UNIVERSITY OF PISA

BIOS - Research Doctorate School in **BIO**molecular **S**ciences

Ph.D. *in* **BIOMATERIALS** - *XXII Cycle*

Biocompatible Polymeric Materials for Regenerative Medicine Applications

Mamoni Dash

Supervisor: Prof./Dr. Emo Chiellini

Tutor: Dr. Federica Chiellini

Laboratory of Bioactive Polymeric Materials for Biomedical and Environmental Applications (BIOlab)

Department of Chemistry and Industrial Chemistry

To, Mummy, Babu & Bhauni

INDEX

LIST OF ABBREVIATIONS

ANOVA:	Analysis of Variance
DEX:	Statistical Design Experiment
DSC:	Differential Scanning Calorimetry
DTGA:	Derivative Thermogravimetric Analysis
FTIR:	Fourier Transform Infrared Spectroscopy
T_d:	Decomposition Temperature
T_g:	Glass Transition Temperature
TGA:	Thermogravimetric Analysis
T_m:	Melting Temperature
T_p:	Peak Degradation Temperature
UV:	Ultraviolet
X_c:	Crystallinity Degree
LCST	Lower Critical Solution Temperature
PEC	Polyelectrolyte Complex
ECM	Extra-cellular Matrix
BAL	Bioartificial Liver
IBL	Implanatable Bioartificial Liver
ASGPR	Asialoglycoproteins
RII	Retrograde Intrabiliary Infusion
IL	Inter Leukin
BMP	Bone Morphogenetic Protein
FRET	Fluorescence Resonance Energy Transfer
TE	Tissue Engineering
HSA	Human Serum Albumin
TPP	Tripolyphosphate
MW	Molecular weight
DD	Degree of Deacetylation
DA	Degree of Acetylation
BAPNA	N-α-benzoyl-DL-arginine-4-nitroanilide
MAGlyGly	Methacryloylglycylglycine
GlyGly	Glycyl glycine

PIDS	Polarization Intensity Differentiation Scattering
SEM	Scanning Electron Microscopy
FEM	Field Emission Microscopy
NMR	Nuclear Magnetic Resonance Spectroscopy
XPS	X-ray Photoelectron Spectroscopy
DMSO	Dimethyl sulphoxide
EGDMA	Ethylene glycol dimethacrylate
Semi-IPN	Semi Interpenetrating Networks

GLOSSARY

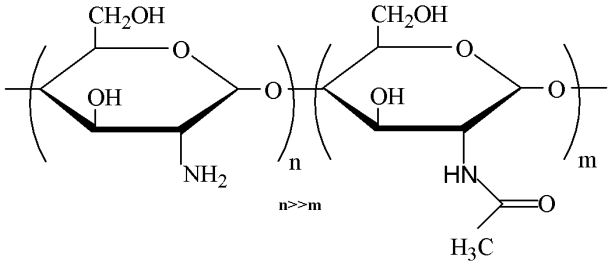

Chitosan

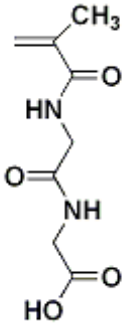

Methacryloylglycylglycine

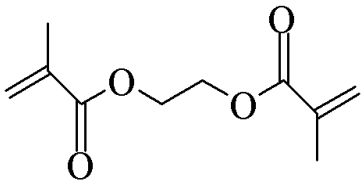

Ethylene glycol dimethacrylate

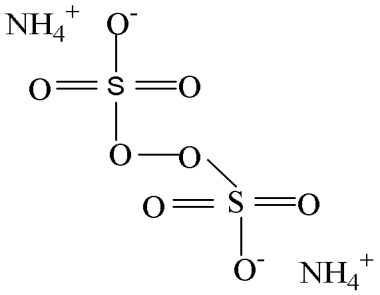

Ammonium persulfate

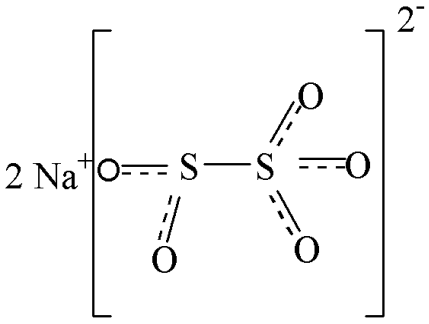

Sodium metabisulphite

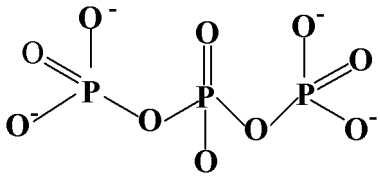

Tripolyphosphate

OBJECTIVES

The present doctorate thesis aims at studying in detail the behaviour and properties of a naturally derived semi-synthetic origin polymer, chitosan and its combination with a synthetic polymer belonging to the class of poly(acrylamides). To accomplish the above objective, micro/ nano particles as well as semi-interpenetrating hydrogel networks were prepared for biomedical applications. Various physico-chemical characterizations of the prepared materials have been performed and evaluated in detail.

Chitosan is a biodegradable polymer with great potential for various applications due to its biocompatibility, high charge density, non-toxicity and mucoadhesivity. It is a semi-crystalline polymer and most of its properties are known to be a function of the degree of acetylated monomeric units. Much of the potential of chitosan as a biomaterial stems from its cationic nature and high charge density in solution. The charge density allows chitosan to form insoluble ionic complexes or complex coacervates with a wide variety of water-soluble anionic polymers. Different strategies are adopted in this thesis to develop systems based on chitosan which would offer better application for Regenerative Medicine applications.

As mentioned above, the degree of deacetylation (DD) that represents indeed the number of acetylated amino glucosidic units and is one of the most important properties of chitosan. A simple, rapid and reliable method for the determination of DD of chitosan is essential. An economical and accurate determination of DD for highly acetylated amino polysaccharides has always been a challenge for researchers dealing with chitin and chitosan. Our aim was to prepare chitosan from its parent polymer chitin and to determine the DD values using spectroscopic and thermal techniques. Different reaction parameters were varied and using these data a statistical model was designed to define the best preparative condition for such reactions.

The use of microsphere or bead-based therapies allow drug release to be carefully tailored to the specific treatment sites through the choice and formulation of various drug–polymer combinations. Chitosan beads are used to provide controlled release of many drugs and to improve the bioavailability of degradable substances such as protein or enhance the uptake of hydrophilic substances across the epithelial compartments. Chitosan possess a unique capability of forming beads in the presence of non-toxic polyanion. We tried to exploit this ability of chitosan for the loading of two model proteins Human Serum Albumin (HSA) and Porcine Trypsin (PT). Both the proteins were successfully loaded into the beads and their release behaviour was studied.

A number of studies have been conducted with the aim of using chitosan-based nanoparticles as the carriers of drugs, vaccines and even DNA. Chitosan-based nanoparticles

have provided the opportunities for the site-specific delivery of drugs because they can solubilize various hydrophobic drugs, increase bioavailabilty and possess a long residence time in blood circulation system. With this objective in mind, chitosan nanoparticles were prepared by interaction with poly(methacryloylglycylglycine) (MAGlyGly). Poly(MAGlyGly) is an poly(acrylamide) based polymer with wide application in the delivery of anti-cancer drugs. Our main focus in this work has been in understanding the physico-chemical characteristics of the prepared nanoparticles as suited to be used in drug delivery practice.

The same underlying concept has been explored again to prepare hydrogels with semi- interpenetrating hydrogel networks (semi-IPN's) composed of chitosan and Poly(MAGlyGly). Hydrogels are of special interest in controlled release applications because of their tissue biocompatibility, the ease with which drugs are dispersed in the matrix and the high degree of control achieved by the design of the physical and chemical properties of the polymer network. A major disadvantage of the hydrogels is represented by their relatively low mechanical strength that can be mitigated and even overcome either by crosslinking, or by formation of interpenetrating networks (IPNs). We used the later approach to prepare semi-IPN's by varying different compositions of the polymer and crosslinker with a aim of allowing it to be used for tissue engineering purposes. The selected strategy was dictated and tailored to the ultimate expected application of the prepared IPN's in tissue engineering.

.

1. CHITOSAN- A VERSATILE MATERIAL FOR REGENERATIVE MEDICINE APPLICATIONS

1.1. Abstract

Regenerative medicine, one of the upcoming fields in present and future life science, finally aims at the restoration or replacement of lost or damaged organ or body part with transplantation of new tissues in combination with supportive scaffolds and biomolecules. Regenerative medicine is usually defined by connecting the fields of tissue engineering, stem cell research, gene therapy and therapeutic cloning [1, 2]. Recently, functional biomaterial research has been directed toward the development of new drug delivery systems and improved scaffolds for regenerative medicine. In this regard, increasing attention has been given to chitosan and its derivatives. Chitosan is becoming an undisputed biomolecule of great potential because of its polyelectrolyte properties, including the presence of reactive functional groups, gel-forming ability, high adsorption capacity, complete biodegradability, bacteriostatic, and fungistatic, even anti-tumor influence [3]. Chitosan is also bio-compatible and non-toxic for living tissues [4,5]. These investigations confirm the suitability and extensive applications of chitosan in regenerative medicine. The present chapter outlines the major new findings on the most common chitosan-based materials. Micro/nanoparticulate and hydrogels are widely used forms of chitosan, a survey of the publications related to them over the past decade has been done. Methods of their preparation, drug loading, release characteristics, and applications are covered. Herein, the potential value of chitosan in tissue engineering, wound healing and gene therapy have been mainly focused. The chemical structure and relevant biological properties of chitosan for regenerative medicine have also been summarized.

1.2. Introduction

The history of chitosan dates back to the last century, when Rouget [6] discussed the deacetylated forms of the parent chitin natural polymer in 1859. During the past 20 years, a substantial amount of work has been published on this polymer and its potential use in various applications. Recently, chitosan has been considered for pharmaceutical formulation and drug delivery applications in which attention has been focused on its absorption-

enhancing, controlled release and bioadhesive properties. Synthesized from a naturally occurring source, this polymer has been shown to be both biocompatible and biodegradable [7]. Chitosan is a linear copolymer of β-(1-4) linked 2-acetamido- 2-deoxy- β -D-glucopyranose and 2-amino-2- deoxy- β -D-glycopyranose (*figure. 1(a)*). It is easily obtained by deacetylation of chitin, a polysaccharide widely distributed in nature (e.g. crustaceans, insects and certain fungi) [8,9]. Due to the limited solubility of chitin in aqueous solutions, chitosan is more suitable for industrial applications [10]. Chitin and chitosan polymers are a natural and a semi-synthetic desired aminopolysaccharides respectively having unique structures, multidimensional properties, highly sophisticated functions and wide ranging applications in biomedical and other industrial areas [11–13]. The positive attributes of excellent biocompatibility and admirable biodegradability with ecological safety and low toxicity with versatile biological activities such as antimicrobial activity and low immunogenicity have provided ample opportunities for further development [14-19]. It has become of great interest not only as a cheap and easily available resource but also as a new functional biomaterial of high potential in various fields [20-22].

1.3. General Aspects of Chitosan

1.3.1 Structure of Chitosan

Chitosan [poly(1,4-β-D-glucopyranosamine)], is produced generally by partial deacetylation of chitin obtained from the shells of crustaceans. Chitosan molecule is a copolymer of N-acetyl-D-glucosamine and D-glucosamine available in different grades depending upon the degree of deacetylated moieties (*figure 1(a)*) [23]. It is a polycationic polymer that has one amino group and two hydroxyl groups in the repeating hexosaminide residue (*figure 1(b)*). The sugar backbone consists of β-1,4-linked D-glucosamine with a high degree of N-acetylation, a structure very similar to that of cellulose, except that the acetylamino group replaces the hydroxyl group on the C2 position. Thus, chitosan is poly(N-acetyl-2-amino-2-deoxy-D-glucopyranose), where the N-acetyl-2-amino-2-deoxy-D-glucopyranose (or Glu-NH_2) units are linked by (1→4)-β-glycosidic bonds[24]. Chitosan has a rigid crystalline structure through inter- and intra-molecular hydrogen bonding.

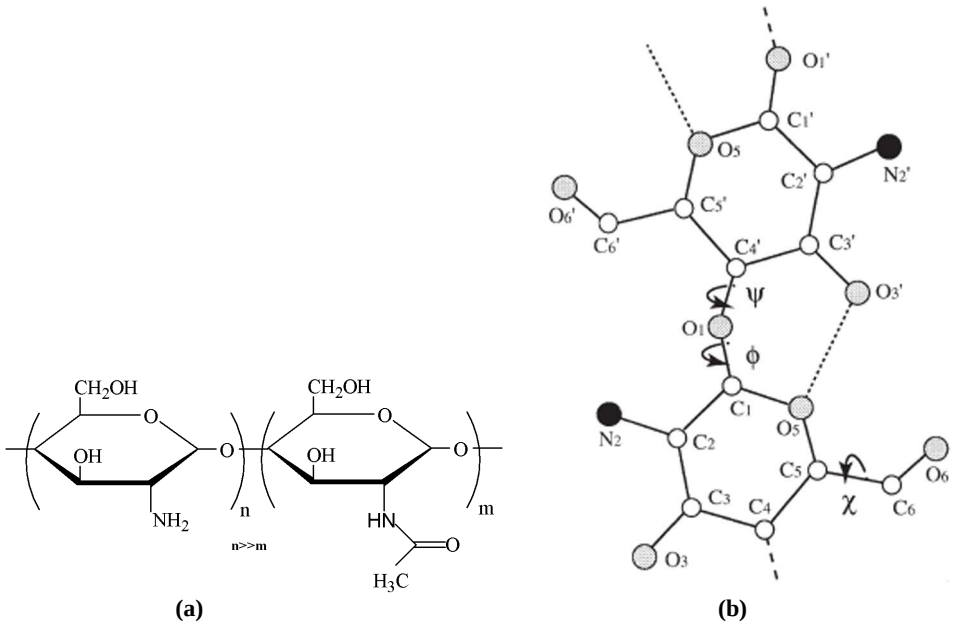

(a) **(b)**

Figure 1. *(a) Structure of chitosan ; (b) Chemical structure of chitosan. Individual atoms are numbered. Dashed lines denote O3—O5 hydrogen bonds. Two dihedral angles (φ, ψ) defining the main chain conformation and one dihedral angle χ defining the O6 orientation are indicated.*

1.3.2 Source & Availability of Chitosan

Chitin is the second most abundant polysaccharides in nature, cellulose being the most abundant. Chitin is found in the exoskeleton of crustacea, insects, and some fungi. The main commercial sources of chitin are the shell wastes of shrimp, lobster, krill and crab. In the world several millions tons of chitin are harvested annually [24-26]. Chitosan is obtained by the deacetylation of chitin. Treatment of chitin with an aqueous 40-45%(w/v) NaOH solution at 90-120°C for 4-5 h results in N-deacetylation of chitin. The insoluble precipitate is washed with water to give a crude sample of chitosan. The conditions used for deacetylation determines the polymer molecular weight and the degree of deacetylation (DD). Generally, further purification is necessary to prepare medical and pharmaceutical grade chitosan.

1.3.3 Physicochemical Properties of Chitosan

Chitosan is insoluble at neutral and alkaline pH, but forms water-soluble salts with inorganic and organic acids including glutamic, hydrochloric, lactic and acetic acids. Upon

dissolution in acidic media, the amino groups of the polymer become protonated rendering the molecule positively charged. The DD represents the proportion of D-glucosamine units with respect to the total number of units. The properties of chitosan (e.g. pKa and solubility) can be modified by changing the DD and formulation properties such as the pH and ionic strength. At neutral pH, most chitosan molecules lose their charge and precipitate from solution.

The primary amino groups on the molecule are reactive and provide sites for side group attachment using a variety of mild reaction conditions, this property renders it to be an easy molecule for side chain reactions and derivatization. In addition, the characteristic features of chitosan such as being cationic, hemostatic and insoluble at high pH, can be completely reversed by a sulfation process which can render the molecule anionic and water-soluble, and also introduce anticoagulant properties [27].

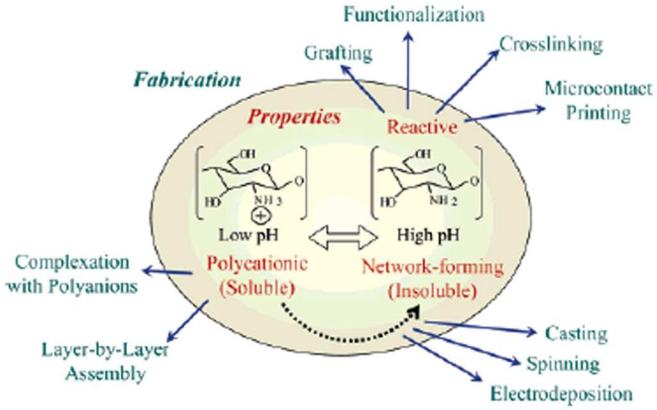

Figure 2. *Schematic illustration chitosan's versatility for fabrication. At low pH (less than about 6), chitosan's amine groups are protonated conferring polycationic behavior to chitosan. At higher pH (above about 6.5), chitosan's amines are deprontonated and reactive. Also at higher pH, chitosan can undergo interpolymer associations that can lead to fiber and network (i.e., film and gel) formation.*

The variety of groups that can be attached to chitosan is almost unlimited, and side groups can be chosen to provide specific functionality, alter biological properties or modify physical properties. Due to its high molecular weight and a linear unbranched structure, chitosan is an excellent viscosity- enhancing agent in acidic environments. It behaves as a pseudoplastic material exhibiting a decrease in viscosity with increasing rates of shear. The viscosity of chitosan solution increases with an increase in chitosan concentrations, decrease in temperature and with increasing DD, which is a structural parameter also influencing physiochemical properties such as the molecular weight, the elongation at break and the tensile strength [28]. Viscosity also influences biological properties such as wound-healing

properties and osteogenesis enhancement as well as biodegradation by lysozyme [29]. Chitosan, which is polycationic in acidic environments, possesses an ability to form gels at acidic pH values because it is hydrophilic and can retain water in its structure. Exposure to high temperatures can change the physical properties of chitosan, affecting its aqueous solubility, rheology, and appearance.

1.3.4 Biological Properties of Chitosan

Chitosan has been used as a safe excipient in drug formulations over the last two decades [30]. This polymer also attracted the attention of pharmaceutical scientists as a mucoadhesive polymer. Chitosan in the swollen state has been shown to be an excellent mucoadhesive and a natural bioadhesive polymer that can adhere to hard and soft tissues; it has been used in dentistry, orthopaedics, ophthalmology and in surgical procedures. It adheres to epithelial tissues and to the mucus coat present on the surface of the tissues. A variety of chitosan-based colloidal delivery systems have been described in the literature for the mucosal delivery of polar drugs, peptides, proteins, vaccines and DNA. Clinical tests carried out in order to promote chitosan-based biomaterials do not report any inflammatory or allergic reactions following implantation, injection, topical application or ingestion in the human body [31]. It has been demonstrated that degree of deacetylation has no significant influence on the *in vitro* and *in vivo* cytocompatibility of chitosan films with keratinocytes and fibroblasts. The chitosan films with a low degree of deacetylation are very good biomaterials for superficial wound-healing [31]. Once placed on the wound, they adhere to fibroblasts and favor the proliferation of keratinocytes and thereby epidermal regeneration.

1.3.5 Biodegradability of Chitosan

An important aspect in the use of polymers as drug delivery systems is their metabolic fate in the body or biodegradation. In the case of the systemic absorption of hydrophilic polymers such as chitosan, they should have a suitable molecular weight for renal clearance. If the administered polymer's size is larger than this, then the polymer should undergo degradation. Biodegradation (chemical or enzymatic) would provide fragments suitable for renal clearance. Chemical degradation in this case refers to acid catalysed degradation i.e. in the stomach. Although oxidation–reduction depolymerisation and free radical degradation [32] have been reported [33] these are unlikely to be a significant source or degradation in vivo. Chitosan can be degraded by enzymes which hydrolyse glucosamine–

glucosamine, glucosamine–N-acetyl-glucosamine and N-acetyl-glucosamine–N-acetyl-glucosamine linkages [34].

Chitosan is thought to be degraded in vertebrates predominantly by lysozyme and by bacterial enzymes in the colon [35]. However, eight human chitinases (in the glycoside hydrolase 18 family) have been identified, three of which have shown enzymatic activity [36]. A variety of microorganisms synthesises and/or degrades chitin, the biological precursor of chitosan. In general, chitinases in microorganisms hydrolyze N-acetyl-β-1,4-glucosaminide linkages randomly i.e. they are endo-chitinases (EC 3.2.1.14). Chitinases are also present in higher plants, even though they do not have chitin structural components. In general, both rate and extent of chitosan biodegradability in living organisms are dependent on the DD [37,38]. Increasing DD decreases the degradation rate. The extent of degradation is related to the rate, as all the studies are conducted over a finite lifetime. It is likely that, given adequate time and appropriate conditions, the chitosans would degrade sufficiently for consequent excretion.

1.3.5.1 Biodegradation- In-vitro

Chemical characterisation assays determining the degradation of chitosan commonly use viscometry and/or gel permeation chromatography to evaluate a decrease in molecular weight [39]. Lysozyme has been found to efficiently degrade chitosan; 50% acetylated chitosan had 66% loss in viscosity after a 4 h incubation in vitro at pH 5.5 (0.1 M phosphate buffer, 0.2 M NaCl, 37 °C) [39]. This degradation appears to be dependent on the degree of acetylation with degradation of acetylated chitosan (more chitin like) showing the faster rate [40,41]. Surprisingly, a range of proteases were found to degrade chitosan films to varying degrees, with leucine amino-peptidase being the most effective, degrading the film by 38% over 30 days [42]. Pectinase isozyme from Aspergilus niger has also been shown to digest chitosan at low pH providing lower molecular weight chitosans [43,44]. More therapeutically relevant, is the digestion of chitosan with rat cecal and colonic bacterial enzymes. It was found that degradation was caused predominantly by extracellular enzymes and that degradation was related to both DD and molecular weight. Compounds of lower molecular weight and lower DD are more susceptible [41]. In a similar experiment, McConnell *et al*. used human faecal preparations and showed significant degradation of chitosan films, glutaraldehyde crosslinked films and tripolyphosphate crosslinked films [45]. Porcine pancreatic enzymes were shown to degrade films over the time periods investigated (4 h and 18 h). The type of crosslinker used for the film formation influenced the degradation

rate; glutaraldehyde to a greater degree than tripolyphosphate, an effect that was more pronounced with the high (310–600 kDa) and medium (190–310 kDa) molecular weight chitosans.

1.3.5.2 Biodegradation- In-vivo

Chitosan degradation after intravenous administration has been reported scarcely. It is somewhat unclear what the mechanism of degradation is when chitosan is injected intravenously. Some authors are of the view that distribution degradation and elimination processes are strongly dependent on molecular weight. Possible sites of degradation, inferred due to the localisation of chitosan, may be the liver and kidney. In one of the few studies reported, chitosan oligosaccharides were found to upregulate lysozyme activity in the blood of rabbits injected intravenously with 7.1–8.6 mg/kg [46]. Chitosan has also been administered subcutaneously, in most cases as an implant. A proposed skin substitute of glutaraldehyde crosslinked chitosan/collagen was relatively stable over time compared to collagen alone when implanted subcutaneously in rabbits [47]. Oral administration of chitosan has shown some degradation in the gastrointestinal tract. The digestion of chitosan, occurring predominantly in the gut, was found to be species dependent with hens and broilers being more efficient digesters (67–98% degradation after oral ingestion) than rabbits (39–83% degradation) [48].

1.3.6 Biodistribution of Chitosan

One of the most studied aspects of chitosan is its biodistribution, especially using methods other than intravenous administration. This distribution is related to all aspects of the chitosan formulation from the molecular weight and DD to the size of the delivery vehicle. In the case of a nanoparticulate formulation, the kinetics and biodistribution will initially be controlled by the size and charge of the nanoparticles and not by chitosan. However, after particle decomposition to chitosan and free drug, inside the cells or target tissue, free chitosan will distribute in the body and eliminate accordingly. Elimination processes may be preceded by biodegradation. To understand chitosan biodistribution the kinetics of its labeled (radio or fluorescent) modifications should be followed, assuming that the label is neither labile nor affecting the physicochemical properties of the chitosan.

1.3.6.1 Distribution after Intravenous Administration

In an attempt to prepare Holmium-166 based radiopharmaceuticals for tumours, Suzuki *et al*. [49] administered chitosan (700 kDa) with Holmium-166 in a chelate complex form and studied its distribution in rats and mice. They found that 72 h after intravenous administration, 4.2% and 4.8% of the radioactivity was recovered in the urine and feces respectively, whereas 90.6% was found in the carcass [49]. Banerjee *et al*. describe the distribution of intravenously injected 99mTc labeled nanoparticles (<100 nm) in Swiss albino mice. Nanoparticles were tested for radiolabel stability and 80% of the radioactivity was associated with the particles after 3 h. Nanoparticles were administered in mice and an apparent evasion of the reticuloendothelial system (RES) was suggested as radioactivity decreased in organs of this system but remained stable in the blood after 1 h [50]. Unfortunately, the nanoparticles were not sufficiently stable to look at long term distributions. However accumulation in the liver was detected.

Richardson *et al*. reported on radio-labeled chitosan (125I) of three different molecular weight fractions (<5 kDa, 5–10 kDa and >10 kDa) and biodistribution was assessed at 5 min and 1 h in male Wistar rats [51]. The authors found ~45% of the recovered dose of the <5 kDa chitosan in the blood at 5 min and ~30% remaining in the blood at 1 h. This was not the case for the 5–10 kDa and >10 kDa chitosans where the 5 min blood recovery was ~15% and ~12% and the 1h ~8% and ~4% respectively. The main organ of uptake appears to be the liver, where accumulation was found to increase with increasing molecular weight. However, there was a recovery of less than 60% of the total administered dose (in harvested tissue) in all cases and it was not normalized to the tissue weight [51]. All three studies found the liver to be a significant site of accumulation; this could be due to this organ being a primary site of metabolism as seen with radio-labeled dextran [52].

A potential method to study native chitosan without significant modification would be to use 14C as a label e.g. in the food source for the animal/fungi producing the chitin so that the saccharide backbone is labeled, as detection of native chitosan is somewhat of a challenge [53].

1.3.6.2 Distribution after intraperitoneal administration

FITC-labeled chitosan (50% DD, 100 kDa) was prepared by FITC coupling and chromatographed for purification. This labeled chitosan was administered intraperitoneally and it was completely absorbed form the peritoneal cavity (no evidence in abdominal fluid

after 14 h). FITC-chitosan was found to be predominantly localised in the kidney at 1 h in a mouse model. There was a rapid renal excretion rate (25% at 1 h, 100% in 14 h) with evidence of degradation due to a decrease in the molecular weight [54].

1.3.6.3 Tissue distribution after oral administration

Oral dosage forms use chitosan as an excipient, although chitosan does not strictly fit the definition of excipient as it has many biological effects. It has been suggested that chitosan chelates fat and reduces cholesterol but this, and its mechanism, is somewhat debatable [55,56]. Apart from the effect that chitosan may have on bile salts and gastrointestinal milieu, the uptake of chitosan into the bloodstream is generally not investigated in oral administration studies. Chitosan's systemic absorption and distribution from this route of delivery has been observed to be largely dependent on the molecular weight. It has been seen in some cases that oligomers showed some absorption whereas larger molecular weight chitosans were excreted without being absorbed. This effect was seen with FITC-labeled chitosans with 3.8 kDa (88.4% DD) chitosan having the greatest plasma concentration after oral administration vs 230 kDa (84.9% DD) having almost no uptake. Increasing molecular weight was seen to decrease the plasma concentration in this, one of the only studies investigating plasma concentration after oral administration [57].

2.1.6.4 Intracellular chitosan distribution

Although native chitosan has not been investigated, the intracellular uptake and distribution of chitosan/DNA complexes have been studied in vitro [58-60]. Chitosan polyplex uptake at 37 °C was 3-fold higher than at 4 °C [58] but this could be due to increased interaction and not an ATP dependent endocytic mechanism. The authors suggested nuclear localization and they also stated little dissociation of the DNA from the chitosan. In a more comprehensive study, Leong *et al*. stained for lysosomes and found some co-localization with chitosan DNA nanoparticles. However, the majority of the polyplexes were found in the cytosol [59]. A complex of doxorubicin with chitosan has also been studied; complexes enter cells through an endocytic mechanisms which was not further elucidated [61].

1.3.7 Toxicity of Chitosan

Chitosan is widely regarded as being a non-toxic, biologically compatible polymer [62]. It is approved for dietary applications in Japan, Italy and Finland [63] and it has been approved by the FDA for use in wound dressings [64]. The modifications perfomed on chitosan could make it more or less toxic and any residual reactants should be carefully removed.

1.3.7.1 In-vitro toxicity

In a series of articles Schipper *et al*. described the effects of chitosans with differing molecular weights and DD on CaCo-2 cells, HT29-H and in situ rat jejunum. Toxicity was found to be DD and molecular weight dependent. At high DD the toxicity is related to the molecular weight and the concentration, at lower DD toxicity is less pronounced and less related to the molecular weight. However most of the chitosans tested did not increase dehydrogenase activity significantly in the concentration range tested (1–500 μg/ml) on Caco-2 cells. The in situ rat jejunum study showed no increase in LDH activity with any of the chitosans tested (50 μg/ml) [65,66]. A study that reveals safety of materials is the red cell haemolysis assay. Haemolysis was not observed (<10%) over 1 h and 5 h with chitosans of <5 kDa, 5–10 kDa and >10 kDa at concentrations of up to 5 mg/ml [51]. As well, no red blood cell lysis was observed with paclitaxel chitosan micelles at 0.025 mg/ml [67].

Interestingly, chitosan and its derivatives seem to be toxic to several bacteria [68], fungi [69] and parasites [70]. This pathogen related toxicity is an effect which could aid in infectious disease control. When emulsions containing chitosans were tested, bacterial inhibition took place in acidic solutions pH 5–5.3, and a 87 kDa 92% DD chitosan was more effective than a 532 kDa 73% DD chitosan against both Pseudomonas aeruginosa and Staphylococcus aureus. A lipid emulsion of the same chitosans was found to have antimycotic effect against Candida albicans and Aspergillus niger [68]. In tests of meglumine antimoniate against Leishmania infantum it was found that the chitosan excipient had anti-parasitic properties (IC50 112.64± 0.53 mg/ml for promastigotes and 100.81±26.45 mg/ml for amastigotes) [70]. None of these studies hypothesized a mechanism of action for the inhibitory effect observed.

1.3.7.2 In-vivo toxicity

In vivo toxicity particularly after long term administration is of high importance for the design of drug delivery forms based on chitosan. In a relatively long study (65 days), no detrimental effect on body weight was found when chitosan oligosaccharides were injected (7.1–8.6 mg/kg over 5 days). An increase in lysozyme activity was apparent on the first day post injections [71].

Rao *et al.* stated no "significant toxic effects" of chitosan in acute toxicity tests in mice, no eye or skin irritation in rabbits and guinea pigs respectively. In the same study it was also concluded that chitosan was not pyrogenic. However, no concentration or DD of the chitosan used was noted [72]. Even though no dose is stated in his work , no detrimental effects were noted by Richardson *et al*. [51]. The LD50 of paclitaxel chitosan micelles in mice was 72.16 mg/kg, no anaphylaxis was observed in guinea pigs and no intravenous irritation was observed histopathologically in rabbits at 6 mg/kg [67]. No adverse effects at 3.3–4 mg/kg were reported by Banerjee *et al*. [50]. In a study on fat chelation, 4.5 g/day chitosan (molecular weight and DD not noted) in humans was not reported toxic, although no significant reduction in fat was found [73]. Arai *et al*. found that chitosan has an LD50 comparable to sucrose of >16 g/kg in oral administration to mice [74]. No oral toxicity was found in mice treated with 100 mg/kg chitosan nanoparticles (80 kDa, 80% DD) [75]. Exposure of rat nasal mucosa to chitosan solutions at 0.5% (w/v) over 1 h caused no significant changes in mucosal cell morphology compared to control [76]. From most studies reported it appears that chitosan shows minimal toxic effects and this justifies its selection as a safe material in drug delivery.

1.4. Chitosan Based Systems for Regenerative Medicine Applications

1.4.1 Chitosan Micro/nano Particles

If DD and molecular weight of chitosan can be controlled, then it would be a material of choice for developing micro/nanoparticles. Chitosan has many advantages, and these include its ability to control the release of active agents and the avoid use of hazardous organic solvents while fabricating particles since it is soluble in aqueous acidic solution. In view of the above-mentioned properties, chitosan is extensively used in developing drug delivery systems [77–84]. Particularly, chitosan has been used in the preparation of mucoadhesive formulations [85,86,76,87], improving the dissolution rate of the poorly

soluble drugs [80,88,89], drug targeting [90,91] and enhancement of peptide absorption [86,76,92]. Different types of chitosan based drug delivery systems are summarized in Table 1. The micro/nanoparticulate drug delivery systems offer numerous advantages over the conventional dosage forms. These include improved efficacy, reduced toxicity and improved patient compliance [93,94-96]. In the present section we have addressed the trends in the area of micro/nanoparticulate chitosan-based drug delivery systems. Literature of the past decade has been covered and results are evaluated.

Table 1 *Chitosan based drug delivery systems prepared by different methods.*

Type of system	Method of preparation
Tablets	Matrix coating
Capsules	Capsule shell
Microspheres	Emulsion cross-linking
	Coacervation/Precipitation
	Spray drying
	Ionic gelation
	Sieving method
Nanoparticles	Emulsion-droplet coalescence
	Coacervation/Precipitation
Beads	Coacervation/Precipitation
Films	Solution casting
Gel	Crosslinking

1.4.1.1 Methods for the preparation of Chitosan micro/nanoparticles

Different methods have been used to prepare chitosan particulate systems. Selection of any of the methods depends upon factors such as particle size requirement, thermal and chemical stability of the active agent, reproducibility of the release kinetic profiles, stability of the final product and residual toxicity associated with the final product. However, selection of any of these methods depends upon the nature of the active molecule as well as the type of the delivery device.

1.4.1.1.1 Emulsion crosslinking

This method utilizes the reactive functional amine group of chitosan to cross-link with the possible reactive groups of the cross-linking agent. In this method, a water-in-oil (w/o) emulsion is prepared by emulsifying the chitosan aqueous solution in the oil phase. Aqueous droplets are stabilized using a suitable surfactant. The stable emulsion is cross-linked by using an appropriate cross-linking agent to harden the droplets. Microspheres are filtered and washed repeatedly with alcohol and then dried [97]. By this method, size of the particles can be controlled by controlling the size of aqueous droplets. However, the particle size of final product depends upon the extent of cross-linking agent used while hardening in addition to speed of stirring during the formation of emulsion. This method is schematically represented in *figure 3*. The emulsion cross-linking method has few drawbacks since it involves tedious procedures as well as use of harsh cross-linking agents, which might possibly induce chemical reactions with the active agent. Also, complete removal of the un-reacted crosslinking agent may be difficult in this process.

Agnihotri *et al*. [98] have used the emulsion crosslinking method to prepare chitosan microspheres to encapsulate diclofenac sodium using three crosslinking agents viz, glutaraldehyde, sulfuric acid and heat treatment. Microspheres were spherical with smooth surfaces. The size of the microparticles ranged between 40 and 230 µm. Among the three cross-linking agents used, glutaraldehyde cross-linked microspheres showed the slowest release rates while a quick release of diclofenac sodium was observed by the heat cross-linked microspheres. Sankar *et al*. [99] prepared the chitosan-based pentazocine microspheres for intranasal delivery. Formulation parameters such as drug loading, polymer concentration, stirring speed during cross-linking and oil phase were altered to develop microspheres having good in vivo performance. *In vivo* studies indicated a significantly improved bioavailability of pentazocine. Application of *in vitro* data to various kinetic models indicated that these systems followed the diffusion controlled release kinetics.

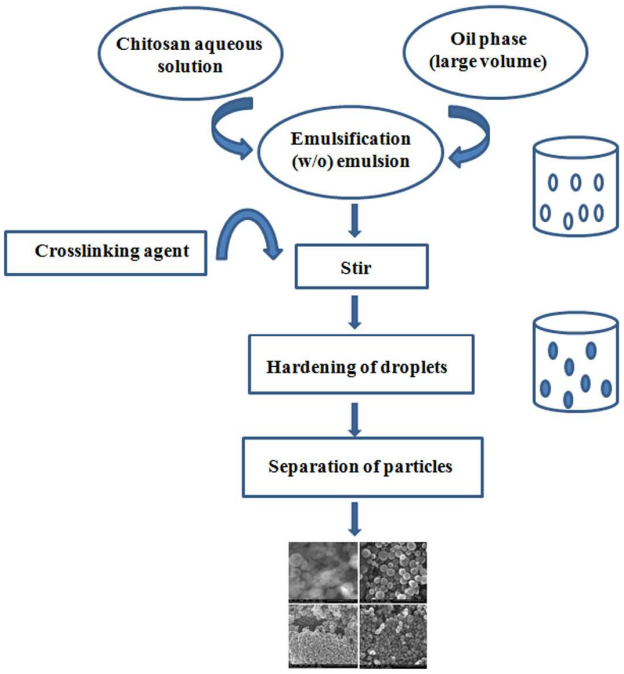

Figure 3. *Schematic representation of preparation of chitosan particulate systems by emulsion cross-linking method*

1.4.1.1.2 Coacervation/ Precipitation

This method utilizes the physicochemical property of chitosan since it is insoluble in alkaline pH medium, but precipitates/coacervates when it comes in contact with alkaline solution. Particles are produced by blowing chitosan solution into an alkali solution like sodium hydroxide, NaOH-methanol or ethanediamine using a compressed air nozzle to form coacervate droplets. Separation and purification of particles are done by filtration/centrifugation followed by successive washing with hot and cold water. The method is schematically represented in *figure 4*. Varying compressed air pressure or spray-nozzle diameter controlled the size of the particles and then using a crosslinking agent to harden particles can control the drug release. Chitosan microspheres loaded with recombinant human interleukin-2 (rIL-2) have been prepared by dropping of rIL-2 with sodium sulfate solution in acidic chitosan solution [100]. When protein and sodium sulfate solutions were added to chitosan solution and during the precipitation of chitosan, the protein was incorporated into microspheres. This method is devoid of cross-linking agent. The rIL-2 was released from microspheres in a sustained manner for up to 3 months. Efficacy of the systems developed was studied by using two model cells viz., HeLa and Lstrain cell lines.

Microspheres were taken up by the cells and rIL-2 was released from the microspheres. Chitosan–DNA nanoparticles have been prepared using the complex coacervation technique [101]. Important parameters such as concentrations of DNA, chitosan, sodium sulfate, temperature, pH of the buffer and molecular weights of chitosan and DNA have been investigated. At the amino to phosphate group ratio between 3 and 8 and chitosan concentration of 100 ng/ mL, the particle size was optimized to 100–250 nm with a narrow distribution. Surface charge of these particles was slightly positive with a zeta potential of 112 to 118 mV at pH lower than 6.0, and became nearly neutral at pH 7.2. The chitosan–DNA nanoparticles could partially protect the encapsulated plasmid DNA from nuclease degradation.

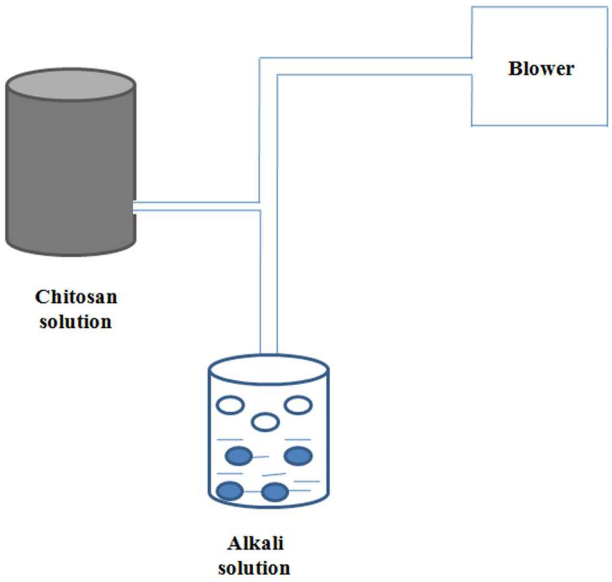

Figure 4. *Schematic representation of preparation of chitosan particulate systems by coacervation/precipitation method*

1.4.1.1.3 Spray-drying

Spray-drying is a well-known technique to produce powders, granules or agglomerates from the mixture of drug and excipient solutions as well as suspensions. The method is based on drying of atomized droplets in a stream of hot air. In this method, chitosan is first dissolved in aqueous acetic acid solution, drug is then dissolved or dispersed in the solution and then, a suitable cross-linking agent is added. This solution or dispersion is

then atomized in a stream of hot air. Atomization leads to the formation of small droplets, from which solvent evaporates instantaneously leading to the formation of free flowing particles [102]. Various process parameters are to be controlled to get the desired size of particles. Particle size depends upon the size of nozzle, spray flow rate, atomization pressure, inlet air temperature and extent of crosslinking. This method is however more commonly used for the preparation of microparticles than for nanoparticles. Huang *et al*. [103] prepared chitosan microspheres by the spray-drying method using type-A gelatin and ethylene oxide–propylene oxide block copolymer as modifiers. Surface morphology and surface charges of the prepared microspheres were investigated using SEM and microelectrophoresis. Shape, size and surface morphology of the microspheres were significantly influenced by the concentration of gelatin. Betamethasone disodium phosphate-loaded microspheres demonstrated a good drug stability (less 1% hydrolysis product), high entrapment efficiency (95%) and positive surface charge (37.5 mV). In vitro drug release from the microspheres was related to gelatin content. Microspheres containing gelatin/chitosan ratio of 0.4–0.6 (w/w) showed a prolonged release up to 12 h. In another study [104], vitamin D2 (VD2), also called as ergocalciferol, was efficiently encapsulated into chitosan microspheres prepared by spray-drying method. The microencapsulated product was coated with ethyl cellulose. The sustained release property of VD2 microspheres was used for the treatment of prostatic disease [105].

1.4.1.1.4 Emulsion-droplet coalescence method

The novel emulsion-droplet coalescence method was developed by Tokumitsu *et al*. [106], which utilizes the principles of both emulsion cross-linking and precipitation. However, in this method, instead of cross-linking the stable droplets, precipitation is induced by allowing coalescence of chitosan droplets with NaOH droplets. First, a stable emulsion containing aqueous solution of chitosan along with drug is produced in liquid paraffin oil and then, another stable emulsion containing chitosan aqueous solution of NaOH is produced in the same manner. When both emulsions are mixed under high-speed stirring, droplets of each emulsion would collide at random and coalesce, thereby precipitating chitosan droplets to give small size particles. The method is schematically shown in *figure 5*. Gadopentetic acid-loaded chitosan nanoparticles have been prepared by this method for gadolinium neutroncapture therapy. Particle size depends upon the type of chitosan, i.e., as the % deacetylation degree of chitosan decreased, particle size increased, but drug content decreased. Particles produced using 100% deacetylated chitosan had the mean particle size

of 452 nm with 45% drug loading. Nanoparticles were obtained within the emulsion-droplet. Size of the nanoparticle did not reflect the droplet size. Since gadopentetic acid is a bivalent anionic compound, it interacts electrostatically with the amino groups of chitosan, which would not have occurred if a cross-linking agent is used that blocks the free amino groups of chitosan. Thus, it was possible to achieve higher gadopentetic acid loading by using the emulsion-droplet coalescence method compared to the simple emulsion crosslinking method.

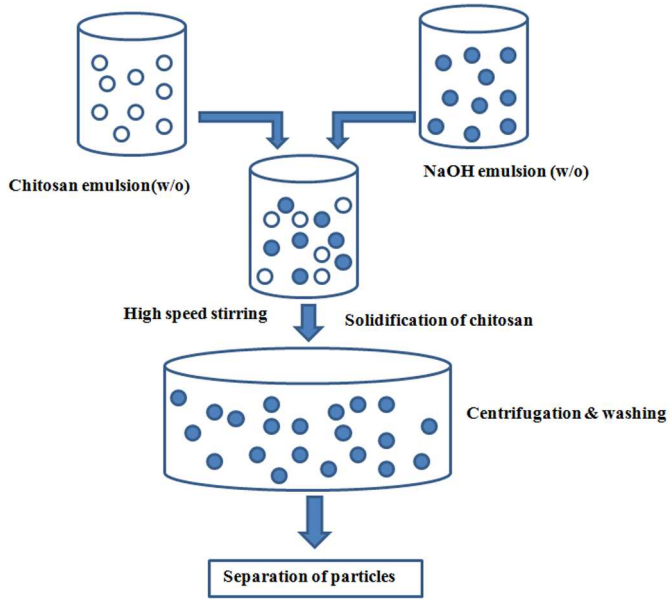

Figure 5. *Schematic representation of preparation of chitosan particulate systems by emulsion – droplet coalescence method*

1.4.1.1.5 Ionic gelation

The use of complexation between oppositely charged macromolecules to prepare chitosan microspheres has attracted much attention because the process is very simple and mild [107,108]. In addition, reversible physical cross-linking by electrostatic interaction, instead of chemical cross-linking, has been applied to avoid the possible toxicity of reagents and other undesirable effects. Tripolyphosphate (TPP) is a polyanion, which can interact with the cationic chitosan by electrostatic forces [109,110]. Bodmeier *et al.* [111] reported the preparation of TPP–chitosan complex by dropping chitosan droplets into a TPP solution, many researchers have explored its potential pharmaceutical usage [112-117]. In the ionic gelation method, chitosan is dissolved in aqueous acidic solution to obtain the cation of

chitosan. This solution is then added dropwise under constant stirring to polyanionic TPP solution. Due to the complexation between oppositely charged species, chitosan undergoes ionic gelation and precipitates to form spherical particles. The method is schematically represented in *figure 6*.

Ko *et al*. [118] prepared chitosan microparticles with TPP by the ionic cross-linking method. Particle sizes of TPP-chitosan microparticles varied from 500 to 710 nm with drug encapsulation efficiencies more than 90%. Morphologies of TPP-chitosan microparticles have been examined by SEM. As the pH of TPP solution decreased and molecular weight of chitosan increased, microparticles acquired better spherical shape having smooth surface. Release of felodipine as a model drug was affected by the preparation method. Chitosan microparticles prepared at lower pH or higher concentration of TPP solution resulted in a slower release of felodipine. With a decreasing molecular weight and concentration of chitosan solution, the drug release increased. The release of drug from TPP-chitosan microparticles decreased when the cross-linking time was increased. Xu and Du [119] have studied different formulations of chitosan nanoparticles produced by the ionic gelation of TPP and chitosan. TEM indicated their diameter ranging between 20 and 200 nm with spherical shape. FTIR confirmed tripolyphosphoric groups of TPP linked with ammonium groups of chitosan in the nanoparticles. Factors that affect the delivery of bovine serum albumin (BSA) as a model protein have been studied. These include molecular weight and deacetylation degree of chitosan, concentrations of chitosan and BSA, as well as the presence of polyethylene glycol (PEG) in the encapsulation medium.

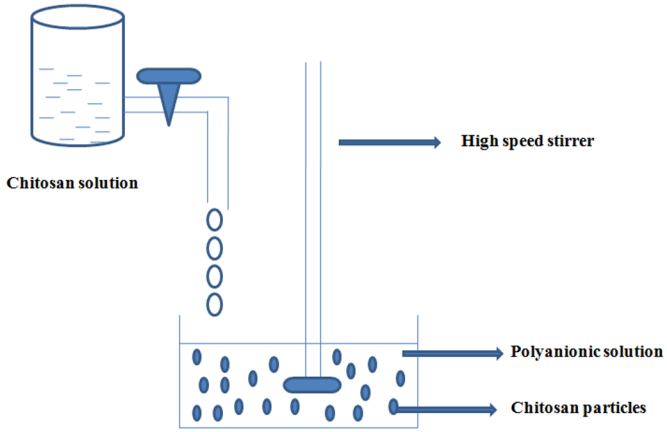

Figure 6. *Schematic representation of preparation of chitosan particulate systems by ionic gelation method*

1.4.1.1.6 Reverse micellar method

Reverse micelles are thermodynamically stable liquid mixtures of water, oil and surfactant. Macroscopically, they are homogeneous and isotropic, structured on a microscopic scale into aqueous and oil microdomains separated by surfactant-rich films. One of the most important aspects of reverse micelle hosted systems is their dynamic behavior. Nanoparticles prepared by conventional emulsion polymerization methods are not only large (>200 nm), but also have a broad size range. Preparation of ultrafine polymeric nanoparticles with narrow size distribution could be achieved by using reverse micellar medium [120]. Since micellar droplets are in Brownian motion, they undergo continuous coalescence followed by re-separation on a time scale that varies between millisecond and microsecond [121]. The size, polydispersity and thermodynamic stability of these droplets are maintained in the system by a rapid dynamic equilibrium. In this method, the surfactant is dissolved in a organic solvent to prepare reverse micelles. To this, aqueous solutions of chitosan and drug are added with constant vortexing to avoid any turbidity. The aqueous phase is regulated in such a way as to keep the entire mixture in an optically transparent microemulsion phase. Additional amount of water may be added to obtain nanoparticles of larger size. To this transparent solution, a cross-linking agent is added with constant stirring, and cross-linking is achieved by stirring overnight. The maximum amount of drug that can be dissolved in reverse micelles varies from drug to drug and has to be determined by gradually increasing the amount of drug until the clear microemulsion is transformed into a translucent solution. The method is schematically represented in *figure 7*. Mitra *et al*. [122] have encapsulated doxorubicin– dextran conjugate in chitosan nanoparticles prepared by reverse micellar method. The surfactant sodium bis(ethyl hexyl) sulfosuccinate (AOT), was dissolved in n-hexane. This procedure produced chitosan nanoparticles encapsulating doxorubicin–dextran conjugate.

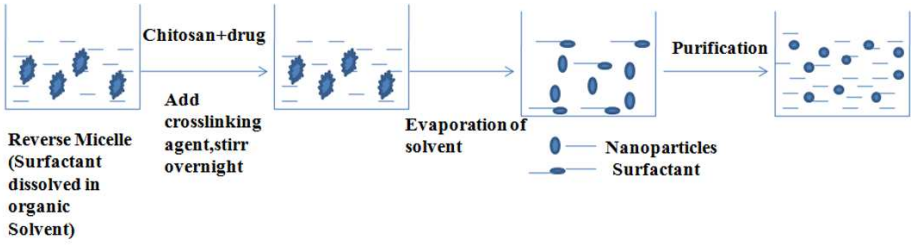

Figure 7. *Schematic representation of preparation of chitosan particulate systems by reverse micellar method*

1.4.1.1.7 Seiving method

Recently, Agnihotri and Aminabhavi [123] have developed a simple, yet novel method to produce chitosan microparticles. In this method, microparticles were prepared by cross-linking chitosan to obtain a non-sticky glassy hydrogel followed by passing through a sieve as shown in *figure 8*. In the work by Agnihotri *et al*., a suitable quantity of chitosan was dissolved in 4% acetic acid solution to form a thick jelly mass that was cross-linked by adding glutaraldehyde. The non-sticky cross-linked mass was passed through a sieve with a suitable mesh size to get microparticles. The microparticles were washed with 0.1 N NaOH solution to remove the un-reacted excess glutaraldehyde and dried overnight in an oven at 40 8C. Clozapine was incorporated into chitosan before crosslinking with an entrapment efficiency up to 98.9%. This method is devoid of tedious procedures, and can be scaled up easily. Microparticles were irregular in shape, with the average particle sizes in the range 543–698 nm. The in vitro release was extended up to 12 h, while the in vivo studies indicated a slow release of clozapine.

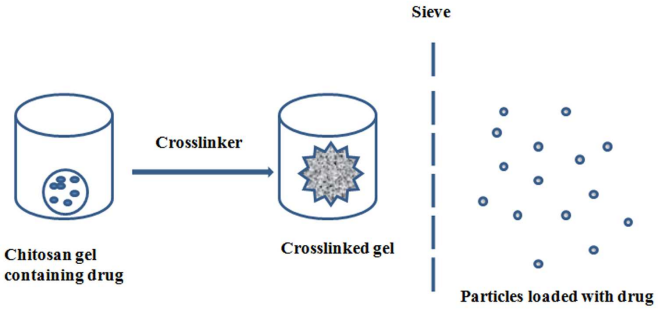

Figure 8. *Schematic representation of preparation of chitosan particulate systems by seiving method*

1.4.1.2 Drug loading into Chitosan micro/nanoparticles

Drug loading in micro/nanoparticulate systems can be done by two methods, i.e., during the preparation of particles (incorporation) and after the formation of particles (incubation). In these systems, drug is physically embedded into the matrix or adsorbed onto the surface. Various methods of loading have been developed to improve the efficiency of loading, which largely depends upon the method of preparation as well as physicochemical properties of the drug. Maximum drug loading can be achieved by incorporating the drug during the formation of particles, but it may get affected by the process parameters such as

method of preparation, presence of additives, etc. Both water-soluble and water-insoluble drugs can be loaded into chitosan-based particulate systems. Water soluble drugs are mixed with chitosan solution to form a homogeneous mixture, and then, particles can be produced by any of the methods discussed before.

Water-insoluble drugs and drugs that can precipitate in acidic pH solutions can be loaded after the formation of particles by soaking the preformed particles with the saturated solution of drug. Diclofenac sodium, which precipitates in acidic pH conditions, has been loaded by the soaking method [98]. In this method, loading depends upon the swelling of particles in water. Percentage loading of drug decreased with increasing cross-linking due to decreased swelling. Water-insoluble drugs can also be loaded using the multiple emulsion technique. In this method, drug is dissolved in a suitable solvent and then emulsified in chitosan solution to form an oil-in-water (o/w) type emulsion. Sometimes, drug can be dispersed into chitosan solution by using a surfactant to get the suspension. Thus, prepared o/w emulsion or suspension can be further emulsified into liquid paraffin to get the oil-water-oil (o/w/o) multiple emulsion. The resulting droplets can be hardened by using a suitable cross-linking agent. Hejazi and Amiji [124] have prepared chitosan microspheres by ionic cross-linking and precipitation with sodium sulfate. Two different methods were used for drug loading. In method I, tetracycline was mixed with chitosan solution before simultaneous cross– linking and precipitation. In method II, drug was incubated with the pre-formed microspheres for 48h. Cumulative amount of tetracycline that was released from chitosan microspheres and stability of drug was examined in different pH media at 37 °C. Microspheres with a spherical shape having an average diameter of 2– 3 nm were formed. When drug was added to chitosan solution before cross-linking and precipitation, only 8% (w/w) was optimally incorporated in the final microsphere formulation. When drug was incubated with the pre-formed microspheres, a maximum of 69% (w/w) could be loaded. About 30% of tetracycline either in solution or when released from the microspheres was found to degrade at pH 1.2 in 12 h. Preliminary results of this study suggested that chitosan microspheres can be used to incorporate antibiotic drugs, which may be effective when administered locally in the stomach against H. pylori.

1.4.1.3 Drug release & release kinetics

Drug release from chitosan-based particulate systems depends upon the extent of cross– linking, morphology, size and density of the particulate system, physicochemical properties of the drug as well as the presence of adjuvants. In vitro release also depends upon

pH, polarity and presence of enzymes in the dissolution media. The release of drug from chitosan particulate systems involves three different mechanisms: (a) release from the surface of particles, (b) diffusion through the swollen rubbery matrix and (c) release due to polymer erosion. In majority of cases, drug release follows more than one type of mechanism. In case of release from the surface, adsorbed drug instantaneously dissolves when it comes in contact with the release medium. Drug entrapped in the surface layer of particles also follows this mechanism. This type of drug release leads to burst effect. He *et al*. [102] observed that cemetidine-loaded chitosan microspheres have shown burst effect in the early stages of dissolution. Most of the drug was released within few minutes when particles were prepared by spray drying technique. Increasing the cross-linking density can prevent the burst release. This effect can also be avoided by washing microparticles with a proper solvent, but it may lead to low encapsulation efficiency.

Drug release by diffusion involves three steps. First, water penetrates into particulate system, which causes swelling of the matrix; secondly, the conversion of glassy polymer into rubbery matrix takes place, while the third step is the diffusion of drug from the swollen rubbery matrix. Hence, the release is slow initially and later, it becomes fast. This type of release is more prominent in case of hydrogels. Al-Helw *et al*. [125] observed a high initial release of the drug in all the prepared formulations. Nearly, 20– 30% of the incorporated drug was released in the first hour. Release was dependent on the molecular weight of chitosan and particle size of the microspheres. The release rate from microspheres prepared from high molecular weight chitosan was slow compared to those prepared from medium and low molecular weight chitosan. This could be attributed to both lower solubility of high molecular weight chitosan and higher viscosity of the gel layer formed around the drug particles upon contact with the dissolution medium. The release within the first 3 h was fast (75– 95%) from microspheres within the size range of 250– 500 µm, but for particles in the size range of 500– 1,000 µm, drug release was 56– 90% in 5 h. This was attributed to large surface area available for dissolution with a small particle size, thus favoring rapid release of the drug compared to larger microspheres.

Analysis of drug release data has several approaches. Ganza-Gonzalez *et al*. [126] analyzed the drug release data using the classic Higuchi equation [127]. Higuchi equation was used to describe the release of a solute from a flat surface, but not from a sphere [128], but the good fit obtained suggested that the release rate depends upon the rate of diffusion through the cross-linked matrix. Authors have also fitted the release data to equations developed by Guy *et al*. [129] to describe the diffusion from a sphere. The most commonly used equation for diffusion controlled matrix system is an empirical equation used by Ritger

and Peppas [130], in which the early time release data can be fitted to obtain the diffusion parameters,

$$\frac{Mt}{M\infty} = ktn \quad (1)$$

Here, M_t/M_∞ is the fractional drug release at time t, k is a constant characteristic of the drug-polymer interaction and n is an empirical parameter characterizing the release mechanism. Based on the diffusional exponent [131], drug transport is classified as Fickian (n=0.5), Case II transport (n=1), non-Fickian or anomalous (0.5< n< 1) and super Case II (n>1).

Agnihotri and Aminabhavi [123] have analyzed the dynamic swelling data of chitosan microparticles using Eq. (1) to predict drug release from the water uptake data of the microparticles cross-linked with (5.0, 7.5 and 10.0)*10^{-4} mL of glutaraldehyde/mg of chitosan. It was observed that as the cross-linking increases, swelling of chitosan microparticles decreases. Values of n obtained in the range of 0.160 to 0.249 indicating that the release mechanism deviates from the Fickian trend. The values of n are < 0.5 due to the irregular shaped particles and these decrease systematically with increasing cross-linking. In the swelling controlled release systems, drug is dispersed within a glassy polymer. Upon contact with biological fluid, the polymer swells, but no drug diffusion occurs through the polymer phase. As the penetrant enters the glassy polymer, glass transition temperature of the polymer is lowered due to relaxation of the polymer chains. Drug could diffuse out of the swollen rubbery polymer. This type of system is characterized by two moving boundaries: the front separating the swollen rubbery portion and the glassy region, which moves with a front velocity and the polymer fluid interface. The rate of drug release is controlled by the velocity and position of the front dividing the glassy and rubbery portions of the polymer. Jameela *et al*. [132] have obtained a good correlation fit for the cumulative drug released *vs.* square root of time, demonstrating that the release from the microsphere matrix is diffusion-controlled and obeys Higuchi equation [127]. It was demonstrated that the rate of release depends upon the size of microspheres. Release from smaller size microspheres was faster than those from the large size microspheres due to smaller diffusional path length for the drug and the larger surface area of contact of smaller particles with the dissolution medium.

1.4.2 Chitosan hydrogels

Chitosan hydrogels have been prepared with a variety of approaches. In each preparation chitosan is either physically associated or chemically cross-linked to form the

hydrogel. Our discussion below will focus on these two distinct hydrogel engineering approaches.

1.4.2.1 Physical association networks

In order to satisfy the requisite features of a hydrogel, the chitosan polymer network must satisfy two conditions: (1) inter-chain interactions must be strong enough to form semi-permanent junction points in the molecular network, and (2) the network should promote the access and residence of water molecules inside the polymer network. Gels that meet these demands may be prepared by non-covalent strategies that capitalize on electrostatic, hydrophobic, and hydrogen bonding forces between polymer chains [133,134]. *Figure 9* shows the schematics of four major physical interactions (i.e. ionic, polyelectrolyte, interpolymer complex, and hydrophobic associations) that lead to the gelation of a chitosan solution.

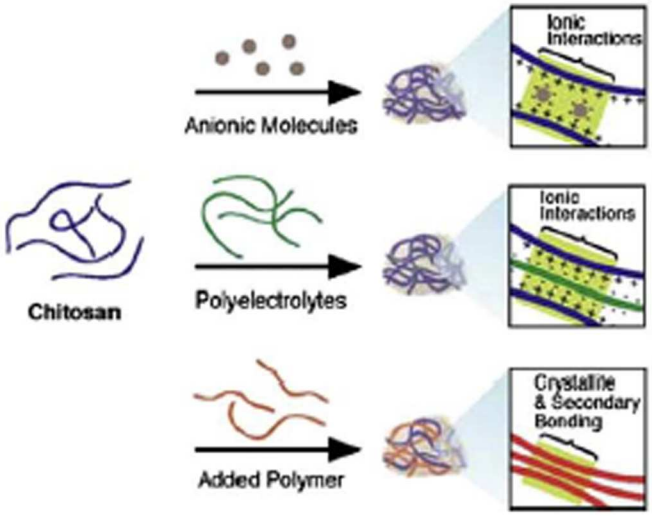

Figure 9. *Schematic representation of chitosan based hydrogel networks derived from different physical associations: (a) networks of chitosan formed with ionic molecules, polyelectrolyte polymer and neutral polymers*

Because the network formation by all of these interactions is purely physical, gel formation can be reversed. Tunable gel swelling behavior can be readily achieved in a physical gel by adjusting the concentration and nature of the second component used during the fabrication process. A chitosan-based physical gel can often be obtained by simply mixing the components that make up the gel under the appropriate conditions. These gels have a short

life time in physiological media, ranging from a few days to a month. Therefore, physical gels are good for short-term drug release applications. Because the gelation does not require any toxic covalent linker molecules, it is always safe for clinical applications. However, their widespread application is limited due to the weak mechanical strength and uncontrolled dissolution [135].

1.4.2.1.1 Ionic complexes

Thanks to the cationic amino groups of chitosan, ionic interactions can occur between chitosan and negatively charged molecules and anions. Ionic complexation of mixed charge systems can be formed between chitosan and small anionic molecules, such as sulfates, citrates, and phosphates [136,137] or anions of metals like Pt (II), Pd (II), and Mo (VI) [138,139]. These interactions can yield hydrogels with varying material properties that depend upon the charge density and size of the anionic agents, as well as the degree of deacetylation and concentration of the chitosan polymer.

Both anions and small molecules bind chitosan via its protonated amino groups, but metal ions form coordinate–covalent bonds with the polymer instead of electrostatic interactions [138,139]. Ionic complexation can be accompanied by other secondary interchain interactions including hydrogen bonding between chitosan's hydroxyl groups and the ionic molecules, or interactions between deacetylated chitosan chains after neutralization of their cationic charge [138,140]. These interactions can enhance the physical properties of the hydrogel, and can be modulated to express unique material properties, such as pH sensitivity.

1.4.2.1.2 Polyelectrolyte complexes (PEC's)

While polyelectrolytes form electrostatic interactions with chitosan, they are different from the ions or ionic molecules used in ionic complexation in that they are larger molecules with a broad molecular weight range, such as polysaccharides, proteins and synthetic polymers. The associations between the chitosan polymer and polyelectrolytes are stronger than other secondary binding interactions like hydrogen bonding or van der Waals interactions. The advantages of this type of complex are significant. They are complexed without the use of organic precursors, catalysts, or reactive agents, alleviating the concern

about safety in the body or cross-reactions with a therapeutic payload. In addition, because PEC's consist of only chitosan and the polyelectrolyte, their complexation is straightforward and reversible. Chitosan-based PEC networks have been produced by anionic macromolecules like DNA, anionic polysaccharides (e.g. alginate, GAGs (chondroitin sulfate, hyaluronic acid, or heparin), carboxymethyl cellulose, pectin, dextran sulfate, xanthan, etc.), proteins (e.g. gelatin, albumin, fibroin, keratin, and collagen) and anionic synthetic polymers (e.g. polyacrylic acid). The stability of these compounds is dependent on charge density, solvent, ionic strength, pH, and temperature [141,142]. The choice of the anionic molecule for PEC formation is highly dependent upon its charge under physiological conditions because the pH of the hydrogel environment modulates ionic interactions and, subsequently, PEC hydrogel properties. If the electrostatic interactions of the polymer are strong enough, the physical associations between the polymers at physiological pH can be maintained.

1.4.2.1.3 Physical mixtures and secondary bonding

In addition to the specific physical interactions described, hydrogels can be formed by polymer blends between chitosan and other water-soluble nonionic polymers, such as Poly(vinly alcohol) (PVA). These polymer mixtures form junction points in the form of crystallites and interpolymer complexation after lyophilization or after a series of freeze–thaw cycles [133,143]. The chain–chain interactions act as crosslinking sites of the hydrogel. In the case of chitosan–PVA polymer blends, increasing the chitosan content negatively affects the formation of PVA crystallites, leading to the formation of hydrogels with less ordered structures. Recently, a new hydrogel consisting of a polymer blend of chitosan and polyethylenimine (PEI) was prepared [144]. PEI is a polycationic material that has been extensively used as a gene transfection agent [145]. By mixing the polymer with chitosan, a 3D hydrogel was formed within 5 min that was stable under cell culture conditions and could support the growth of primary human fetal skeletal cells. Ladet *et al*. demonstrated the preparation of a hydrogel using a hydro-alcohol method of gel formation that relied upon the neutralization of chitosan's amino groups using a sodium hydroxide solution [146]. This prevented ionic repulsion between the polymer chains, allowing for the formation of hydrogen bonds, hydrophobic interactions, and chitosan crystallites. Using this technique, hydrogels on the order of cubic centimeters could be prepared. Macroscopic shrinkage of the hydrogel during neutralization and gel depletion with the increase in the concentration of neutralizing agent was observed (*figure 10*). Interestingly, an interrupted gelation method

was used that led to the preparation of multilayered, "onion-like" hydrogels (*figure 10*), which could be used to encapsulate drugs for the co-delivery of multiple therapeutics or pulse-like delivery of a given payload [147,148].

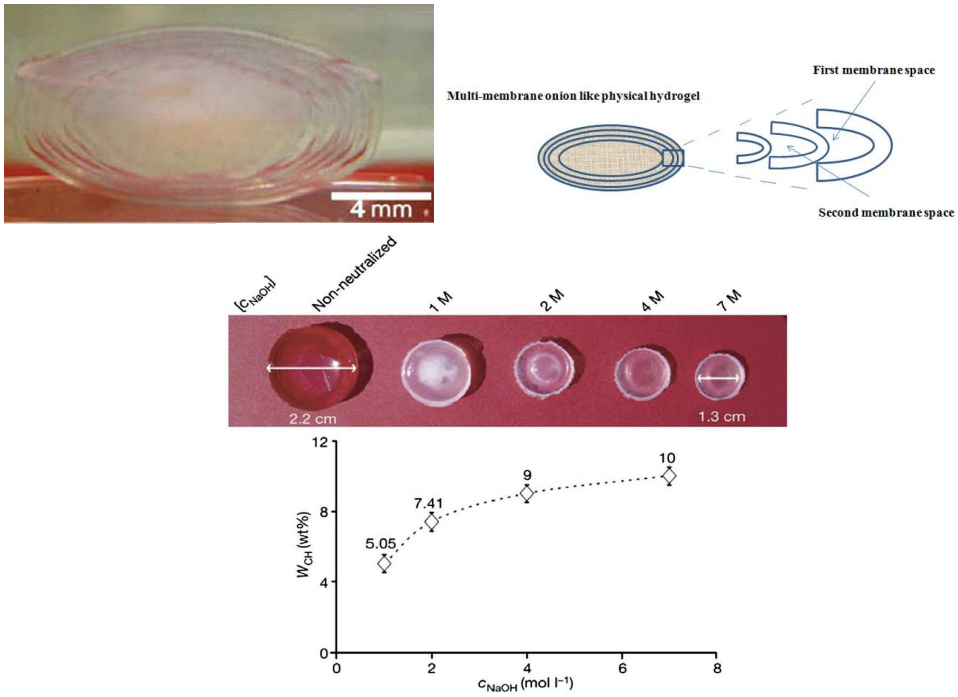

Figure 10. *(a) multimembrane biomaterial with 'onion-like' structure based on chitosan hydrogel. (b) Schematic diagram of the multi-membrane onion-like structures; (c) Variation of hydrogel shrinkage during neutralization as a function of the concentration of sodium hydroxide. The initial polymer concentration in the non-neutralized alcohol gel is constant and close to 4.5wt.% in each case. (d) Evolution of the chitosan mass fraction in the gel (WCH) at different steps of the hydrogel neutralization as a function of the NaOH concentration in the neutralization bath. [146].*

1.4.2.1.4 Thermoreversible hydrogels and hydrophobic associations

Researchers have engineered a class of hydrogel systems called thermoreversible gels that form transient gel or liquid states depending upon the environmental temperature. These polymers take advantage of hydrophobic interactions or secondary bonding to form junctions between chains that yield a semi-rigid gel from a flowable liquid solution. Specifically, when system temperatures pass a lower critical solution temperature (LCST), the material undergoes a hydrophilic– hydrophobic transition. The importance of a polymer

solution that has a low viscosity at room temperature, but forms a gel above a LCST is significant for its use in biomedical applications. These materials can be injected into the body as a liquid, forming a gel in situ where the body temperature is above the LCST, offering the potential to serve as carrier matrices for a wide range of biomedical and pharmaceutical applications [149,150]. These injectable, gelling systems can be introduced into the body without the need for invasive surgeries, and deliver the bioactive agents to a defect site without significant negative effects (local heating, use of organic solvents, formation of toxic byproducts, etc.). Hydrogels prepared by aggregation of chitosan-based co-polymers or by neutralization with polyol salts show promising thermoreversible gelation properties in aqueous media [151–155]. One such engineering strategy used the temperature-sensitive behavior of a physical mixture of glycerol phosphate disodium salt (GP) and chitosan. The phosphates of the GP salt are believed to neutralize the ammonium groups of chitosan, allowing increased hydrophobic and hydrogen bonding between the chitosan chains at elevated temperatures. The mixture remains a clear liquid at room temperature and gels at 37 °C [155]. The chitosan/GP gel showed promise as a biotherapeutic system capable of delivering a bioactive bone protein (an osteogenic mixture of TGF β family members), and as a cell matrix whereby chondrocytes were implanted in vivo and showed normal cartilage formation over 3 weeks.

1.4.2.2 Crosslinked networks

While physically bonded hydrogels have the advantage of gel formation without the use of cross-linking entities, they have limitations. It is also difficult to precisely control the physical gel pore size, chemical functionalization, and degradation or dissolution, leading to inconsistent performance in vivo. Alternatively, robust chitosan hydrogels can be produced using irreversible networks. Polymeric chains of these hydrogels are covalently bonded together either by using small cross-linker molecules, secondary polymerizations, or irradiation chemistry. Most of these linker molecules react with the primary amines of chitosan and form irreversible inter- or intramolecular bridges among the chitosan chains. Covalently cross-linked hydrogels are also obtained by attaching photo-reactive or enzyme-sensitive molecules on the chitosan, followed by their subsequent exposure to UV or sensitive enzymes, respectively. The properties of cross-linked hydrogels depend mainly on their crosslinking density and the ratio of moles of cross-linker molecules to the moles of polymer repeating units [156]. The following sections describe the different ways of making irreversible chitosan hydrogels.

1.4.2.2.1 Chemical crosslinking

Chemical cross-linking is a straight forward method to produce permanent hydrogel networks using covalent bonding between polymer chains. Cross-linked chitosan networks can be prepared using the available –NH2 and –OH chemical handles and cross-linkers that can form a number of linkage chemistries, including amine carboxylic acid bonding and Schiff base formation [157-159]. Specifically, these networks can be formed by using small molecule cross-linkers, polymer–polymer reactions between activated functional groups, as well as photosensitive agents or enzyme-catalyzed reactions.

The new cross-linking agent, genipin, is a naturally derived chemical from the gardenia that has been shown to be one such biocompatible cross-linking agent [160]. Genipin has been reported to bind biological tissues [161] and biopolymers, such as chitosan and gelatin, leading to covalent coupling. It works as an effective cross-linking agent for polymers containing amino groups and is much less cytotoxic than glutaraldehyde [162]. In addition, genipin cross-linked chitosan membranes exhibit a slower degradation rate than their glutaraldehyde crosslinked counterpart [163]. Use of genipin also showed extended drug release by chitosan hydrogels cross-linked in situ [152,164]. Even though genipin shows good biocompatibility, it is still liable to negatively interact with encapsulated drugs, an unavoidable problem for gelation in the presence of a therapeutic [165]. A thermo-sensitive, chitosan-pluronic hydrogel was also produced by UV photo-cross-linking [166]. The chitosan and pluronic groups were functionalized with photosensitive acrylate groups that were cross-linked by UV exposure. The resultant polymers could then form a physical network at temperatures above the LCST. The hydrogel showed the sustained release of encapsulated human growth hormone (hGH) and plasmid DNA, demonstrating its potential application for different types of drugs [166,167].

1.4.2.2.2 Interpenetrating networks (IPN's)

Entangled polymer networks can be further strengthened by interlacing secondary polymers within the cross-linked networks. Here, a cross-linked chitosan network is allowed to swell in an aqueous solution of polymer monomers. These monomers are then polymerized, forming a physically entangled polymer mesh called an interpenetrating network. There are also semi-IPNs where only one of the polymer networks is cross-linked, while the second polymer remains in its linear state. If the second polymer is also cross-

linked, a full-IPN is formed. There are several chitosan-based semi-IPNs (prepared with polyether [168,169], silk [170], PEO[171], and PVP [172] and full-IPNs (prepared with PNIPAM [173]). This technique allows for the specific selection of polymers that can complement the deficiencies of one another. For instance, a hydrophilic polymer can be chosen to enhance the structural characteristics of the hydrogel, while a biocompatible polymer may limit the immunological response. Although the cross-linking density, hydrogel porosity, and gel stiffness can be adjusted in IPN-based hydrogels according to the target application, they have difficulty encapsulating a wide variety of therapeutic agents, especially sensitive biomolecules. In addition, IPN preparation requires the use of toxic agents to initiate or catalyze the polymerization or to catalyze the cross-linking. Complete removal of these materials from the hydrogel is challenging, making the clinical application problematic.

1.4.2.3 Drug loading in chitosan hydrogels

The drug loading in a hydrogel depends upon both the physical and chemical properties of the gel as well as the therapeutic itself. In fact, the choice of hydrogel materials, network conformation, and drug loading mechanism must be made to complement the properties of the drug (e.g. hydrophobilicity, charge) and its mechanism of action (sustained drug release versus rapid, high exposure). Three major approaches to drug loading can be summarized as : diffusion, entrapment, and tethering [174-178]. Each method bears specific advantages and disadvantages and should be selected after taking into consideration the hydrogel network used as well as the nature of the drug. The easiest drug loading method is to place the fully formed hydrogel into medium saturated with the therapeutic [179,180]. Depending upon the porosity of the hydrogel, the size of the drug, and the chemical properties of each, the drug will slowly diffuse into the gel. When placed in vivo, the drug will then freely diffuse back out of the hydrogel into the neighboring tissue. This approach is effective for loading small molecules, but larger therapeutics peptides and proteins in particular are not readily able to migrate through the small pores of the hydrogel [165]. In addition, this drug loading process can take long time. In the case of larger drugs and bioligands, the payload must be entrapped during the gelation process. Here, the drug is mixed with the polymer solution, and the cross-linking or complexation agent is added. It is important to consider the chemistry of the drug molecule to prevent unwanted cross-linking or deactivation of the therapeutic during gelation. Both diffusion and entrapment allow for free movement of the therapeutic out of the hydrogel network. This can lead to an initial

burst release after implantation of the hydrogel in vivo due to the concentration gradient formed between the gel and the surrounding environment. In order to limit the loss of the therapeutic reserve (and the risk of toxic exposure), drugs can be covalently or physically linked to the polymer chains prior to gelation. This tethering method limits tissue exposure to the agent to only when the hydrogel breaks down or the molecular tether is broken [181]. Linkages between the drug and polymer that are susceptible to environmental enzymes have been used to control the speed and timing of release. Drug loading is also complicated by molecules that have the opposite hydrophilicity or the same charge as the constituent polymer. For instance, hydrophobic molecules like paclitaxel must be complexed with amphiphilic additives before the hydrogel and payload will blend in solution [183, 184]. This has been accomplished by binding the drug to albumin (Abraxane) or by mixing it in an aqueous citric acid/glyceryl monooleate solution prior to hydrogel loading [184]. Therapeutics have also been loaded into small secondary release vehicles (e.g. microparticles, microgels, liposomes, and micelles) prior to hydrogel encapsulation [185, 186].

1.4.2.4 Drug release from chitosan hydrogels

Release of loaded therapeutics from a hydrogel can occur by one of three different modes: diffusion, chemical/environmental stimulation, and enzyme-specific stimulation [187]. Diffusion is regulated by movement through the polymer matrix or by bulk erosion of the hydrogel as it breaks down in vivo. Environmentally responsive hydrogels are gels that swell in response to external cues like pH and temperature and effectively open their pores for enhanced diffusion of the entrapped therapeutic under predetermined conditions[165]. This type of controlled release can be used to limit drug release outside of the effective range of the diseased tissue. Environmental cues are specific to limited regions within the body, but better specificity has also been widely investigated with new release mechanisms that release a drug payload only when triggered by local enzymatic cues. These biochemically stimulated responses occur by tethering drugs to the hydrogel via labile domains that are susceptible to matrix remodeling enzymes or using polymers that are targeted by enzymes [188]. This method has received the least amount of attention, but offers selective, sustained release mechanisms that are beginning to receive attention from chitosan hydrogel engineers.

1.5. Applications

1.5.1 Chitosan for Tissue Engineering Applications

Tissue engineering is an interdisciplinary field that applies the principles and methods of engineering and the life sciences toward the fundamental understanding of structural and functional relationships in normal and pathological tissue and the development of biological substitutes to restore, maintain, or improve function [189]. It involves the *in vitro* seeding and growing of relevant cells onto a scaffold. The scaffold therefore is a very important component for tissue engineering. Several requirements have been identified as crucial for the production of tissue engineering scaffolds: 1) the scaffold should possess interconnecting pores of appropriate scale to favor tissue integration and vascularization, 2) be made from material with controlled biodegradability or bioresorbability so that tissue will eventually replace the scaffold, 3) have appropriate surface chemistry to favor cellular attachment, differentiation and proliferation, 4) possess adequate mechanical properties to match the intended site of implantation and handling, 5) should not induce any adverse response and, 6) be easily fabricated into a variety of shapes and sizes [190]. The versatility of chitosan offer a wide range of applications since they are biodegradable, non-toxic and can be formulated in a variety of forms including powders, gels and films for applications. They can also provide controlled release of growth factors and extracellular matrix components. To improve the adherent ability for seeding cells, chitosan allow for a wide range of molecules to be modified. With these promising features, they are considered as a very interesting biomaterial for use in cell transplantation and tissue regeneration. This technology has been used to create various tissue analogs including cartilage, bone, liver, and nerve in the past decades.

1.5.1.1 Chitosan in bone tissue engineering

Chitosan has been extensively used in bone tissue engineering since it was shown to promote growth and mineral rich matrix deposition by osteoblasts in culture [191]. Also chitosan is biocompatible (minimizes additional local inflammation), biodegradable, and can be molded into porous structures (allows osteoconduction) [192]. Several studies have focused on the use of chitosan–calcium phosphate (CP) composites for this purpose [193,194]. A 3D macroporous CP bioceramic embedded with porous chitosan sponges is developed by Zang *et al*. [195]. In this scaffold, a nested chitosan sponge enhanced the

mechanical strength of the ceramic phase via matrix reinforcement and preserved the osteoblast phenotype [196]. Macroporous chitosan scaffolds incorporating hydroxyapatite (HA) or CP glass with an interconnected porosity of approximately 100 mm have been synthesized [196]. Overall composites of chitosan–CP appear to have a promising clinical application in the future [197]. The issue of mechanical resistance of chitosan-based composites was addressed by Hu *et al*. [198], who reported a chitosan–HA multilayer nanocomposite with high strength and bending modulus rendering the material suitable for possible application for internal fixation of long bone fractures. A macroporous chitosan-gel/b-TCP composite scaffold for bone tissue engineering using freeze-drying process was developed [199]. This study investigated the effects of concentration of composite suspension and the freezing temperature on the ability to resist compression by the scaffold [200]. Chitosan was used as an adjuvant with bone cements to increase their injectability while keeping the chemico-physical properties suitable for surgical use (e.g. setting time and mechanical properties). The rationale of using chitosan for this purpose is based on the property that chitosan solutions gel in response to a pH change from slightly acidic to physiological; in fact, the chitosan–CP composites address the need to develop bone fillers that set in response to physiological conditions, but not while mixing the components in vitro. Likewise, when chitosan is added to calcium phosphate cements (CPC), octocalcium phosphate is obtained; a material that is shown to improve injectability and strength [200]. Many of these chitosan gel composites are proposed mainly for non load bearing bony defects [201]. Xu *et al*. studied the feasibility of creating macropores in CPC using chitosan and/or absorbable mesh. A synergistic effect of adding chitosan and bioabsorbable mesh to CPC was seen. This injectable, bioabsorbable composite material possessed interconnected macropores (osteoconductive) and provided strength to the implant during tissue regeneration [202]. The intramolecular hydrogen bonds of chitosan provide interacting macromolecules with a good resistance to heat. Zhao *et al*. used phase separation technique to fabricate biomimetic HA/chitosan–gelatin network composites in the form of 3D-porous scaffolds and they showed improved adhesion, proliferation and expression of rat calvaria osteoblasts on these highly porous scaffolds [203]. Kim *et al*. showed the application of this property through composites of chitosan with poly methyl-methacrylate (PMMA). This specially developed composite material exhibited lower exothermic curing temperatures and possessed higher inter-connected porosity with a pore size suitable for osteoconduction with better anchorage to the surrounding bone. It was observed that the pore size of this composite material increased with time due to biodegradation of the chitosan [204]. Also, chitosan has

been used to modify the surface properties of prosthetic materials for the attachment of osteoblasts [205, 206].

In another recent work by Zhao *et al.*, scaffold with calcium phosphate cement (CPC) and chitosan fibres were prepared and studies. It was found that human umbilical cord mesenchymal stem cells (hUCMSCs) can be harvested without an invasive procedure required for the commonly studied bone marrow mesenchymal cells (MSCs). The objectives of this study were to develop CPC scaffolds with improved resistance to fatigue and fracture, and to investigate hUCMSC delivery for bone tissue engineering. In fast fracture, CPC with 15% chitosan and 20% polyglactin fibers (CPC–chitosan–fiber scaffold) had flexural strength of 26 MPa, higher than 10 MPa for CPC control ($p < 0.05$). In cyclic loading, CPC–chitosan–fiber specimens that survived $2 * 10^6$ cycles had the maximum stress of 10 MPa, compared to 5 MPa of CPC control. CPC–chitosan–fiber specimens that failed after multiple cycles had a mean stress-to-failure of 9 MPa, compared to 5.8 MPa for CPC control ($p < 0.05$).

1.5.1.2 Chitosan in cartilage tissue engineering

In cartilage repair, the choice of biomaterial is very critical for the success of tissue engineering approaches [208]. The ideal cell-carrier substance should mimic the natural environment in the articular cartilage matrix. It has been shown that cartilage-specific extracellular matrix (ECM) components such as type II collagen and GAGs play a critical role in regulating expression of the chondrocytic phenotype and in supporting chondrogenesis in vitro as well as in vivo [209,210]. Three-dimensional (3D) scaffolds are essential for the development of engineered articular cartilage. Ideal scaffolds are designed to be biocompatible, bioabsorbable and exhibit predictable porosity and degradation rate. They provide a framework that facilitates new tissue in growth; moreover, mechanical characteristics are matched to those of the native tissue increasing the chances that the reparative process will be compatible with the host's tissue physiology [211,212]. Chitosan has been used as a scaffolding material in articular cartilage engineering [213,214], due to its structural similarity with various GAGs found in articular cartilage. This is of high importance because GAGs are considered to play a pivotal role in modulating chondrocyte morphology, differentiation, and function. Iwasaki *et al.* [215] reported an alginate-based chitosan hybrid polymer fibers which showed increased cell attachment and proliferation in vitro compared to alginate. These hybrid polymer fibers showed increased tensile strength, implying a possible use in developing a 3D load bearing scaffold for cartilage regeneration

[215]. Chondrocytes cultured on chitosan substrates in vitro maintained round morphology and preserved synthesis of cell -specific ECM molecules [216,214].

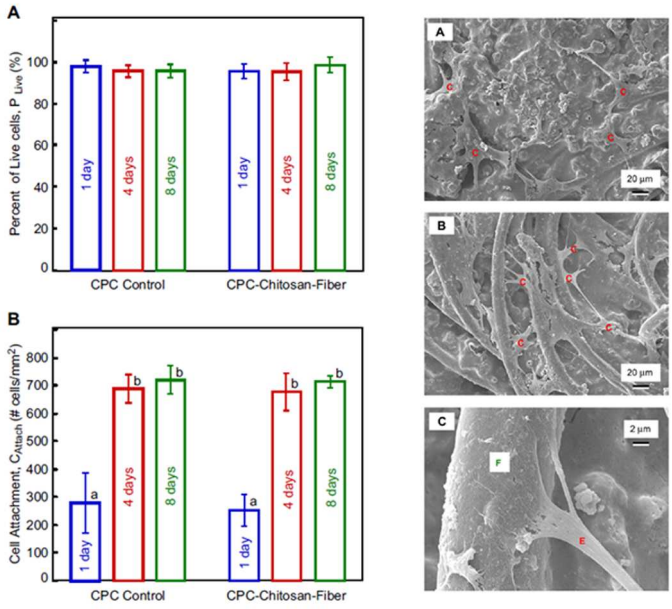

(1) (2)

Figure 11. *(1) hUCMSCs were cultured on CPC control and CPC–chitosan–fiber for 1, 4, and 8 days: (A) Percent of live cells, and (B) live cell attachment (mean _ sd; n ¼ 5). P_{Live} reached 96–99%, not different from each other ($p > 0.1$). C_{Attach} was less than 300 cells/mm^2 at day 1; it more than doubled to 700 cells/mm2 at day 4, due to hUCMSC proliferation. In (B), dissimilar letters indicate values that are significantly different ($p < 0.05$).(2) SEM of hUCMSC attachment on: (A) CPC control, and (B) CPC–chitosan–fiber scaffold. Cells are designated as ''C'', which anchored to CPC in (A), and to the fibers in the scaffold in (B). Cells developed long, cytoplasmic extensions ''E'', shown in (C) at a higher magnification, attaching firmly to the fiber in the CPC–chitosan–fiber scaffold [207].*

Chitosan was used to improve chondrocyte attachment to PLLA films; the modified substrate showed increased cell adhesion, proliferation and biosynthetic activity [217]. chitosan was also conjugated with hyaluronan to obtain a biomimetic matrix for chondrocytes. Chondrocyte adhesion, proliferation, and the synthesis of aggrecan and type II collagen were significantly higher on the hybrid fiber than on chitosan [218]. Similarly, to increase the cellular adhesiveness of chitosan, Hsu *et al*. have developed chitosan–alginate–hyaluronan complexes with or without covalent attachment with RGD containing protein. Cell-seeded scaffolds showed neocartilage formation in vitro. When chondrocyte seeded scaffolds were implanted into rabbit knee cartilage defects, partial repair was observed after

1 month both in presence or absence of RGD indicating potential of this composite material for cartilage regeneration [219].

Chitosan-based scaffolds can deliver growth factors in a controlled fashion to promote the in growth and biosynthetic ability of chondrocytes. Lee *et al*. [220] reported porous collagen/chitosan/GAG scaffolds loaded with TGF-b1. This scaffold exhibited controlled release of TG F-b1 and promoted cartilage regeneration. Moreover, addition of chitosan to the collagen scaffold was seen to improve mechanical properties [220] and stability of the collagen network by inhibiting the action of collagenases [221]. Kim *et al*. [222] used a porous freeze-dried chitosan scaffold incorporating TGF-b1-containing microspheres, for the treatment of cartilage defects. TGF-b1 was released in a sustained fashion, and promoted chondrocyte proliferation and matrix synthesis. In a similar trial, Lu *et al*. studied the effect of intraarticular injection of chitosan on regeneration of articular cartilage. An increase in epiphyseal cartilage in the tibial and femoral joints was seen with an activation of chondrocyte proliferation. Similarly, an intra-articular fibrous tissue was observed for the 6 weeks of the experiment, together with residual injected chitosan [223].

A noteworthy accomplishment was achieved by Buschmann *et al*. who showed that microfractured ovine defects are repaired with more hyaline cartilage when the defect is treated with in situ-solidified implants of chitosan–GP mixed with autologous whole blood, compared to microfracture alone in an ovine model at 6 months [224]. Since bleeding has been identified as an initiating event in post-surgical repair, they hypothesized that microfracture-based repair could be improved by stabilizing the clot formed in the lesion with chitosan that is thrombogenic and actively stimulates the wound repair process. Furthermore, these chitosan– GP/blood clots are adhesive and contract much less than whole blood clots, thereby maintaining a voluminous scaffold [224]. Chitosan–GP/blood implants were applied to marrow-stimulated chondral defects in rabbit cartilage repair models [225], where they induced greater fill of chondral defects with repair tissue compared to marrow-stimulation alone [224] and, in addition, produced a more cellular and hyaline repair cartilage well integrated with a porous subchondral bone structure [224-226]

In a recent work by Haoya *et al*.[227] chitosan hydrogel in the form of a scaffold was prepared for chondrocytes that would act to reconstruct tissue-engineered cartilage and repair articular cartilage defects in the sheep model. In this study, temperature-responsive chitosan hydrogels were prepared by combining chitosan, b-sodium glycerophosphate (GP) and hydroxyethyl cellulose (HEC). Tissue-engineered cartilage reconstructions were made in vitro by mixing sheep chondrocytes with a chitosan hydrogel. Cell survival and matrix accumulation were analyzed after 3 weeks in culture *(figure 12(a))*. To collect data for in

vivo repair, reconstructions cultured for 1 day were transplanted to the freshly prepared defects of the articular cartilage of sheep. Then at both 12 and 24 weeks after transplantation, the grafts were extracted and analyzed histologically and immune-histochemically. The results showed that the chondrocytes in the reconstructed cartilage survived and retained their ability to secrete matrix when cultured in vitro. Transplanted in vivo, the reconstructions repaired cartilage defects completely within 24 weeks*(figure 12(b))*. The implantation of chitosan hydrogels without chondrocytes also helps to repair cartilage defects. The chitosan-based hydrogel could support matrix accumulation of chondrocytes and could repair sheep cartilage defects in 24 weeks. This study showcased the success of a new technique in its ability to repair articular cartilage defects.

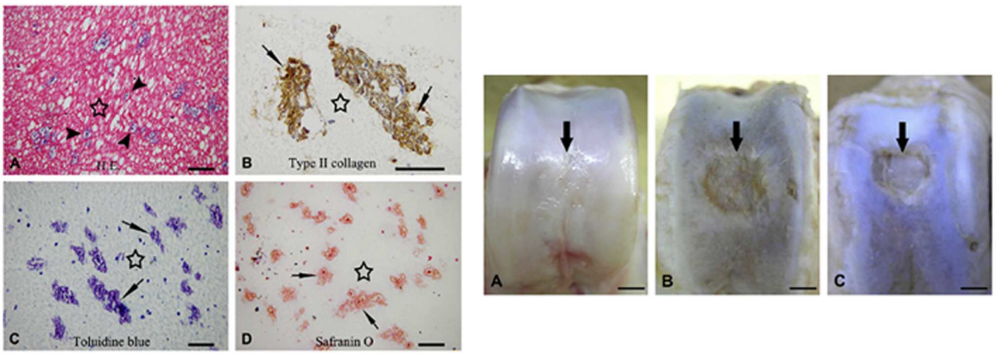

(a) (b)

Figure. 12.*(a) Accumulation of matrix in the tissue-engineered cartilage. Histology and immunohistochemistry of chondrocytes cultured in chitosan hydrogels 3 weeks. The results showed that the chondrocytes in the chitosan hydrogels accumulated pericellular sulfated GAG-containing matrix. A, H.E. staining; B, Type II collagen immunohistochemical staining; C, Toluidine blue staining; D, Safranin O staining. Star: chitosan hydrogel; Arrowhead: cell nucleus; Arrow: matrix of the chondrocytes. Bar = 100 µm. (b) Gross observation of the articular cartilage repair at 24 weeks post-operation. A, the defect part of the cartilage in the experimentalgroup was covered by the smooth, consistent, glistening white hyaline tissue nearly indistinguishable from the surrounding normal cartilage. No clear signs of margin with normal cartilage could be spotted on the surface of the regenerated areas; B, The defects in control group 1 were partially repaired with fiber-like tissue, leaving a small depression in the defect areas; C, The defects in control group 2 detected a thin and irregular surface tissue, with obvious defects and cracks surrounding the normal cartilage. Arrow: the defect; Bar =0.5 cm[227]*

1.5.1.3 Chitosan in liver tissue engineering

Insufficient donor organs for orthotopic liver transplantation worldwide have urgently increased the requirement for new therapies for acute and chronic liver disease [228]. Bioartificial liver (BAL) is a promising application of tissue engineering for the treatment of fulminant hepatic failure (FHF). One of the important issues for BAL devices is the proper choice of cell sources, such as primary hepatocytes, hepatic cell lines, and liver stem cells. The primary hepatocyte of these cells represents the most direct approach to BAL devices. BAL devices require a suitable ECM for hepatocyte culture because hepatocytes are anchorage dependent cells and are highly sensitive to the ECM milieu for the maintenance of their viability and differentiated functions [229-231]. Chitosan as a promising biomaterial can be applied in liver tissue engineering due to its various properties. One of the reasons for selecting chitosan as a scaffold for hepatocytes culture is that its structure is similar to GAGs, which are components of the liver ECM prepared chitosan/ collagen matrix (CCM) by cross-linking agent EDC in NHS buffer system[232-235]. The EDC cross-linked CCM showed moderate mechanical strength, good hepatocyte compatibility as well as excellent blood compatibility. On the other hand, implantable bioartificial liver (IBL) can restore, maintain or improve liver functions or offer the possibility of permanent liver replacement. Unlike the general approach for bioartificial skin, bone and cartilage, development of IBL has extreme difficulties. Appropriate design of the complex architecture, as well as the anti-thrombogenic extracellular component, are necessary for developing this blood-contacting device, because thrombus formation can lead to occlusion and decrease membrane efficiency [236]. Wang et al. showed a superior blood compatibility through chitosan/collagen / heparin matrix in implantable bioartificial liver (IBL) applications [237].

Another strategy in liver tissue engineering focuses on the ability of highly concentrated, multivalent galactose residues to bind to the asialoglycoprotein receptor (ASGPR) expressed on the surface of hepatocytes. Typical cell–matrix interaction is mediated by adhesion receptor such as integrin which specifically binds RGD sequence [238]. The ASGPR was the first reported mammalian lectin, or carbohydrate-binding protein. It was discovered in the mid-1960s by Ashwell *et al*. in their studies of the metabolism of plasma glycoproteins in mammals [239-240]. Since then, hepatic ASGPR has been a classical system for studying receptor-mediated endocytosis. Chung *et al*. suggested a potential ability to improve hepatocyte attachment to alginate (AL)/GC scaffolds for short-term culture[241]. In study by Kim & Seo, they further showed enhanced hepatocyte functions in AL/GC scaffolds for long periods. That is, hepatocyte cultured in AL/GC

scaffolds could enhance the functions through its spheroid formation (*figure 13*) in co-culture condition with fibroblast [228]. Li *et al*. conjugated fructose onto the porous chitosan scaffold by the reaction between amino and aldehyde group. Fructose is also known as a specific ligand of ASGPR in hepatocyte. They showed that the chitosan surface modified with fructose induced the formation of cellular aggregates with enhancing liver specific metabolic activities and cell density to a satisfactory level [233-234].

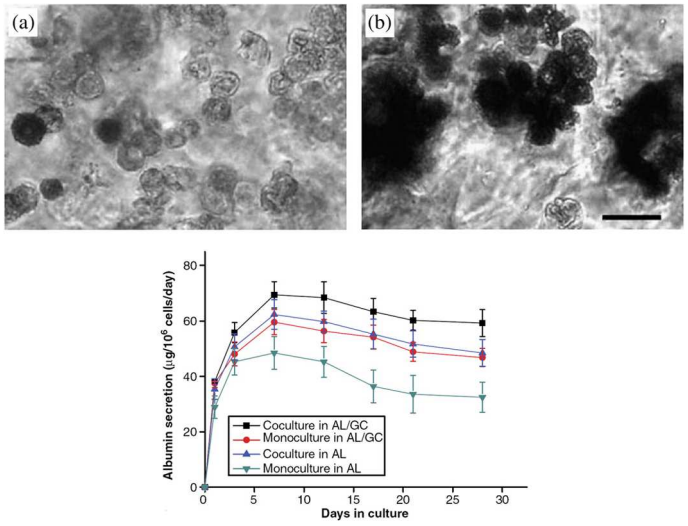

Figure 13. *Phase-contrast micrographs of hepatocytes within the AL (A) and AL/GC (B) scaffold stained with MTT and comparisons of liver-specific albumin secretion function [228].*

4.1.1.3 Chitosan in nerve tissue engineering

More than any other form of trauma, nerve injuries complicate successful rehabilitation since it is difficult for mature neurons (like many other cells in the body) to replicate, as they do not undergo cell division. Once the nervous system is impaired, its recovery is difficult and malfunction of other parts of the body occurs [242]. The repair of nerve lesions has been attempted in many different ways, which have in common the goal of directing the regenerating nerve fibers into the proper endoneurial tubes. The strategies developed for nerve repair can be classified into two categories: (1) bridging, which includes grafting and tubulization techniques, (2) end-to-end suturing of the nerve stumps. The former technique has been shown to be more effective, as it avoids tension across the repair site [243]. A wide variety of materials have been suggested for the production of artificial tubes for nerve repair, including biocompatible, non-degradable and degradable materials. A

variety of artificial tubes have been used to repair nerve injuries, but the artificial tubes do not have enough internal surface area for nerve fibers and Schwann cells (SCs) to cohere [236]. Thus, artificial tubes to bridge large defects in nerve repair should contain a biodegradable matrix, which can provide an optimal structural, cellular, and molecular framework for SCs and neurite migration across a nerve gap. Chitosan has been studied as a candidate material for nerve regeneration due to its properties such as antitumor, antibacterial activity, biodegradability and biocompatibility. Jianchun *et al*. reported that neurons cultured on the chitosan membrane can grow well and that chitosan tube can greatly promote the repair of the peripheral nervous system [244]. Yuan *et al*.[245] also showed that chitosan fibers supported the adhesion, migration and proliferation of SCs, which provide a similar guide for regenerating axons to Büngner bands in the nervous system. Matsuda *et al*. developed a new biomaterial for nerve regeneration through immobilization of laminin peptide in molecularly aligned chitosan by covalent bonding [246]. Chávez-Delgado *et al*. showed that progesterone delivered from chitosan prostheses provides better facial nerve regenerative response of the rabbits than chitosan prostheses without progesterone [247]. Mingyu *et al*. showed an improved attachment, differentiation and growth on the chitosan/ poly(L-lysine) composite materials when compared to cells cultured on chitosan membranes. The improved nerve cell affinity on the chitosan/poly(L-lysine) composite materials had been attributed to the increased hydrophilicity by the abundant hydroxyl group and the positive surface charge of chitosan [248]. Cheng *et al*. added gelatin to chitosan for preparation of soft and elastic complex that has good nerve cell affinity. The chitosan/gelatin composite film showed a lower modulus and a higher percentage of elongation at break compared with chitosan film. Also, PC12 cells cultured on the composite films differentiated more rapidly and extended longer neutites than on chitosan films [249]. Frier *et al*. also developed chitin hydrogel tubes which were fabricated from chitosan solutions using acylation chemistry and mold casting techniques for the preservation of the natural chemical composition of chitin, and no toxic crosslinking agent was necessary for the hydrogel preparation (*figure 14*). Chitin and chitosan support nerve cell adhesion and neurite outgrowth, making these materials potential candidates for scaffolds in neural tissue engineering [250].

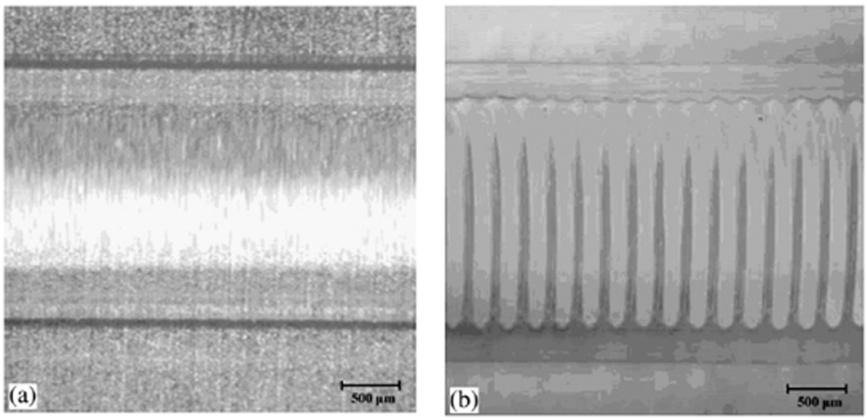

Figure 14. *Optical microscope longitudinal view of (a) a chitin hydrogel tube and (b) a chitin gel tube reinforced with a PLGA coils embeddedin the wall [250].*

1.5.2 Drug Delivery Applications

Drug delivery has been a very active area, especially for chitosan as a carrier for various active agents including drugs and biologics. Chitosan films are very commonly used for this purpose, a novel inorganic–organic pH-sensitive membrane based on an interpenetrating network utilizing inorganic silicate and organic chitosan was proposed by Park *et al.* for drug delivery [251]. The membrane was evaluated for its response to pH changes; the intended method of application. Percolation of lidocaine-HCl, sodium salicylate and 4-acetomidophenol into this membrane was studied and found to be sensitive to the external pH as well as the drugs' ionic interactions with chitosan. The membrane was proposed to also be sensitive to other stimuli such as temperature and light that may be alternative channels for drug loading. In a similar fashion, the in-situ light initiated polymerization of acrylic acid in the presence of chitosan was used to derive a novel mucoadhesive membrane [252]. The interactions between the two polymers were determined to be based on hydrogen bonding. The strong adhesive property of this membrane rendered it suitable for transmucosal drug delivery applications. The loading and release study of triamcinolone acetonide (TAA), a drug used to reduce inflammation in the treatment of mouth ulcers, was subsequently reported [252]. TAA was loaded into the chitosan–PAA membrane from solution. The drug loaded membrane was found to meet the requirements for a transmucosal drug delivery system with drug release a function of pH and the amount of drug loaded. Another method of generating membranes was the interaction of oxidized glucose dialdehyde with chitosan [254]. N-alkyl groups of varying chain lengths were used

to modify the hydrophobicity of these chitosan membranes. The longer the alkyl chain, the more hydrophobic the chitosan membrane becomes and that had bearing on the drug release rate. Using vitamin B2 as the drug model various parameters were studied, the permeation and diffusion of B2 decreased with increasing pH 8 and when the hydrophobicity of chitosan increased, i.e. as the alkyl chains increased in length. In vitro studies indicated no toxic effects for this membrane system. Another example of membrane methodology is the chitosan–gelatin drug containing films incorporating danshen, an herbal extract, without the need for crosslinking, for delivery in the abdominal cavity [255]. Again, Hu *et al*. [256] utilised the same in situ polymerization of acrylic acid in the presence of chitosan, to form nanoparticles. The yield of nanoparticles was found to be a function of the molecular weight of chitosan; the lower molecular weight, the better the yield of around 70%. A silk peptide was incorporated into the nanoparticles. The release of the silk peptide occurred as an initial burst followed by continued release for up to 10 days. The dependence of the release on pH was noted and the authors suggested the nanospheres were useful for drug release applications in the gastric cavity.

Cisplatin loaded chitosan microspheres were prepared using a w/o emulsion system [257]. Variables such as chitosan concentration, cisplatin, glutaraldehyde concentration, type of chitosan and oil were studied and found to have a significant effect on cisplatin entrapment in chitosan microspheres. Incorporation efficiency was found to be between 28 and 29%. The type of oil used was found to affect release properties of cisplatin, which showed an initial burst effect. Pharmacokinetics, targeting, embolization effects and alteration of liver function using cisplatin chitosan microspheres were studied after hepatic arterial embolization in dogs. Results showed a remarkable decrease in the number of arterioles in liver, necrosis of nodules and hepatic cell degeneration in the embolized region. Shiraishi *et al*. also prepared indomethacin loaded chitosan microspheres but by polyelectrolyte complexation of sodium tripolyphosphate and chitosan. A pH-dependent disintegration of the beads was observed in the in vitro study [258]. The plasma concentrations of indomethacin after oral administration of chitosan gel beads to beagle dogs exhibited a sustained-release pattern. Good correlation was observed between the molecular weight of chitosan and dissolution rate constant or the mean absorption time or area under the plasma concentration–time curve. Another study reported, the preparation of inomethacin loaded chitosan microspheres using only aqueous solvents [259]. The influence of formulation variables on indomethacin content in the microspheres and time for release of indomethacin from the microspheres was also investigated.

Hejazi and Amiji examined the gastric residence time of tetracycline loaded chitosan microspheres (prepared by ionic crosslinking and precipitation method) following their oral administration in gerbils [260]. Gastric retention studies were performed by administering radioiodinated [125I] chitosan microsphere suspension in the nonacid-suppressed and acid-suppressed states. At different time points, animals were sacrificed and the radioactivity in tissues and fluids was measured with a gamma counter. The results indicated that chitosan microspheres did not provide a longer residence time in the fasted gerbil stomach. The tetracycline concentration profile in the stomach following administration of microsphere formulation was similar to that of aqueous solution. Huang *et al*. [261] observed that betamethasone disodium phosphate-loaded microspheres demonstrated good drug stability (<1% hydrolysis product), high entrapment efficiency (95%) and positive surface charge (37.5 mV). The results also indicated that yield and size of particle was increased with increasing betamethasone amount but both zeta potential and tap density of the particles decreased with increasing betamethasone loaded amount. The in vitro release of betamethasone showed a dose-dependent burst followed by a slower release phase that was proportional to the drug concentration in the concentration range between 5 and 30% (w/w) [262].

Chitosan hydrogels coupled with BMP-7 have shown the ability to enhance lesion repair [263]. For instance, to enhance cartilage formation, chondroitin sulfate, a GAG molecule found in cartilage, has been immobilized in chitosan hydrogels [264]. Platelet derived growth factor has also been loaded into chitosan gels to enhance osteoinduction by release of the growth factor as the hydrogel degraded at the defect site [265,266]. Chitosan–alginate hydrogels loaded with BMP-2 and mesenchymal stem cells (MSCs) were shown to induce subcutaneous bone formation [267]. Chitosan– laminin nerve guides loaded with glial cell line-derived nerve growth factor (GDNF) enhanced both the functional and sensory nerve recovery by releasing GDNF in the early stage of implantation [268]. Treatment with some growth factors that have short therapeutic half-lives, such as endothelial growth factor, require frequent administration to maintain an effective concentration. Chitosan–albumin hydrogel microspheres have shown continuous release for over 3 weeks after subcutaneous implantation in rats, indicating possible success in vivo [269]. Azab *et al*. developed a chitosan-based hydrogel cross-linked with glutaraldehyde [270,271] and loaded with 131Inorcholesterol (131I-NC), and tested the hydrogel in a breast cancer xenograft mouse model. This hydrogel showed a reduction in the progression rate of the tumor, and prevented 69% of tumor recurrence and metastatic spread. Importantly, there was little or no systemic distribution of the radioisotope after hydrogel implantation.

Zeng *et al*. prepared chitosan-based nanocomplexes with various forms were prepared by ionically crosslinking with tripolyphosphate (TPP) in different acidic media under mild conditions. It was found that the self-assembly and ionic interactions of chitosan and TPP were greatly affected by reaction media, and chitosan-based nanofibers could be obtained in adipic acid medium while nanoparticles were formed in acetic acid medium *(figure 15(A))*. Using bovine serum albumin (BSA) as a macromolecular model-drug, in vitro drug release studies indicated that chitosan-based nanofibers and nanoparticles exhibited a similar prolonged release profile. In addition, the bioinspired mineralization of both chitosan-based nanofibers and nanoparticles was carried out by soaking them in synthetic body fluids (SBF). Transmission electron microscopy (TEM) *(figure 15(B))* and X-ray Diffraction (XRD) results indicated that chitosan-based nanofibers have better inductivity for nanohydroxyapatite formation than chitosan-based nanoparticles. The results suggested that biomimetic chitosan-based systems with controlled release capacity of bioactive factors may be of use in bone tissue engineering for enhancing the bioactivity and bone inductivity [272]. Recently, novel asymmetric chitosan membranes were developed for the guided tissue regeneration (GTR) by using the two-step phase separation in this study [273]. The bicontinuous structure on the top layer was formed due to the liquid–liquid demixing by non-solvent induction and the pore size was ranged from 0.5 to 2 µm. The interconnected cellular pores ranged from 80 to 120 µm on the bottom layer would be created by the formation of ice crystals. The membrane developed in this research possessed good biocompatibility, tissue integration, cell occlusivity and osteoconduction, which lasted for at least 3 months. The chitosan membrane also successfully prevented the proliferation of bacterial, which was significantly superior to all the commercial GTR products for now. The asymmetric structure would be appropriate for the release of complex drugs with different effective periods. The results showed that the asymmetric chitosan GTR membranes prepared in this study are promising for the treatment of periodontal diseases.

In another study by Saber *et al*. [274] was investigated the feasibility of using chitosan to deliver drugs to the inner ear across the round window membrane (RWM). Three structurally different chitosans loaded with a tracer drug, neomycin, were injected into the middle ear cavity of albino guinea pigs (n = 35). After 7 days the effect of chitosans and neomycin was compared among the treatment groups. The hearing organ was analysed for hair cell loss and the RWM evaluated in term of thickness. All tested chitosan formulations successfully released the loaded neomycin, which then diffused across the RWM, and exerted ototoxic effect on the cochlear hair cells in a degree depending on the concentrations

used. Chitosans had no noxious effect on the cochlear hair cells. It is concluded that chitosan, is safe and effective carriers for inner ear therapy.

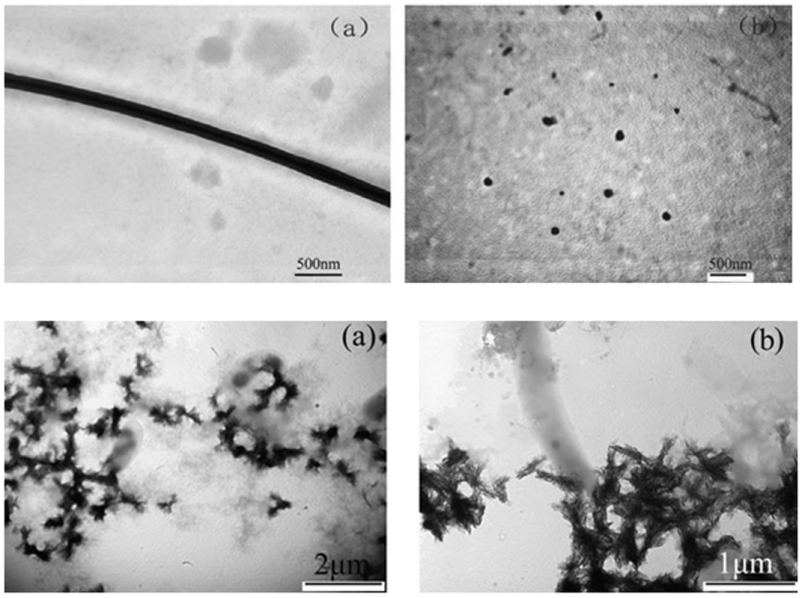

Figure 15.*(A) TEM images of Chitosan-TPP nanocomplexes formed by ionically crosslinking in (a) adipic acid medium and (b) acetic acid medium.(B) TEM photos of (a) chitosan-TPP nanoparticles and (b) chitosan-TPP nanofibers after soaking in SBF at 37.0 ±0.5_C for 7 days[272].*

Several studies of chitosan particles or polyelectrolytes complexes for nasal delivery of therapeutic proteins have been done [275-278]. It has been shown that insulin-loaded chitosan nanoparticles enhanced nasal absorption of proteins to a greater extent than chitosan solutions [275, 278]. Powder formulations of protein-loaded chitosan nanoparticles suitable for pulmonary delivery were prepared by spray drying [279-281]. Insulin-loaded nanoparticles were obtained by ionic gelation of a chitosan solution with a TPP solution also containing insulin. The nanoparticles were suspended in a solution of mannitol and lactose. Spray-drying yielded microparticle powders with a suitable aerodynamic diameter (1-3 mm) for alveolar deposition. The insulin-loaded chitosan nanoparticles had a good loading capacity (65–80%) and were fully recovered from the powder formulations after contact with an aqueous medium, and showed a fast release of insulin [281]. Yang *et al.* prepared an inhalable chitosan-based powder formulation of salmon calcitonin containing mannitol (as a cryoprotecting agent) using a spray drying process. The effect of chitosan on the physicochemical stability of the protein was investigated with chromatographic and

spectrometric techniques. The dissolution rate of the protein decreased when formulated with chitosan, which might be due to irreversible complex formation between the (aggregated) protein and chitosan during the drying process [282]. In a recent study, Ma *et al*. prepared protein-loaded chitosan microspheres using a modified ionotropic gelation method combined with a high voltage electrostatic field BSA was chosen as a model protein. The preparation process and major parameters were discussed and optimized. The morphology, particle size, encapsulation efficiency and in vitro release behavior of the prepared microspheres were investigated. The results revealed that the microspheres exhibited good sphericity and dispersity when the mixture of sodium tripolyphosphate (TPP) and ethanol was applied as coagulation solution. Higher encapsulation efficiency (>90%) was achieved for the weight ratio of BSA to chitosan below 5%. 35% of BSA was released from the microspheres cured in 3% coagulation solution, and more than 50% of BSA was released from the microspheres cured in 1% coagulation solution at pH 8.8. However, only 15% of BSA was released from the microspheres cured in 1% coagulation solution at pH 4. The results suggested that ionotropic gelation method combined with a high voltage electrostatic field will be an effective method for fabricating chitosan microspheres for sustained delivery of protein.[283]

Chitosan-based carriers have been extensively studied for parenteral and mucosal delivery of antigens [284-302]. In these studies mucosal and parenteral immunizations with various antigen co-administered with soluble chitosan, antigen-loaded chitosan powders/ micro/nanoparticles demonstrated various levels of both systemic and local immune responses. Moreover, in a phase I clinical study, intranasal immunization with influenza vaccine formulated with soluble chitosan glutamate showed positive effects of the polymer on the immune responses raised in the vaccinees [303]. The adjuvant activities of chitosan and its precursor chitin with DD of 30 and 70%, after intraperitoneal administration in mice and guinea pigs, were studies in terms of induction of cytokines, long-lasting circulating antibodies and cell-based immunity against bacterial alpha-amylase and an *Escherichia coli* infection [304,305]. In another study, chitosan (DD 70%) showed induction of cytokines, interleukin (IL)-1 and colony-stimulating factor (CSF) in macrophages *in vitro* [306]. Zaharoff *et al*. showed that chitosan dissolved in buffer pH 6.2 enhanced the immunoadjuvant properties of cytokines such as granulocyte-macrophage colony-stimulating factor (GM-CSF), when co-administered subcutaneously. Likely, chitosan prolonged dissemination of GM-CSF at the site of injection resulting in prolonged exposure of immune cells to this cytokine and enhancing the immunoadjuvant properties of GM-CSF. After single subcutaneous injection of GM-CSF/chitosan solution, the cytokine expanded lymph nodes

about 5-fold higher than GM-CSF alone, which was injected four times. It was also suggested that chitosan could enhance the antigen presenting capability of DCs and induced greater allogeneic T-cell proliferation [307]. In a subsequent paper, the same authors demonstrated that chitosan substantially increased antigen-specific antibody titers and antigen-specific CD4+ proliferation upon subcutenous administration of an aqueous solution of β-galactosidase, as a mode antigen and chitosan. The authors suggested that the ability of soluble chitosan to enhance humoral and cell-mediated immunity is related to its physicochemical characteristics such as viscosity, which increases the retention of formulations at the injection sites and also its ability to induce transient cellular expansion in draining lymph nodes [308]. Ghendon *et al*. showed that intramuscular administration of soluble chitosan with monovalent and trivalent split inactivated influenza vaccine resulted in strong humoral and cell-immunity responses against drift variants of A- and B-type human influenza viruses [309,310]. They showed that soluble chitosan admixed with inactivated influenza vaccine increased cytotoxic activity of splenic NK T-lymphocytes and enhanced the proliferative activity of mononuclear lymphocytes in the spleen. Moreover, it was shown that the number of CD3, C3/NK and CD25 T-cells also increased. The authors suggested that chitosan activates cell immunity because of its proliferation activity, which is initiated through receptor complex TCR-CD3 as well as activation signals linked with lectin receptors [310].

1.5.3 Chitosan in Gene Therapy

The transfection efficiency of chitosan as a gene delivery vehicle has been studied by Sato *et al*. [311]. The molecular weight of chitosan, the charge ratio between the luciferase plasmid to chitosan and the pH of the culture media were found to be determinants of the transfection efficiency in vitro. Nakao *et al*. reports on the use of chitosan for enhancing adenovirus infectivity to mammalian cells in gene therapy [312]. Lower concentrations of chitosan and lower molecular weight chitosans were better at enhancing adenovirus activity [313]. Chitosan-based gene delivery systems are promising candidates for non-viral gene therapy [314]. The chitosan- DNA complexes are very easy to synthesize and were superior to polygalactosamine-DNA complexes, but their use is limited because of the lower transfection efficiency [315]. The stability of the DNA-chitosan complexes is an important parameter and depends on both the chitosan chain length and the amount of chitosan, increasing the chitosan chain length and chitosan concentration could yield more stable complexes, indicating that varying the chitosan chain length may provide a tool for

controlling the ability of the polyplex to deliver therapeutic gene vectors to cells [316,317]. The preparation of chitosan and chitosan/ DNA nanospheres by using a novel and simple osmosis-based method has been recently patented [318]. With this method, they were able to prepare chitosan/DNA particles of spherical morphology with an average diameter 38 ± 4 nm. Also, the DNA incorporation was pretty high (up to 30%) and the release process is gradual and prolonged in time. Another advantage of this method is that, varying the solvent/ non-solvent couple, temperature and membrane cut-off, affording useful nanostructured systems of different size and shape to employ in several biomedical and biotechnological applications, may easily modify the process. As a novel technique, Hui *et al*. studied the gene delivery by chitosan–DNA nanoparticles through retrograde intrabiliary infusion (RII) and examined the efficacy of liver specific targeting [319]. The transfection efficiency of chitosan–DNA nanoparticles, as compared with PEI–DNA nanoparticles, was evaluated in Wistar rats by infusion into the common bile duct, portal vein, or tail vein. Chitosan–DNA nanoparticles administrated through the portal vein or tail vein did not produce detectable luciferase expression. In contrast, rats that received chitosan– DNA nanoparticles showed more than 500 times higher luciferase expression in the liver 3 days after RII; and transgene expression levels decreased gradually over 14 days. Luciferase expression in the kidney, lung, spleen, and heart was negligible compared with that in the liver. RII of chitosan–DNA nanoparticles did not yield significant toxicity and damage to the liver and biliary tree as evidenced by liver function analysis and histopathological examination. Luciferase expression by RII of PEI–DNA nanoparticles was 17-fold lower than that of chitosan–DNA nanoparticles on day 3, but it increased slightly over time. These results suggest that gene delivery by chitosan–DNA nanoparticles through RII is a promising routine to achieve liver-targeted gene delivery and both gene carrier characteristichitosan and mode of administration significantly influence gene delivery efficiency.

Probing for a solution to track the efficiency of DNA delivery, *Lee et al.* [320] employed fluorescence resonance energy transfer (FRET) to monitor the molecular dissociation of a chitosan/ DNA complex with different molecular weights of chitosan. Chitosan with different molecular weights was complexed with plasmid DNA and the complex formation was monitored using dynamic light scattering and a gel retardation assay. Plasmid DNA and chitosan were separately labeled with quantum dots and Texas Red, respectively, and the dissociation of the complex was subsequently monitored using confocal microscopy and fluorescence spectroscopy. As the chitosan molecular weight in the chitosan/ DNA complex increased the Texas Red-labeled chitosan gradually lost FRET-induced fluorescence light. This observation was noticed when HEK293 cells incubated with

chitosan/DNA complex and were examined with confocal microscopy. This suggested that the dissociation of the chitosan/DNA complex was more significant in the high molecular weight chitosan/DNA complex. Fluorescence spectroscopy also determined the molecular dissociation of the chitosan/DNA complex at pH 7.4 and pH 5.0 and confirmed that the dissociation occurred in acidic environments. This finding suggested that the high molecular weight chitosan/DNA complex could easily be dissociated in lysosomes compared to a low molecular weight complex. Furthermore, the high molecular weight chitosan/DNA complex showed superior transfection efficiency in relation to the low molecular weight complex. Therefore, it could be concluded that the dissociation of the chitosan/DNA complex is a critical event in obtaining the high transfection efficiency of the gene carrier/DNA complex [320]. Lee, Kim, and Yoo prepared chitosan/pluronic hydrogels as injectable depot systems for gene therapy to enhance local transgene expression at injection sites. Transfection studies employing HEK293 cells showed that released fractions from chitosan/pluronic hydrogels showed better transfection efficiency than those from pluronic hydrogels [321].

In another study, Khatri *et al*. investigated the preparation and vivo efficacy of plasmid DNA(pDNA) loaded chitosan nanoparticles for nasal mucosal immunization against hepatitis B. Chitosan pDNA nanoparticles were prepared using a complex coacervation process [322]. Prepared nanoparticles were characterized for size, shape, surface charge, plasmid loading and ability of nanoparticles to protect DNA against nuclease digestion and for their transfection efficacy. In this study, chitosan nanoparticles produced humoral (both systemic and mucosal) and cellular immune responses upon nasal administration. The study signified the potential of chitosan nanoparticles as DNA vaccine carrier and adjuvant for effective immunization through non-invasive nasal route. Albeit, the conventional high molecular chitosans have a few drawbacks such as aggregated shapes, low solubility at neutral pH, and high viscosity at concentrations used for in vivo delivery and a slow onset of action [323], the non-viral gene delivery systems based on chitosan are still regarded as one of the most efficient system for DNA vaccine delivery.

In an approach to develop chitosan nanoparticles for siRNA delivery, Katas & Alpar, prepared chitosan nanoparticles by two methods of ionic cross-linking, simple complexation and ionic gelatin using sodium tripolyphosphate (TPP). Both methods produced nanosize particles, less than 500 nm depending on type, molecular weight as well as concentration of chitosan. In the case of ionic gelation, two further factors, namely chitosan to TPP weight ratio and pH, affected the particle size. In vitro studies in two types of cells lines, CHO K1 and HEK 293, revealed that preparation method of siRNA association to the chitosan plays an important role on the silencing effect. Chitosan–TPP nanoparticles

with entrapped siRNA are shown to be better vectors as siRNA delivery vehicles compared to chitosan–siRNA complexes possibly due to their high binding capacity and loading efficiency. This report suggested that, chitosan–TPP nanoparticles show much potential as viable vector candidates for safer and cost-effective siRNA delivery [324]. Exploring the efficiency of chitosan/siRNA nanoparticles as a therapeutic agent, Liu *et al*. reported that the physicochemical properties (size, zeta potential, morphology and complex stability) and in vitro gene silencing of chitosan/siRNA nanoparticles are strongly dependent on chitosan molecular weight and DD [325]. High molecular weight and DD chitosan resulted in the formation of discrete stable nanoparticles of 200 nm in size. Chitosan/siRNA formulations (N/P: 50) prepared with low molecular weight (10 kDa) showed almost no knockdown of endogenous enhanced green fluorescent protein (EGFP) in H1299 human lung carcinoma cells, whereas those prepared from higher moleculr weight (64.8– 170 kDa) and DD (80%) showed greater gene silencing ranging between 45% and 65%. The highest gene silencing efficiency (80%) was achieved using chitosan/siRNA nanoparticles at N:P 150 using higher molecular weight (114 and 170 kDa) and DD (84%) that correlated with formation of stable nanoparticles of 200 nm. From their conclusions it is evident that there is still room for improvement and for the optimization of gene silencing using chitosan/siRNA nanoparticles and the fine-tuning of the polymeric properties would make lots of difference.

1.5.4 Chitosan in Bioimaging Applications

Chitosan is an exemplary polymer in biological applications owing to its biocompatible properties, in this context, its use in bioimaging applications is also gaining rapid attention. The incorporation of imaging agents such as Fe_3O_4 for Magnetic Resonance Imaging(MRI) into the self-assembled nanoparticles could enhance hepatocyte-targeted imaging [326] and the particle could serve as MR molecular imaging agent. Various inorganic materials including metals can be incorporated in the chitosan composite preparations and their combined characteristics have proven beneficial for several biomedical applications. Chitosan polyion complex composites can be prepared by interactions of chitosan with natural and synthetic polyanion molecules [327]. Preparing fluorescent chitosan quantum dot composites enables the combination of targeted drug and gene delivery with optical imaging [328, 329]. Polyacrylic acid (Carbopol), an anionic synthetic polymer having mucoadhesive properties, is extensively used with chitosan to form polymer composites, which have longer circulation times in vivo, resulting in higher bioavailability of incorporated therapeutic agents [327,330-332]. The latter composites can

also be made to contain contrast agents for imaging purposes. Lee *et al*. have developed novel self-assembling nanoparticles composed of amphipathic water-soluble chitosan–linoleic acid (WSC–LA) conjugates for encapsulation of super paramagnetic iron oxide (SPIOs) as a contrast agent to target hepatocytes [333]. The WSC–LA conjugates self-assembled into core–shell structures in aqueous solution. Since its incorporation in nanoparticles, its potential for in vivo molecular imaging applications has increased tremendously (*figure 16*). In a similar fashion, chitosan-based Gd-nanoparticles have been prepared by incorporating Gd-DTPA using the emulsion-droplet coalescence technique [334]. DTPA is diethyl triamine penta acetic acid, which is a chelating group that binds tightly with Gd(III) ion and are widely used as contrast agents for clinical MRI. Their release properties and their ability for long-term retention of Gd-DTPA in the tumor indicated that these Gd nanoparticles might be useful as an intratracheal injectable device for gadolinium neutron-capture therapy (Gd-NCT) [335]. The extent of Gd loading was different for different types of chitosans used in the preparation. The highest Gd load was achieved with 100% deacetylated chitosan in 15% Gd-DTPA aqueous solution, and the particle size was 452 nm, whereas chitosan with lower deacetylation level produced much larger particles with decreased Gd-DTPA content. Gadolinium-loaded chitosan nanoparticles displayed prolonged retention in tumor tissue after in vivo intratumoral injection [336,337]. Kumar *et al*. also described the chemistry and preparations of Holmium-166 and Samarium-153 chitosan complexes, which are mainly suited for radiopharmaceutical applications [334].

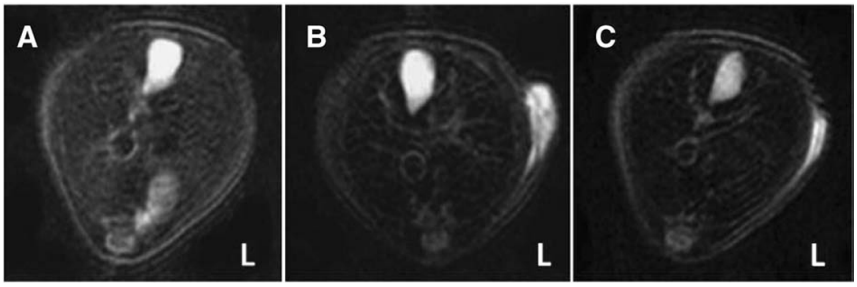

Figure 16. *MR images of the central region of mouse liver before (A) and after (B–C) injection of SPION-loaded WSC–LA nanoparticles. Images were obtained at (B) 30 min and (C) 1 h after injection of the nanoparticles. L = left[333].*

1.5.5 Chitosan in wound healing applications

In the area of wound healing, an ideal dressing should protect the wound from bacterial infection, provide a moist and healing environment, and be biocompatible [338]. Chitosan-based materials, produced in varying formulations, have been used in a number of wound healing applications. Chitosan itself can induce faster wound healing and produce smoother scarring, possibly due to enhanced vascularization and the supply of chito-oligomers at the lesion site, which have been implicated in better collagen fibril incorporation into the extracellular matrix [339,340]. While different material dressings have been used to enhance endothelial cell proliferation, the delivery of growth factors involved in the wound-healing process can improve that process [341]. Chitosan hydrogels take advantage of the reparative nature of the polymer and simultaneously deliver a therapeutic payload to the local wound. For instance, fibroblast growth factor-2 (FGF-2) stimulates angiogenesis by activating capillary endothelial cells and fibroblasts [342,343]. In order to sustain its residence at the wound site, the factor was incorporated into a high molecular weight chitosan hydrogel, formed by UV-initiated cross-linking. The growth factor remained bound tightly within the hydrogel until exposed to chitinase, after which it showed bioactivity, indicating that there was no loss of functionality during the material preparation [344]. Park *et al*. developed a chitosan hydrogel scaffold impregnated with bFGF-loaded microspheres that can accelerate wound closure in the treatment of chronic ulcers [342].

1.6. Conclusions

Regenerative medicine has entered a new era with the development of modern science and technology. The novel properties of chitosan make it one of the most promising bio-based polymers for drug delivery, tissue engineering and gene therapy. Chitosan, a native chitin derived polymer represents a vast resource with great medical potential. Current studies show that, in general, chitosan is a relatively non-toxic, biocompatible material. However, care must be taken to ensure that it is pure, as protein, metal or other contaminants could potentially cause many deleterious effects both in crosslinking approaches and in dosage forms. In this review we have seen how the unique cationic properties of chitosan offer it to be an excellent biomaterial. We presented the various forms of chitosan, its preparative procedures and its applications in drug delivery, tissue engineering, gene therapy and bioimaging field. The various approaches on the preparation techniques presented herein can be helpful to decide its use in the context of localized drug delivery to selectively capture

a therapeutic payload and control its release in local proximity to its target or to use it for tissue engineering purposes. The study demonstrates that for encapsulation and controlled release using chitosan particle/hydrogel as carriers, there is a window of preparative conditions for systematically manipulating the process of incorporation and for controlling some properties, especially size and surface charge density etc. After crosslinking or any such changes, unreacted reagents have to be thoroughly removed to prevent confounding results as many reagents are cytotoxic if uncoupled. The biodistribution is both molecular weight and formulation dependent, with relatively long circulation times achievable. The liver appears to be a primary site of localization for chitosan. It should be appreciated that many characteristics of chitosan affect its biological activity, including but not limited to: the molecular weight, the DD, the salt form, and the superstructural form should be performed. Chitosan has been shown to improve the dissolution rate of poorly soluble drugs and thus can be exploited for bioavailability enhancement of such drugs making it an interesting candidate for delivery applications. Various therapeutic agents such as anticancer, anti-inflammatory, antibiotics, antithrombotic, steroids, proteins, amino acids, antidiabetic and diuretics have been incorporated in chitosan based systems to achieve controlled release. Recalling chitosan's promise as a biopolymer for tissue engineering purposes, the possibility to generate structures with predictable pore sizes and degradation rates makes it a suitable material for bone and cartilage regeneration. However, efforts to improve the mechanical properties of chitosan-based composite biomaterials are essential for this type of application. One of a great ability of chitosan is its capability to bind anionic molecules such as growth factors , glucosamine glycans and DNA. In fact, the combination of good biocompatibility, intrinsic antibacterial activity, ability to bind to growth factors and to be processed in a variety of different shapes makes chitosan an appropriate candidate as scaffold material for cartilage, and bone tissue engineering in clinical practice. Moreover, the ability to link chitosan to DNA molecules renders this material a good candidate as a substrate for gene activated matrices in gene therapy applications. Another upcoming application related to chitosan is in bioimaging, a survey about the recent advances has also been done, and it was found that chitosan based particles provide an excellent template for this imaging application. Although some of the parameters such as molecular weight, DD, viscosity have to be considered to use chitosan at its full potential, the benefits are significant enough to make the effort worthwhile.

1.7. References

[1]. Conrad, C., Huss, R.; *J Surg Res*, **2005**,201.

[2]. Wobus, A.M., Boheler, K.R.; *Physiol Rev*, **2005**, 635.

[3]. Shahidi, F., Abuzaytoun, R., *Adv Food Nutr*, **2005**, 93.

[4]. Hejazi, R., Amiji, M.; *J Control Release*, **2003**, 151.

[5]. Khor, E., Lim, L.Y., *Biomaterials*, **2003**, 2339.

[6] Rouget, C.;*C.R.Acad. Sci. Ser. III* **,1859,** 792.

[7] Hirano, S., in *Progress in Biomedical Polymers* (Gebelein, G.G. and Dunn, R.L., eds), **1990**,pp. 283–289, Plenum Press

[8] Muzzarelli, R.A.A.; in *Natural Chelating Polymers:Alginic Acid, Chitin, and Chitosan* (Muzzarelli, R.A.A., ed.), **1973**,pp. 83–252, Pergamon Press

[9] Braconnot, H.; *Ann. Chim. Phys.* **1811**, 265.

[10] Mima, S.;*J.Appl. Polym. Sci.*, **1983**, 1909.

[11] Chandy, T., Sharma, C.P.; *Biomater Artif Cells Artif Organs*, **1990**, 1.

[12] Paul, W., Sharma, C.P.; *STP Pharma Sci*, **2000**, 5.

[13] Muzzarelli, R.A.A., Muzzarelli, C.; *Adv Polym Sci* ,**2005**, 151.

[14] Jayakumar, R., New, N., Tokura, S., Tamura, H.; *Int J Biol Macromol* , **2007**,175.

[15] Rinaudo, M.; *Polym Int*, **2008**, 397.

[16] Mourya, V.K., Inamdar, N.N.; *React Funct Polym*, **2008**,1013.

[17] Kurita, K.; *Mar Biotechnol*, **2006**, 203.

[18] Hirano, S.; *Polym Int*, **1999**, 732.

[19] Yi, H., Wu, L.Q., Bentley, W.E., Ghodssi, R., Rubloff, G.W., Culver, J.N.; *Biomacromolecules,* **2005,** 2881

[20] Kumar, M.N., Muzzarelli, R.A., Muzzarelli, C., Sashiwa, H., Domb, A.J., *Chem Rev*, **2004**, 6017.

[21] Kurita, K., *Polym Degrad Stabil*, **1995**, 117.

[22] Hirano, S.; *Biotechnol Annu Rev*, **1996**, 237.

[23] Hoppe-Seiler, F.; *Ber. Dtsch. Chem. Ges.*, **1994**, 3329.

[24] Roberts, G.A.F.; Structure of chitin and chitosan in: G.A.F: Roberts (Ed), Chitin Chemistry, MacMillan, Houndsmills, **1992**, pp. 1-53.

[25] C.K.Rha, D. Rodrigues-Sanchez, C.Kienel-Sterzer, Novel applications of chitosan, in:R.R.Colwell, E.R. Parsier, A.J.Sinkey (Eds.), Biotechnology of Marine Polysaccharides, Hemisphere,Washington, 1984,pp.284-311.

[26] H. Struszcyk, D.Wawro, A.Niekraszewicz, Biodegradability of chitosan fibres,in:C.J.Brine, PA. Stanford,J.P. Zikakis (Eds.), Advances in Chitin and Chitosan, Elsiever Applied Science, London, 1991, pp.580-585.

[27] Suh, J.K.F., Matthew, H.W.T. ; *Biomaterials*, **2000**, 2589.

[28] Wang,W., Xu, D.; *Int. J. Biol. Macromol.* , **1994**, 149.

[29] Glerentes, P., Vachoud, L., Doury, J., Domard, A.; *Biomaterials,* **2002**, 1295.

[30] Felt, O., Buri, P., Gurny, R.; *Drug Dev. Ind. Pharm.*, **1998**, 979.

[31] Chatelet, C., Damour, O., Domard, A.; *Biomaterials*, **2001**, 261.

[32] Hsu, S. C., Don, T. M., Chiu, W. Y.; *Polym. Degrad. Stab.*, **2002** , 73.

[33] Zoldners, J., Kiseleva, T., Kaiminsh, I.; *Carbohydr. Polym.*, **2005**, 215.

[34] KEGG Pathway, Amino sugar and nucleotide sugar metabolism. 2009, Kanehisa Laboratories.

[35] Kean, T., Thanou, M.; Chitin and chitosan—sources, production and medical applications, in: P.A. Williams, R. Arshady (Eds.), Desk reference of Natural Polymers, their Sources, Chemistry and Applications, Kentus Books, London, **2009**, pp. 327–361.

[36] Funkhouser, J.D., Jr Aronson N.N., Chitinase family gh18: evolutionary insights from the genomic history of a diverse protein family, BMC Evol. Biol. , **2007**,96.

[37] Yang, Y.M., Hu,W., Wang, X.D., Gu, X.S.; *J. Mater. Sci. Mater. Med.*, **2007**, 2117.

[38] Xu, J., McCarthy, S.P., Gross, R.A., Kaplan, D.L.; *Macromolecules*, **1996**, 3436.

[39] Onishi, H., Machida, Y.; *Biomaterials*, **1999**, 175.

[40] Senel, S., McClure, S.J.; *Adv. Drug Deliv. Rev.*, **2004**, 1467
.

[41] Zhang, H., Neau, S.H., *Biomaterials*, **2002**, 2761.

[42] Rao, S.B., Sharma, C.P.; *J. Biomed. Mater. Res.*,**1997**, 21.

[43] Kittur, F.S., Vishu Kumar, A.B., Tharanathan, R.N.; *Carbohydr. Res.*, **2003**, 1283.

[44] Kittur, F.S., Vishu Kumar, A.B., Varadaraj, M.C., Tharanathan, R.N.; *Carbohydr. Res.*, **2005**, 1239.

[45] McConnell, E.L., Murdan, S., Basit, A.W.; *J. Pharm. Sci.* , **2008**, 3820.

[46] Guo, Z., Chen, R., Xing, R., Liu, S., Yu, H., Wang, P., Li, C., Li, P.; *Carbohydr. Res*., 2006, 351.

[47] Ma, L., Gao, C., Mao, Z., Zhou, J., Shen, J. Hu, X., Han,C.; *Biomaterials*, **2003**, 4833.

[48] Hirano, S., Seino, H., Akiyama, Y., Nonaka, I.; Proceedings of the ACS Division of Polymeric Materials: Science and Engineering, American Chemical Society, Los Angeles, California, 1988.

[49] Suzuki, Y.S., Momose,Y., Higashi, N., Shigematsu, A., Park, K.B., Kim,Y.M., Kim, J.R., Ryu, J.M. ; J. *Nucl. Med.* ,**1998**, 2161.

[50] Banerjee, T., Mitra, S., Kumar Singh, A., Kumar Sharma, R., Maitra, A.; *Int. J. Pharm*., **2002**, 93.

[51] Richardson, S.C., Kolbe, H.V., Duncan, R.; *Int. J. Pharm*.,**1999**, 231.

[52] Line, B.R., Weber, P.B., Lukasiewicz, R., Dansereau, R.N.; *J. Nucl. Med.*, **2000**,1264.

[53] Kean, T., Thanou, M.; *Adv. Drug Deliv. Rev.*, **2009**, doi:10.1016/j.addr.2009.09.004

[54] Onishi, H., Machida, Y.; *Biomaterials*, **1999**, 175.

[55] Kumar, R.M.N.V.; *React. Funct. Polym.* , **2000**, 1.

[56] Xu, G., Huang, X., Qiu, L., Wu, J., Hu,Y.; *Asia Pac. J. Clin. Nutr.*; **2007**,313.

[57] Chae, S.Y., Jang, M.K., Nah, J.W.; *J. Control. Release* , **2005**, 383.

[58] Ishii, T., Okahata,Y., Sato,T.; *Biochim. Biophys. Acta* , **2001**,51.

[59] Leong, K.W., Mao, H.Q., Truong-Le, V.L., Roy, K., Walsh, S.M., August, J.T.; *J. Control. Release* ,**1998**,183.

[60] Park, I.K., Kim, T.H., Kim, S.I., Park, Y.H., Kim, W.J., Akaike, T., Cho, C.S.; *Int. J. Pharm.*, **2003**, 103.

[61] Janes, K.A., Fresneau, M.P., Marazuela, A., Fabra, A., Alonso, M. J.; *J. Control. Release*, **2001**, 255.

[62] Thanou, M., Verhoef, J.C., Junginger, H.E.; *Adv. Drug Delivery Rev.*, **2001**, 117.

[63] Illum, L.; *Pharm. Res.*, **1998**, 1326.

[64] Wedmore, I., McManus, J.G., Pusateri, A.E., Holcomb, J.B.; *J. Trauma* ,**2006**, 655.

[65] Schipper, N.G., Varum, K.M., Artursson, P.; *Pharm. Res.* , **1996**, 1686.

[66] Schipper, N.G., Varum, K.M., Stenberg, P., Ocklind, G., Lennernas, H., Artursson, P.; *Eur. J. Pharm. Sci.*, **1999**, 335.

[67] Zhang, C., Qu, G., Sun, Y., Wu, X., Yao, Z., Guo, Q., Ding, Q., Yuan, S., Shen, Z., Ping, Q., Zhou, H.; *Biomaterials*, **2008**, 1233.

[68] Jumaa, M., Furkert, F.H., Muller, B.W.; *Eur. J. Pharm. Biopharm.*, **2002**, 115.

[69] Guo, Z., Chen, R., Xing, R., Liu, S., Yu, H., Wang, P., Li, C., Li, P.; *Carbohydr. Res.*, **2006**, 351.

[70] Pujals, G., Sune-Negre, J.M., Perez, P., Garcia, E., Portus, M., Tico, J.R., Minarro, M., Carrio, J.; *Parasitol. Res.*, **2008**, 1243.

[71] Hirano, S., Iwata, M., Yamanaka, K., Tanaka, H., Toda, T., Inui, H.; *Agric. Biol. Chem.*, **1991**, 2623.

[72] Rao, S.B., Sharma, C.P.; *J. Biomed. Mater. Res.;* **1997**, 21.

[73] Gades, M.D., Stern, J.S., *Obes. Res.*, **2003**, 683.

[74] Arai, K., Kinumaki, T., Fujita, T., *Bull. Tokai Reg. Fish. Res. Lab.*, **1968**, 89.

[75] Sonaje, K., Lin, Y.H., Juang, J.H., Wey, S.P., Chen, C.T., Sung, H.W.; *Biomaterials*, **2009**, 2329.

[76] Illum, L., Farraj, N.F., Davis, S.S.; *Pharm. Res.*, 1994, 1186.

[77] Muzzarelli, R.A.A., Jeuniauk, C., Gooday, G.W.; Chitin in Nature and Technology, Plenum, New York, 1986.

[78] Sjak-Braek, G., Anthonsen, T., Sandford, P.; Chitin and Chitosan, Elsevier, New York, **1992**.

[79] Hou, W.M., Miyazaki, S., Takada, M., Komai, T.; *Chem. Pharm. Bull.*, **1985**, 3986.

[80] Miyazaki, S., Ishii, K., Nadai, T.; *Chem. Pharm. Bull.*, 1981, 3067.

[81] Handa, T., Kasai, A., Takenaka, H., Lin, S.Y., Ando, Y.; *J. Pharm. Sci.*, 1985, 264.

[82] Miyazaki, S., Yamaguchi, H., Yokouchi, C., Takada, M., Hou, W. M.; *Chem. Pharm. Bull.*, **1988**, 4033.

[83] Sawayanagi, Y., Nambu, N., Nagai, T.; *Chem. Pharm. Bull.*,**1982**, 4213.

[84] Shiraishi, S., Imai, T., Otagiri, M.; *J. Control. Release*, **1993**, 217.

[85] Lehr, C.M., Bouwstra, J.A., Schacht, E.H., Junginger, H.E.; *Int. J. Pharm.*, **1992**, 43.

[86] Luehen, H.L., Lehr, C.M., Rentel, C.O., Noach, A.B.J., Boer, A.G., Verhoef, J.C., Junginger, H.E.; *J. Control. Release*, **1994**, 329.

[87] Imai, T., Shiraishi, S., Saito, H., Otagiri, M., *Int. J. Pharm.*, **1991**, 11.

[88] Genta, I., Pavanetto, F., Conti, B., Giunchedi, P., Conte, U., Proc. Int. Symp. Control. Release Bioact. Mater. 21 **1994**, 616.

[89] Sawayanagi, Y., Nambu, N., Nagai, T., *Chem. Pharm. Bull.*, **1983**, 2507.

[90] Gallo, J.M., Hassan, E.E.; *Pharm. Res.* , **1988**, 300.

[91] Hassan, E.E., Parish, R.C., Gallo, J.M.; *Pharm. Res.*, **1992**, 390.

[92] Artursson, P., Lindmark, T., Davis, S.S., lllum, L.; *Pharm. Res.*, **1994**, 1358.

[93] Soppimath, K.S., Aminabhavi, T.M., Kulkarni, A.R., Rudzinski, W.E.; *J. Control. Release*, **2001**, 1.

[94] Kreuter, J., Nanoparticles, in: J. Kreuter (Ed.), Colloidal Drug Delivery Systems, Marcel Dekker, New York, 1994, pp. 219– 342.

[95] Brannon Peppas, L.; *Int. J. Pharm.*, **1995**, 1.

[96] Couvreur, P., Grislain, L., Lenaerts, V., Brasseur, F., Guiot, P.; in: P. Guiot, P. Couvreur (Eds.), Polymeric Nanoparticles and Microspheres, CRC Press, Boca Raton, FL, **1986**.

[97] Akbuga, J., Durmaz, G.; *Int. J. Pharm.*, **1994**, 217.

[98] Kumbar, S.G., Kulkarni, A.R., Aminabhavi, T.M.; *J. Microencapsulation*, **2002**, 173.

[99] Sankar, C., Rani, M., Srivastava, A.K., Mishra, B.; *Pharmazie*, **2001**, 223.

[100] Ozbas-Turan, S., Akbuga, J., Aral, C.; *J. Pharm. Sci.*, **2002**, 124 .

[101] Mao, H.Q., Roy, K., Troung-Le, V.L., Janes, K.A., Lim, K.Y., Wang, Y., August, J.T., Leong, K.W.; *J. Control. Release* , **2001**, 399.

[102] He, P., Davis, S.S., Illum, L.; *Int. J. Pharm.*, **1999**, 53.

[103] Huang, Y.C., Yeh, M.K., Chiang, C.H.; *Int. J. Pharm.*, **2002**, 239.

[104] Shi, X.Y., Tan, T.W.; *Biomaterials*, 2002, 4469.

[105] Bishop, C.W., Knutson, J.C., Valliere, C.R.; US Pat. 5 795 882, **1998**.

[106] Tokumitsu, H., Ichikawa, H., Fukumori, Y.; *Pharm. Res.*, **1999**, 1830.

[107] Polk, A., Amsden, B., Yao, K.D., Peng, T., Goosen, M.F.A., *J. Pharm. Sci.*, **1994**, 178.

[108] Liu, L.S., Liu, S.Q., Ng, S.Y., Froix, M., Ohno, T., Heller, J.; *J. Control. Release*, **1997**, 65.

[109] Kawashima, Y., Handa, T., Takenaka, H., Lin, S.Y., Ando, Y. ; *J. Pharm. Sci.*, **1985**, 264.

[110] Kawashima, Y., Handa, T., Kasai, A., Takenaka, H., Lin, S.Y.; *Chem. Pharm. Bull.*, **1985**, 2469.

[111] Bodmeier, R., Oh, K.H., Pramar, Y.; *Drug Dev. Ind. Pharm.*, **1989**, 1475.

[112] Shirashi, S., Imai, T., Otagiri, M., *J. Control. Release*. 1993, 217.

[113] Sezer, A.D., Akbuga, J.; *Int. J. Pharm.* , **1995**, 113.

[114] Aydin, Z., Akbuga, J.; *Int. J. Pharm.*, **1996**, 101.

[115] Calvo, P., Remunan-Lopez, C., Vila-Jata, J.L., Alonso, M.J., *Pharm. Res.*, **1997**, 1431.

[116] Calvo, P., Remunan-Lopez, C., Vila-Jata, J.L., Alonso, M. J., *J. Appl. Polym. Sci.*, **1997**, 125.

[117] Shu, X.Z., Zhu, K.J.; *Int. J. Pharm.* , **2000**, 51.

[118] Ko, J.A., Park, H.J., Hwang, S.J., Park, J.B., Lee, J.S.; *Int. J. Pharm.*, **2002**, 165.

[119] Xu, Y., Du, Y.; *Int. J. Pharm.*, **2003**, 215.

[120] Leong, Y.S., Candau, F., *J. Phys. Chem.*, **1982**, 2269.

[121] Luisi, P.L., Giomini, M., Pileni, M.P., Robinson, B.H.; *Biochim. Biophys. Acta*, **1988**, 209.

[122] Mitra, S., Gaur, U., Ghosh, P.C., Maitra, A.N.; *J. Control. Release* , **2001**, 317.

[123] Agnihotri, S.A., Aminabhavi, T.M.; *J. Control. Release*, **2004**, 245.

[124] Hejazi, R., Amiji, M.; *Int. J. Pharm.* , **2002**, 87.

[125] Al-Helw, A.A., Al-Angary, A.A., Mahrous, G.M., Al- Dardari, M.M.; *J. Microencapsulation*, **1998**, 373.

[126] Ganza-Gonzalez, A., Anguiano-Igea, S., Otero-Espinar, F.J., Mendez, J.B., *Eur. J. Pharm. Biopharm.*, 1999, 149.

[127] Higuchi, T.; *J. Pharm. Sci.*, **1963**, 1145.

[128] Washington, C.; *Int. J. Pharm.*, **1990**, 1.

[129] Guy, R.H., Hadgraft, J., Kellaway, I.W., Taylor, M.J.; *Int. J. Pharm.*, **1982**, 199.

[130] Ritger, P.L., Peppas, N.A.; *J. Control. Release* , **1987**, 37.

[131] N.A. Peppas, R.W. Korsmeyer, in: N.A. Peppas (Ed.), Hydrogels in Medicine and Pharmacy, vol. 3, CRC Press, Boca Raton, FL, **1987**, p. 103.

[132] Jameela, S.R., Kumary, T.V., Lal, A.V., Jayakrishnan, A.; *J. Control. Release* , **1998**, 17.

[133] Berger, J., Reist, M., Mayer, J.M., Felt, O., Gurny, R.; *Eur. J. Pharm. Biopharm.*, **2004**, 35.

[134] Boucard, N., Viton, C., Domard, A.; *Biomacromolecules*, **2005**, 3227.

[135] N.A. Peppas, Hydrogels in medicine and pharmacy, CRC Press, Boca Raton, FL, 1986.

[136] Shu, X.Z., Zhu, K.J.; *Int. J. Pharm.*, **2002**, 217.

[137] Shen, E.C., Wang, C., Fu, E., Chiang, C.Y., Chen, T.T., Nieh, S.; *J. Periodontal. Res.*, **2008**, 642.

[138] Brack, H.P., Tirmizi, S.A., Risen, W.M., *Polymer* , **1997**, 2351.

[139] Dambies, L., Vincent, T. Domard, A., Guibal, E.; *Biomacromolecules*, **2001**, 1198.

[140] Berger, J., Reist, M., Mayer, J.M., Felt, O., Gurny, R.; *Eur. J. Pharm. Biopharm.*, **2004**, 19.

[141] Meares, P.; *J. Chem. Soc. Faraday Trans.*, **1983**, 2264.
[142] Tsuchida, E., Abe, K.; *Adv. Polym. Sci.*, **1982**, 1.

[143] Cascone, M.G., Maltinti, S., Barbani, N., Laus, M.; *J. Mater. Sci. Mater. Med.*, **1999**, 431.

[144] Khan, F., Tare, R.S., Oreffo, R.O.C., Bradley, M., *Angew. Chem. Int. Ed*., **2009**, 978.

[145] Boussif, O., Lezoualch, F., Zanta, M.A., Mergny, M.D., Scherman, D., Demeneix, B., Behr, J.P.; Proc. Natl Acad. Sci. U. S. A. 92 (1995) 7297–7301.

[146] Ladet, S., David, L., Domard, A.; *Nature*, **2008**, 76.

[147] Chen, R.R., Silva, E.A., Yuen, W.W., Brock, A.A., Fischbach, C., Lin, A.S., Guldberg, R.E., Mooney, D.J.; *FASEB J.*, **2007**, 3896.

[148] Richardson, T.P., Peters, M.C., Ennett, A.B., Mooney, D.J., *Nat. Biotechnol.*, **2001**,1029.

[149] Jeong, B., Kim, S.W., Bae, Y.H.; *Adv. Drug Deliv. Rev.* , **2002**, 37.

[150] J. Kretlow, D., Klouda, L., Mikos, A.G.; *Adv. Drug Deliv. Rev.*, **2007**, 263.

[151] Bhattarai, N., Matsen, F.A., Zhang, M.; *Macromol. Biosci.*, **2005**, 107.

[152] Bhattarai, N., Ramay, H.R., Gunn, J., Matsen, F.A., Zhang, M.Q.; *J. Control. Release*, **2005**, 609.

[153] Boesel, L.F., Reis, R.L., Roman, J.S.; *Tissue Eng. Part A*, **2008**, 223.

[154] Chen, J.P., Cheng, T.H.; *Polymer*, **2009**, 107.

[151] Chenite, A., Chaput, C., Wang, D., Combes, C., Buschmann, M.D., Hoemann, C.D., Leroux, J.C., Atkinson, B.L., Binette, F., Selmani, A.; *Biomaterials*, **2000**, 2155.

[156] Park, H., Park, K., Shalaby, W.S.W.; Biodegradable Hydrogels for Drug Delivery, CRC Press, Boca Raton, FL, **1993**.

[157] Hoare, T.R., Kohane, D.S.; *Polymer* , **2008**, 1993.

[158] Berger, J., Reist, M., Mayer, J.M., Felt, O., Peppas, N.A., Gurny, R.; *Eur. J. Pharm. Biopharm.*, **2004**, 19.

[159] Hennink, W.E., van Nostrum, C.F.; *Adv. Drug Deliv. Rev.*, **2002**, 13.

[160] Jin, J., Song, M., Hourston, D.J.; *Biomacromolecules*, **2004**, 162.

[161] Sung, H.W., Liang, I.L., Chen, C.N., Huang, R.N., Liang, H.F., *J. Biomed. Mater. Res.*, **2001**, 538.

[162] Sung, H.W., Huang, R.N., Huang, L.L.H., Tsai, C.C.; *J. Biomater. Sci. Polym. Ed.*, **1999**, 63.

[163] Mi, F.L., Tan, Y.C., Liang, H.C., Huang, R.N., Sung, H.W. ; *Biomater. Sci. Polym. Ed.*, **2001**, 835.

[164] Chen, S.C., Wu, Y.C., Mi, F.L., Lin, Y.H., Yu, L.C., Sung, H.W.; *J. Control. Release*, **2004**, 285.

[165] Bhattarai, N.; *Adv. Drug Deliv. Rev.*, **2009**, doi:10.1016/j.addr.2009.07.019

[166] Yoo, H.S.; *J. Biomater. Sci. Polym. Ed.* , **2007**, 1429.

[167] Lee, J.I., Kim, H.S., Yoo, H.S.; *Int. J. Pharm.* , **2009**, 93.

[168] Lee, S.J., Kim, S.S., Lee, Y.M.; *Carbohydr. Polym.* , **2000**, 197.

[169] Yao, K.D., Liu, J., Cheng, G.X., Zhao, R.Z., Wang, W.H., Wei, L.; *Polymer Int.*, **1998**, 191.

[170] She, Z., Jin, C., Huang, Z., Zhang, B., Feng, Q., Xu, Y.; *J. Mater. Sci. Mater. Med.*, **2008**, 3545.

[171] Gupta, K.C., Kumar, M.; *J. Appl. Polym. Sci.*, **2001**, 639.

[172] Risbud, M.V., Hardikar, A.A., Bhat, S.V., Bhonde, R.R.; *J. Control. Release*, **2000**, 23.

[173] Wang, M.Z., Fang, Y., Hu, D.D.; *React. Funct. Polym.*, **2001**, 215.

[174] Tessmar, J.K., Gopferich, A.M.; *Adv. Drug Deliv. Rev.*, **2007**, 274.

[175] Holland, T.A., Tessmar, J.K., Tabata, Y., Mikos, A.G.; *J. Control. Release*, **2004**, 101.

[176] Kohane, D.S., Langer, R.; *Pediatr. Res.*, **2008**, 487.

[177] Zisch, A.H., Lutolf, M.P., Ehrbar, M., Raeber, G.P., Rizzi, S.C., Davies, N., Schmokel, H., Bezuidenhout, D., Djonov, V., Zilla, P., Hubbell, J.A.; *Faseb J.* , **2003**, 2260.

[178] Lin, C.C., Anseth, K.S.; *Pharm. Res.*, **2009**, 631.

[179] Kim, S.W., Bae, Y.H., Okano, T.; *Pharm. Res.*, **1992**, 283.

[180] Sokker, H.H., Ghaffar, A.M.A., Gad, Y.H., Aly, A.S.; *Carbohydr. Polym.*, **2009**, 222.

[181] Hoare, T.R., Kohane, D.S.; *Polymer*, **2008**, 1993.

[182] Ruel-Gariepy, E., Shive, M., Bichara, A., Berrada, M., Le Garrec, D., Chenite, A., Leroux, J.C.; *Eur. J. Pharm. Biopharm.*, **2004**, 53.

[183] Obara, K., Ishihara, M., Ozeki, Y., Ishizuka, T., Hayashi, T., Nakamura, S., Saito, Y., Yura, H., Matsui, T., Hattori, H., Takase, B., Kikuchi, M., Maehara, T.; *J. Control. Release*, **2005**, 79.

[184] Jauhari, S., Dash, A.K.; *AAPS PharmSciTech* , **2006**, E53.

[185] Lee, J.E., Kim, S.E., Kwon, I.C., Ahn, H.J., Cho, H., Lee, S.H., Kim, H.J., Seong, S.C., Lee, M.C.; *Artif. Organs* ,**2004**, 829.

[186] Joung, Y.K., Choi, J.H., Park, K.M., Park, K.D.; *Biomed. Mater.*, **2007**, 269.

[187] Petersen, L.K., Narasimhan, B.; *Expert Opin. Drug Deliv.*, **2008**, 837.

[188] Lutolf, M.P., Hubbell, J.A.; *Nat. Biotechnol.*, **2005**, 47.

[189]. Shalak, R., Fox, C.F. Preface. In: Shalak R, Fox CF, eds. Tissue Engineering. New York: Alan R. Liss, **1988**:26.

[190]. Hutmacher, D.W., Schantz, T., Zein, I., Ng, K.W., Teoh, S.H., Tan, K.C.; *J Biomed Mater Res* ,**2001**, 203.

[191] Seol, Y.J., Lee, J.Y., Park, Y.J., Lee, Y.M., Young-Ku, Rhyu, I.C., Lee, S.J., Han, S.B., Chung, C.P.; *Biotechnol Lett*, **2004**, 1037.

[192] Seeherman, H., Li, R., Wozney, J.; *J Bone Jt Surg Am*, **2003**, 96.

[193] Zhang, Y., Zhang, M.; *J Biomed Mater Res*, **2001**, 304.

[194] Zhang, Y., Zhang, M.; *J Biomed Mater Res*, **2002**, 378.

[195] Zhang, Y., Zhang, M.; *J Biomed Mater Res*, **2002**, 1.

[196] Zhang, Y., Ni, M., Zhang, M., Ratner, B.; *Tissue Eng* ,**2003**, 337.

[197] Martino,A. D., Sittinger,Michael., Risbuda, M.V.; *Biomaterials*, **2005**, 5983.

[198] Hu, Q., Li, B., Wang, M., Shen, J.; *Biomaterials*, **2004**, 779.

[199] Yin, Y., Ye, F., Cui, J., Zhang, F., Li, X., Yao, K.; *J Biomed Mater Res*, **2003,** 844.

[200] Leroux, L., Hatim, Z., Freche, M., Lacout, J.L.; *Bone*, **1999**, 31S.
[201] Gutowska, A., Jeong, B., Jasionowski, M.; *Anat Rec*, **2001**, 342.

[202] Xu, H.H., Quinn, J.B., Takagi, S., Chow, L.C.; *Biomaterials*, **2004**, 1029.

[203] Zhao, F., Yin, Y., Lu, W.W., Leong, J.C., Zhang, W., Zhang, J.; *Biomaterials*, **2002**, 3227.

[204] Kim, S.B., Kim, Y.J., Yoon, T.L., Park, S.A., Cho, I.H., Kim, E.J.; *Biomaterials*, **2004**, 5715.

[205] Lee, B.H., Lee, Y.M., Sohn, Y.S., Song, S.C.; *Macromolecules*, **2002a**,3876 .

[206] Lee, J.Y., Nam, S.H., Im, S.Y., Park, Y.J., Lee, Y.M., Seol, Y.J.; *J Control Release*, **2002b**, 187.

[207] Zhao, L., Burguera, E. F., Xu, H.H.K., Amin, N., Ryou, H., Arola, D. D.; *Biomaterials*, **2010**, 840.

[208] Grande, D.A., Halberstadt, C., Naughton, G., Schwartz, R., Ryhana, M.; *J Biomed Mater Res*, **1997**, 211.

[209] Kosher, R.A., Church, R.L.; *Nature*, **1975**, 327.

[210] Kosher, R.A., Lash, J.W., Minor, R.R.; *Dev Biol*, **1973**, 210.

[211] Athanasiou, K.A., Shah, A.R., Hernandez, R.J., LeBaron, R.G.; *Clin Sports Med* , **2001**, 223.

[212] Sittinger, M., Hutmacher, D.W., Risbud, M.V.; *Curr Opin Biotechnol*, **2004**, 411.

[213] Suh, J.K.F., Matthew, H.W.T.; *Biomaterials*, **2000**, 2589.

[214] Lahiji, A., Sohrabi, A., Hungerford, D.S., Frondoza, C.G., Lahiji, A., Sohrabi, A., Hungerford, D.S., Frondoza, C.G.; *J Biomed Mater Res*, **2000**, 586

[215] Iwasaki, N., Yamane, S.T., Majima, T., Kasahara, Y., Minami, A., Harada, K., Nonaka, S., Maekawa, N., Tamura, H., Tokura, S., Shiono, M., Monde, K., Nishimura, S.; *Biomacromolecules*, **2004**, 828.

[216] Risbud, M., Ringe, J., Bhonde, R., Sittinger, M.; *Cell Transplant* , **2001**, 755.

[217] Cui, Y.L., Qi, A.D., Liu, W.G., Wang, X.H., Wang, H., Ma, D.M., Yao, K.D.; *Biomaterials*, **2003**, 3859.

[218] Yamane, S., Iwasaki, N., Majima, T., Funakoshi, T., Masuko, T., Harada, K., Minami, A., Monde, K., Nishimura, S.; *Biomaterials*, **2005**, 611.

[219] Hsu, S.H., Whu, S.W., Hsieh, S.C., Tsai, C.L., Chen, D.C., Tan, T.S.; *ArtifOrgans*, **2004**, 693.

[220] Lee, J.E., Kim, K.E., Kwon, I.C., Ahn, H.J., Lee, S.H., Cho, H., Kim, H.J., Seong, S.C., Lee, M.C.; *Biomaterials*, **2004**, 4163.

[221] Taravel, M.N., Domard, A.; *Biomaterials*, **1996**, 451.

[222] Kim, S.E., Park, J.H., Cho, Y.W., Chung, H., Jeong, S.Y., Lee, E.B., Kwon, I.C.; *J Control Release*, **2003**, 365.

[223] Lu, J.X., Prudhommeaux, F., Meunier, A., Sedel, L., Guillemin, G.; *Biomaterials*, **1999**, 1937.

[224] Hoemann, C.D., Hurtig, M.B., Rossomacha, E., Sun, J., Chevrier, A., Shive, M.S.; *J Bone Joint Surg Am* , **2005**, 2671.

[225] Hoemann, C.D., Sun, J., McKee, M.D., Chevrier, A., Rossomacha, E., Rivard, G.E; *Osteoarthr Cartil* , **2007**, 78.

[226] Chevrier, A., Hoemann, C.D., Sun, J., Buschmann, M.D.; *Osteoarthritis Cartilage*, **2007**, 316.

[227] Haoya, T., Wenza, N., Caoza, J. K., Wangy, H. B., Lu, S.H., Liuy, T., Liny, Q. X., Duany, C. M., Wangy C.Y.; *Osteoarthritis and Cartilage*, **2010**, 257.

[228] Kim, I.Y., Seo, S.J., Moon, H.S., Jiang, H.L., Kim, Y.K., Cho, C.S.; *Tissue Eng Regenerative Med*, **2006a**, 27.

[229] Ben-Ze'ev, A., Robinson, G.S., Bucher, N.L., Farmer, S.R.; *Proc Natl Acad Sci USA* ,**1988**, 2161.

[230] LeCluyse, E.L., Bullock, P.L., Parkinson, A.; *Adv Drug Deliv Rev*, **1996**, 133.

[231] Kang, I.K., Moon, J.S., Jeon, H.M., Meng, W., Kim, Y.I., Hwang, Y.J.; *J Mater Sci Mater Med* , **2005**, 533.

[232] Lindahl,U., Hook, M.; *Annu Rev Biochem*, **1978**, 385.

[233] Li, J., Pan, J., Zhang, L., Guo, X., Yu, Y.; *J Biomed Mater Res A*, **2003a**, 938.

[234] Li, J., Pan, J., Zhang, L., Yu, Y.; *Biomaterials*, **2003b**, 2317.

[235] Wang, X.H., Li, D.P., Wang, W.J., Feng, Q.L., Cui, F.Z., Xu, Y.X.; *Biomaterials*, **2003**, 3213.

[236] Kim, I.Y., Seo, S. J., Moon, H.-S., Yoo, M.-K., Park, I.Y., Kim, B.-C., Cho,C.-S.; *Biotechnol. Adv*., **2008**, 1.

[237] Wang, X., Yan, Y., Lin, F., Xiong, Z., Wu, R., Zhang, R., *J Biomater Sci Polym Ed*, **2005**, 1063.

[238] Adams, J.C.; *J Cell Sci*, **2002**, 257.

[239] Ashwell, G., Morell, A.G.; *Adv Enzymol*, **1974**, 99.

[240] Ashwell, G., Harford, J.; *Ann Rev Biochem*, **1982**, 531.

[241] Chung, T.W., Lu, Y.F., Wang, S.S., Lin, Y.S., Chu, S.H.; *Biomaterials* ,**2002a**, 4803.

[242] Heath, C.A., Rutkowski, G.E.; *TIBTECH*, **1998**, 163.

[243] Ciardelli, G., Chiono, V.; *Macromol Biosci*, **2006**, 13.

[244] Haipeng, G., Yinghui, Z., Jianchun, L., Yandao, G., Nanming, Z., Xiufang, Z.; *J Biomed Mater Res*, **2000**, 285.

[245] Yuan, Y., Zhang, P., Yang, Y., Wang, X., Gu, X.; *Biomaterials*, **2004**, 4273.

[246] Matsuda, A., Kobayashi, H., Itoh, S., Kataoka, K., Tanaka, J.; *Biomaterials*, **2005**, 2273.

[247] Chávez-Delgado, M.E., Mora-Galindo, J., Gómez-Pinedo, U., Feria-Velasco, A., Castro-Castañeda, S., López-Dellamary Toral, F.A.; *J Biomed Mater Res B*, **2003**, 702.

[248] Mingyu, C., Kai, G., Jiamou, L., Yandao, G., Nanming, Z., Xiufang, Z.; *J Biomater Appl* ,**2004**, 59.

[249] Cheng, M., Deng, J., Yang, F., Gong, Y., Zhao, N., Zhang, X.; *Biomaterials*, **2003**, 2871.

[250] Freier, T., Montenegro, R., Shan Koh, H., Shoichet, M.S.; *Biomaterials*, **2005**, 4624.

[251] Park, S.B., You, J.O., Park, H.Y., Haam, S.J., Kim, W.S.; *Biomaterials*, **2001**, 323.

[252] Ahn, J.S., Choi, H.K., Cho, C.S.; *Biomaterials*, **2001**, 923.

[253] Ahn, J.S., Choi, H.K., Chun, M.K., Ryu, J.M., Jung, J.H., Kim, Y.U., Cho, C.S.; *Biomaterials*, **2002**, 1411.

[254] Li, F., Liu, W.G., Yao, K.D.; *Biomaterials*, **2002**, 343.

[255] Zhao, H.R., Wang, K., Zhao, Y., Pan, L.Q.; *Biomaterials*, **2002**, 4459.
[256] Hu, Y., Jiang, X., Ding, Y., Ge, H., Yuan, Y., Yang, C.; *Biomaterials*, **2002**, 3193.

[257]Akbuga, J., Bergisadi, N.; *J. Microencapsul.*, **1999**, 697.

[258] Shiraishi, S., Imai, T., Otagiri, M., *J. Control Rel.*, **1993**, 217.

[259] Aggarwal, A., Kaur, S., Tiwary, A.K., Gupta, S.; *J. Microencapsul.*, **2001**, 819.

[260] Hejazi, R., Amiji, M., *Pharm. Dev. Technol.*, **2003**, 253.

[261] Huang, Y.C., Yeh, M.K., Cheng, S.N., Chiang, C.H.; *J. Microencapsul.*,**2003a.** , 459.

[262] Huang, Y.C., Chiang, C.H., Yeh, M.K.; *J. Microencapsul.* **2003b**, 247.

[263] Mattioli-Belmonte, M., Gigante, A., Muzzarelli, R.A., Politano, R., De Benedittis, A., Specchia, N., Buffa, A., Biagini, G., Greco, F.; *Med. Biol. Eng. Comput.*, **1999**,130.

[264] Suh, J.K., Matthew, H.W.; *Biomaterials,* **2000**, 2589.

[265] Muzzarelli, R.A.A., Biagini, G., Belmonte, M.A., Talassi, O., Gandolfi, M.G., Solmi, R., Carraro, S., Giardino, R., Fini, M.; *J. Bioact. Compat. Polym.*, **1997**, 321.

[266] Lee, Y.M., Park, Y.J., Lee, S.J., Ku, Y., Han, S.B., Klokkevold, P.R., Chung, C.P.; *J. Periodontol.*, **2000**, 418.

[267] Park, D.J., Choi, B.H., Zhu, S.J., Huh, J.Y., Kim, B.Y., Lee, S.H.; *J. Cranio-maxillo-facial Surg.*, **2005**, 50.

[268] Patel, M., Mao, L., Wu, B., Vandevord, P.J.; *J. Tissue Eng. Regen Med* , **2007**, 360.

[269] Elcin, Y.M., Dixit, V., Gitnick, G.; *Artif. Cells Blood Substit. Immobil. Biotechnol.*, **1996**, 257.

[270] Azab, A.K., Kleinstern, J., Doviner, V., Orkin, B., Srebnik, M., Nissan, A., Rubinstein, A.; *J. Control. Release* , **2007**, 116.

[271] Azab, A.K., Orkin, B., Doviner, V., Nissan, A., Klein, M., Srebnik, M., Rubinstein, A.; *J. Control. Release*, **2006**, 281.

[272] Zeng, R., Tu, M., Liu, H., Zhao, J., Zha, Z., Zhou, C., *Carbohydr. Polym.*, **2009**, 107.

[273] Ho, M.H., Hsieh, C.C., Hsiao, S.W., Thien, D. V. H.; *Carbohydr. Polym.*, **2010**, 955.

[274] Sabera, A., Strandc, S.P., Ulfendahla, M.; *Eur. J. Pharm. Biopharm.*, **2010**, 110.

[275] Fernandez-Urrusuno, R., Calvo, P., Remunan-Lopez, C., Vila-Jato, J.L., Alonso, M.J.; *Pharm Res*, **1999**, 1576.

[276] Teijeiro-Osorio, D., Remunan-Lopez, C., Alonso, M.J.; *Biomacromolecules*, **2009**, 243.

[277] Wang, X., Zheng, C., Wu, Z.M., Teng, D.G., Zhang, X., Wang, Z., Li, C.X.; *J. Biomed. Mater. Res. Part B Appl. Biomater.*, **2009**, 150.

[278] Zhang, X.G., Zhang, H.J., Wu, Z.M., Wang, Z., Niu, H.M., Li, C.X.; *Eur. J. Pharm. Biopharm.,* **2008**, 526.

[279] Grenha, A., Grainger, C.I., Dailey, L.A., Seijo, B., Martin, G.P., Remunan-Lopez, C., Forbes, B.; *Eur. J. Pharm. Biopharm.,* **2007**,73.

[280] Grenha, A., Remunan-Lopez, C., Carvalho, E.L.S., Seijo, B.; *Eur. J. Pharm. Biopharm.,* **2008**, 83.
[281] Grenha, A., Seijo, B., Remunan-Lopez, C.; *Eur J Pharm Sci*, **2005**, 427.

[282] Yang, M., Velaga, S., Yamamoto, H., Takeuchi, H., Kawashima, Y., Hovgaard, L., van de Weert, M., Frokjaer, S.; *Int J Pharm*, **2007**,176.

[283] Ma, L., Liu, C.; *Colloids Surf B Biointerfaces*, **2010**,448.

[284] van der Lubben, I.M., Konings, F.A., Borchard, G., Verhoef, J.C., Junginger, H.E.; *J Drug Target*, **2001**, 39.
[285] van der Lubben, I.M., Verhoef, J.C., van Aelst, A.C., Borchard, G., Junginger, H.E.; *Biomaterials,* **2001**, 687.

[286] Vila, A., Sanchez, A., Janes, K., Behrens, I., Kissel, T., Vila Jato, J.L., Alonso, M.J.; *Eur J Pharm Biopharm,* **2004**, 123 .

[287] Illum, L., Jabbal-Gill, I., Hinchcliffe, M., Fisher, A.N., Davis, S.S.; *Adv Drug Deliv Rev*, **2001**, 81.

[288] Amidi, M., Romeijn, S.G., Verhoef, J.C., Junginger, H.E., Bungener, L., Huckriede, A., Crommelin, D.J., Jiskoot, W., *Vaccine*, **2007**, 144.

[289] Boonyo, W., Junginger, H.E., Waranuch, N., Polnok, A., Pitaksuteepong, T.; *J. Control. Release,* **2007**, 168.

[290] Svirshchevskaya, E.V., Alekseeva, L.G., Reshetov, P.D., Phomicheva, N.N., Parphenyuk, S.A., Ilyina, A.V., Zueva, V.S., Lopatin, S.A., Levov, A.N., Varlamov, V.P.; *Eur J Med Chem*, **2009**, 2030.

[291] Ravichandran, E., Al-Saleem, F.H., Ancharski, D.M., Elias, M.D., Singh, A.K., Shamim, M., Gong, Y., Simpson, L.L.; *Infect Immun*, **2007**, 3043.

[292] Sayin, B., Somavarapu, S., Li, X.W., Thanou, M. D.; *Int J Pharm.*, **2008**, 139.

[293] Borges, O., Cordeiro-da-Silva, A., Tavares, J., Santarem, N., de Sousa, A., Borchard, G., Junginger, H.E.; *Eur J Pharm Biopharm.* **2008**, 405.

[294] Kang, M.L., Jiang, H. L. Kang, S.G., Guo, D.D., Lee, D.Y., Cho, C.-S., Yoo, H.S.; *Vaccine*, **2007**, 4602.

[295] Jiang, H.L., Kang, M.L., Quan, J.S., Kang, S.G., Akaike, T., Yoo, H.S., Cho, C.S.; *Biomaterials*, **2008**, 1931.

[296] Klas, S.D., Petrie, C.R., Warwood, S.J., Williams, M.S., Olds, C.L., Stenz, J.P., Cheff, A.M., Hinchcliffe, M., Richardson, C., Wimer, S.; *Vaccine* , **2008**, 5494.

[297] Lameiro, M.H., Malpique, R., Silva, A.C., Alves, P.M., Melo, E.; *J Biotechnol*, **2006**, 152.

[298] Jaganathan, K.S., Vyas, S.P.; *Vaccine*, **2006**, 4201.

[299] Florindo, H.F., Pandit, S., Lacerda, L., Goncalves, L.M.D., Alpar, H.O., Almeida, A.J.; *Biomaterials*, **2009**, 879.

[300] N. Hagenaars, E. Mastrobattista, R. Verheul, I. Mooren, H. Glansbeek, J. Heldens, H. van den Bosch, W. Jiskoot, *Pharm. Res.*, **2009**, 1353.

[301] Baudner, B.C., Giuliani, M.M., Verhoef, J.C., Rappuoli, R., Junginger, H.E., Giudice, G.D., *Vaccine*, **2003**,3837.

[302] Nagamoto, T., Hattori, Y., Takayama, K., Maitani, Y.; *Pharm Res*, **2004**, 671.

[303] Read, R.C., Naylor, S.C., Potter, C.W., Bond, J., Jabbal-Gill, I., Fisher, A., Illum, L., Jennings, R., *Vaccine*, **2005**, 4367.

[304] Nishimura, K., Nishimura, S., Nishi, N., Numata, F., Tone, Y., Tokura, S., Azuma, I.; *Vaccine*, **1985**, 379.

[305] Nishimura, K., Nishimura, S., Nishi, N., Saiki, I., Tokura, S., Azuma, I.; *Vaccine*, **1984**, 93.

[306] Nishimura, K., Ishihara, C., Ukei, S., Tokura, S., Azuma, I.; *Vaccine*, **1986**, 151.

[307] Zaharoff, D.A., Rogers, C.J., Hance, K.W., Schlom, J., Greiner, J.W.; *Vaccine*, **2007**, 8673.

[308] Zaharoff, D.A., Rogers, C.J., Hance, K.W., Schlom, J., Greiner, J.W., *Vaccine*, **2007**, 2085.

[309] Ghendon, Y., Markushin, S., Krivtsov, G., Akopova, I., *Archives of Virology*, **2008**, 831.

[310] Ghendon, Y., Markushin, S., Vasiliev, Y., Alkopova, I., Koptiaeva, I., Krivtsov, G., Borisova, O., Ahmatova, N., Kurbatova, E., Mazurina, S., Gervazieva, V.; *Journal of Medical Virology*, **2009**, 494.

[311] Sato, T., Ishii, T., Okahata, Y.; *Biomaterials*, **2001**, 2075.

[312] Kawamata, Y., Nagayama, Y., Nakao, K., Mizuguchi, H., Hayakawa, T., Sato, T., Ishii, N.; *Biomaterials*, **2002**, 4573.

[313] Khora, E., Limb, L.Y.; *Biomaterials*, **2003**, 2339.

[314] Agnihotri, S.A., Mallikarjuna, N.N., Aminabhavi, T.M.; *J Control Release*, **2004**; 5.

[315] Prabaharan, M., Mano, J.F.; *Drug Delivery*, **2005**, 41.

[316] Danielsen, S., Strand, S., de Lange Davies, C., Stokke, B.T.; *Biochim Biophys Acta*, **2005**,1721.

[317] Mansouri, S., Lavigne, P., Corsi, K., Benderdour, M., Beaumont, E., Fernandes, J.C.; *Eur J Pharm Biopharm*, **2004**, 57.

[318] Masotti, A., Bordi, F., Ortaggi, G., Marino, F., Palocci, C.; *Nanotechnology*, **2008**, 1.

[319] Dai, H., Jiang, X., Tan, G. C. Y., Chen, Y., Torbenson, M., Leong, K. W., et al; *Int J Nanomedicine*, **2006**, 507.

[320] Lee, J. M., Ha, K. S., & Yoo, H. S.; *Acta Biomaterialia*, **2008**, 791.

[321] Lee, J. I., Kim, H. S., & Yoo, H. S.; *Int. J. Pharm*, **2009**, 93.

[322] Khatri, K., Goyal, A. K., Gupta, P. N., Mishra, N., Vyas, S. P.; *Int. J. Pharm*, **2008**, 235.

[323] Zhou, X. F., Zhang, X., Yu, X., Zha, X., Fu, Q., Liu, B., et al.; *Biomaterials*, **2009**, 111.

[324] Katas, H., Alpar, H. O.; *J Control Release*, **2006**, 216.

[325] Liu, X., Howard, K. A., Dong, M., Andersen, M. O., Rahbek, U. L., Johnsen, M. G., et al.; *Biomaterials*, **2007**, 1280.

[326] Lee, C.M., Jeong, H.J., Kim, S.L., Kim, E.M., Kim, D.W., Lim, S.T., Jang, K.Y., Jeong, Y.Y., Nah, J.W., Sohn, M.H.; *Int. J. Pharm.*, **2009**, 163.

[327] Hein, S., Wang, K., Stevens, W.F., Kjems, J.; *Mater. Sci. Technol.* , **2008**, 1053.

[328] Köping-Höggård, M., Tubulekas, I., Guan, H., Edwards, K., Nilsson, M., Vårum, K.M., Artursson, P.; *Gene Ther.* , **2001**, 1108.

[329] Mi, F.L., Shyu, S.S., Peng, C.K., Wu, Y.B., Sung, H.W., Wang, P.S., Huang, C.C.; *J. Biomed. Mater. Res.— Part A*, **2006** ,1.

[330] Sionkowska, A., Wisniewski, M., Skopinska, J., Kennedy, C.J., Wess, T.J.; *Biomaterials*, **2004** 795.

[331] Hsu, S.H., Shu, W.W., Hsieh, S.C., Tsai, C.L., Chen, D.C., Tan, T.S.; *Artif. Organs*, **2004**, 693.

[332] Kweon, D.K., Song, S.B., Park, Y.Y.; *Biomaterials*, **2003**, 1595.

[333] Lee, C.M., Jeong, H.J., Kim, S.L., Kim, E.M., Kim, D.W., Lim, S.T., Jang, K.Y., Jeong, Y.Y., Nah, J.W., Sohn, M.H.; *Int. J. Pharm.*, **2009**, 163.

[334] Kumar, M.N., Muzzarelli, R.A., Muzzarelli, C., Sashiwa, H., Domb, A.J., *Chem. Rev.*, **2004**, 6017.

[335] Tokumitsu H., Ichikawa, H. Fukumori, Y.; *Pharm. Res*. **1999**, 1830.

[336] Saha, T.K., Ichikawa, H., Fukumori, Y.; *Carbohydr. Res.*, **2006**, 2835.

[337] Tokumitsu, H., Ichikawa, H., Saha, T.K., Fukumori, Y., Block, L.H.; *S.T.P. Pharm. Sci.*, **2000**, 49.

[338] Wu, Z., Sheng, Z., Sun, T., Geng, M., Li, J., Yao, Y., Huang, Z.; *Chin. Med. J.(Engl)*, **2003**, 419.

[339] Shigemasa, Y., Minami, S.; *Genet. Eng. Rev.*, **1996**, 383.

[340] Rao, S.B., Sharma, C.P.; *J. Biomed. Mater. Res.*, **1997**, 21.

[341] Hunt, T.K., La Van, F.B.; *N. Engl. J. Med*,**1989**, 111.

[342] Park, C.J., Clark, S.G., Lichtensteiger, C.A., Jamison, R.D., Johnson, A.J.; *Acta Biomater*, **2009**.

[343] Obara, K., Ishihara, M., Ishizuka, T., Fujita, M., Ozeki, Y., Maehara, T., Saito, Y., Yura, H., Matsui, T., Hattori, H., Kikuchi, M., Kurita, A.; *Biomaterials*, **2003**, 3437.

[344] Ishihara, M., Nakanishi, K., Ono, K., Sato, M., Kikuchi, M., Saito, Y., Yura, H., Matsui, T., Hattori, H., Uenoyama, M., Kurita, A.; *Biomaterials*, **2002**, 833.

2. STATISTICAL APPROACH OF CHITIN DEACETYLATION

2.1. Abstract

Chitosan was produced by thermo-chemical deacetylation of chitin. Reaction parameters were varied to obtain different grade of degree of N-acetylation (DA) of chitin following a statistical design. Two different analytical methods namely 1st derivative UV and FTIR spectroscopies have been adopted to determine the values of DA of the prepared chitosan. The values of DA assessed from the 1st derivative UV is in accordance with that using FTIR. Thermogravimetric analysis was also performed to characterize chitin and its derivatives in terms of thermal stability in air and nitrogen.

2.2. Introduction

Chitosan finds numerous applications in agriculture, biomedicine (for example, as drug delivery system), papermaking, water treatment and food industry [1]. The properties of chitosan strongly depend on the degree of N-acetylation (DA), which not only influences its physical-chemical characteristics [2-7] but also its biodegradability [8-10] and immunological activity [11].

Chitosan is derived from chitin and the percentage of N-acetyl group within the polymer chain is a distinguishing factor between the different grades of these biopolymers (Scheme 1). The macromolecule containing 100 % or more than 50 % of amine groups is named chitosan. Conversely, the material will be considered chitin if in its structure there is 100 % or more than 50 % of N-acetyl group.

Various properties of these two biopolymers are closely related to the DA, which is the most fundamental parameter. In other words, if the DA is known, many properties can be predicted and different analytical methods have been employed for its assessment. These methods included ninhydrin test [12], linear potentiometric titration [13], near-infrared spectroscopy [14], nuclear magnetic resonance spectroscopy [15], hydrogen bromide titrimetry [16, 17], infrared spectroscopy [17, 18], and UV-spectrophotometry [19, 20]. Some of these methods are either too tedious (titrimetry), or costly for routine analysis (nuclear magnetic resonance spectroscopy), or destructive to the sample (ninhydrin test).

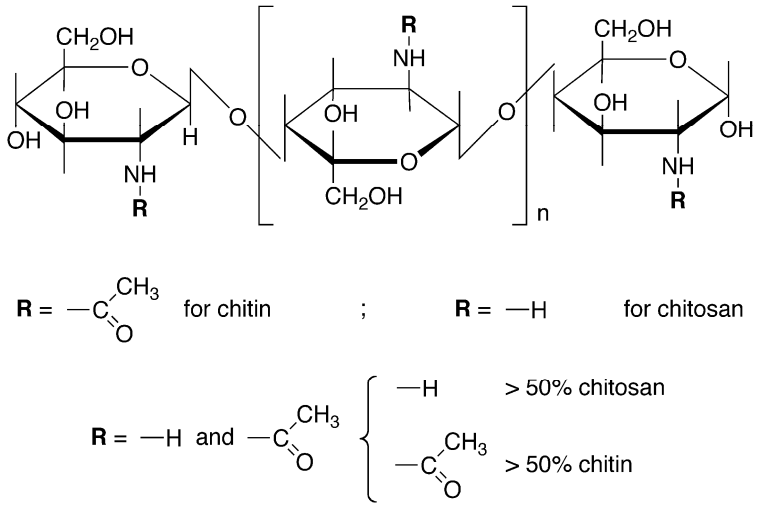

Scheme 1: *Structure of chitin and chitosan and corresponding copolymers*

There are several steps on the manufacturing process of chitosan that depend on the starting material used to extract chitin, which is its precursor. Shrimp, prawn and crab wastes are the principal sources of chitin [21]. However, chitin can be supplied from microorganisms like cultured fungi, Antarctic krill, and insects, too. Scheme 2 illustrates the general steps that are performed traditionally to produce chitosan.

Pre-treatment (PT) is an alternative process, which is required only in some cases where the source of chitin contains others organic substances in considerable quantity [22]. In this step, the material is treated with sodium hydroxide solution (NaOH) at low concentration.

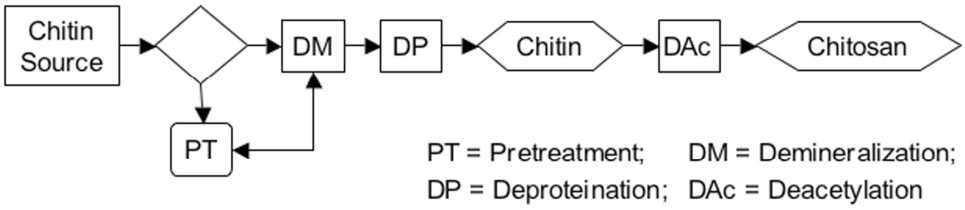

Scheme 2*: Flowsheet of typical chitosan manufacturing process from materials containing chitin*

The process of demineralization (DM) is basically the removing of calcium carbonate ($CaCO_3$) that represents 20-50 % in the shells of marine crustaceans [1]. The condition of this step is bland where a dilute hydrochloric acid (HCl) solution is used at ambient temperature. Following, demineralised material is treated with NaOH solution at 1-2

M and at temperatures higher than that of ambient. In this condition deproteination (DP) will take place. The last step related to the chitin deacetylation (DAc) is the focus of the present work. This step can follow a homogeneous or heterogeneous alkali method. In the first one, temperatures are lower than that of heterogeneous DAc but with long times as for example days. However, the conditions for an heterogeneous DAc of chitin generally uses aqueous NaOH solution at concentration range of 40-50 wt-%, temperature range between 100-150 °C and short times [1, 21].

The aim of the present study is a statistical approach for the optimization of the chitin deacetylation reaction variables using heterogeneous method.

2.3. Materials and Methods

2.3.1 Materials

Chitin from shrimp shells, practical grade powder, was purchased from Sigma (C-7170) [1398-61-4]. Chitosan low molecular weight and DA=75-85%, was purchased from Aldrich (448869) [9012-76-4]. D-(+)-glucosamine hydrochloride (GluN), purity 99%, crystalline (G4875) [66-84-2], N-acetyl-D-glucosamine (GluNAc), purity 99%, (A8625) [7512-17-6], and Potassium bromide (KBr), FTIR grade (221864) [7758-02-3], were purchased from Sigma. Sodium hydroxide pellets and acetic acid were obtained from Carlo Erba and were analytical grades.

2.3.2 Methods

2.3.2.1 Chitin Deacetylation

A screening design of experimente (DEX) for chitin deacetylation process was carried out following a factorial 2^2 with center point [23]. Tables 1 and 2 present levels of variables reaction time and temperature and sample codes for the corresponding processing conditions, respectively.

Table 1: *Settings for the 2^2 design with center point*

Variable	Levels[a)]		
	-1	0	+1
Time (h)	1	2	3
Temperature (°C)	90	110	130

[a)] -1 and +1 are low and high levels and 0 is center point.

Table 2: *Sample codes and processing conditions*

Sample code	Temperature (°C)	Time (h)
CS9-1	90	1
CS13-1	130	1
CS9-3	90	3
CS13-3	130	3
CS11-2	110	2

Alkali concentration and liquor rate were maintained constant at 50 % w/v and 50 mL of NaOH solution to 1g of chitin, respectively. The reaction was performed under nitrogen atmosphere and at constant magnetic stirring.

Completed the DA time, the suspension was filtered off, washed with water to neutral pH and oven dried at 60 °C overnight.

The obtained chitosan was dissolved at 1% w/v in 0.174 M aqueous acetic acid solution. This solution was added into NaOH solution forming a precipitate. The insoluble material was removed by filtration. To the clear filtrate was added again NaOH solution up to pH around 8. The formed white gel was filtered and thoroughly rinsed with distilled water, until neutral pH. Purified chitosan was then freeze-dried, grounded to powder and oven dried at 60 °C overnight.

2.3.2.2 Fourier Transform Infrared Spectroscopy (FTIR)

FTIR measurements were carried out in a Perkin-Elmer Spectrum One spectrophotometer. Sample absorbance spectrum was taken as an average of 32 scans with 2 cm^{-1} of resolution in the frequency range 4000-400 cm^{-1}. Prior analysis, sample and KBr were dried at 60 °C for 2 h under reduced pressure. Sample:KBr disc was prepared with 3 mg:200 mg ratio.

2.3.2.3 Thermogravimetric Analysis (TGA)

TGA evaluations were performed using a Mettler TA 4000 System instrument consisting of TGA-50 furnace with a M3 microbalance, and Star software. Samples of ca. 7 mg were scanned at 10 °C/min from 25 to 900 °C, under 300 mL/min flow rate of both nitrogen and air.

2.3.2.3 Ultraviolet Spectrophotometry (UV)

Ultraviolet spectra were recorded in the range 200-240 nm using a Jasco V-530 UV/V spectrophotometer. A calibration curve was performed by means of standard solutions of GluN and GluNAc. A solution of acetic acid (AcOH) 0.01 M was used as blank. GluN and GluNAc were dissolved in AcOH 0.01 M in the range of 0.08 mM to 0.2 M and 0.01 mM to 0.2 mM, respectively. Accurately weighed (10 mg) chitosan samples were dissolved in 2 mL of AcOH 0.1 M and diluted 10-fold with distilled water to obtain a final AcOH concentration of 0.01M. Chitosan was not dissolved directly in AcOH 0.01M since it would be difficult and time consuming.

2.4. Results and Discussion

The obtained deacetilated chitin was a white powder and the yield was 49.7 ± 2.2 %. The methods to assess the degree of N-acetylation (DA) can be distributed in three groups: 1) spectroscopic; 2) conventional; and 3) destructive [24] In the present study will be compared the values of DA obtained by two spectroscopic (FTIR and UV) and one destructive (TGA) methods using statistical analysis.

2.4.1 FTIR Spectroscopy

FTIR is attractive due to its non-destructive character, be fast, sensitive, user-friendly and low-priced, and suitable for both soluble and non-soluble samples. Hence, this technique is specifically useful for the analysis of insoluble chitin. Nevertheless, FTIR needs a calibration versus an absolute technique like nuclear magnetic resonance (NMR), which permit a direct determination of chitin DA. A big effort has been devoted to identify the right combination of bands and respective baselines, which led to a large number of proposed methods found in the literature. In fact, several methods were attempted to determine the DA by FTIR [16, 17, 24-28].

Sample analysis was in random way as well as the preparation of the three replica performed for each one. This strategy was used to obtain a better estimation of the error of analysis.

As previously described, the method to determine DA using FTIR needs the construction of a calibration curve. However, it was decided to use calibration curve described in literature considering that the statistical analysis of the chitin deacetylation reaction is the focus of the work. Table 3 presents some calibration curves with the respective absorption ratios in literature.

Table 3: *Calibration Curves from absorption ratios versus standard DA values*

DA Calibration Curve	Method for DA standard	Ref.
1) DA = (A_{1655}/A_{3450}) x 155	titration	[16]
2) (A_{1320}/A_{1420}) = 0.3822 + 0.03133 x DA	^{1}H NMR, ^{13}C NMR	[28]
3) (A_{1320}/A_{3450}) = 0.03146 + 0.00226 x DA	^{1}H NMR, ^{13}C NMR	[28]
4) (A_{1560}/A_{2875}) = 0.2 + 0.0125 x DA	elemental analysis	[25]

Figure 1 shows FTIR spectra in transmittance of chitin, its derivatives at the lower and higher levels (see Table 2) and chitosan. The band at around 1320 cm^{-1} is similar for chitin and its derivatives CS9-1 and CS13-3. This band is assigned to the C-N stretching of the N-acetylglucosamine. This result suggests that the process variables ranges do not deacetilated chitin in a significant way. Based on this observation, the calibration curve (2) in the Table 3 was selected to evaluate the extension of chitin deacetylation as a function of process variables. Figure 2 shows FTIR spectrum of chitin with the insert indicating the baselines for the probe (BL1) and internal reference (BL2) absorptions that are in the ranges 1348-1280 cm^{-1} and 1500-1404 cm^{-1}, respectively. The internal reference absorption centered at 1420 cm^{-1} corresponds to $–CH_2$ bending. Using this equation the values of DA for commercial chitin and chitosan were 101 ± 5.2 % and 10 %, respectively. The experiment with commercial chitosan was not replicated. However, considering that the errors of the FTIR measurements were around 5 % (see Tab. 4), it can be confirmed that the equation proposed by Brugnerotto *et al* [28] is a reasonable approach to assess the deacetylation reaction of chitin.

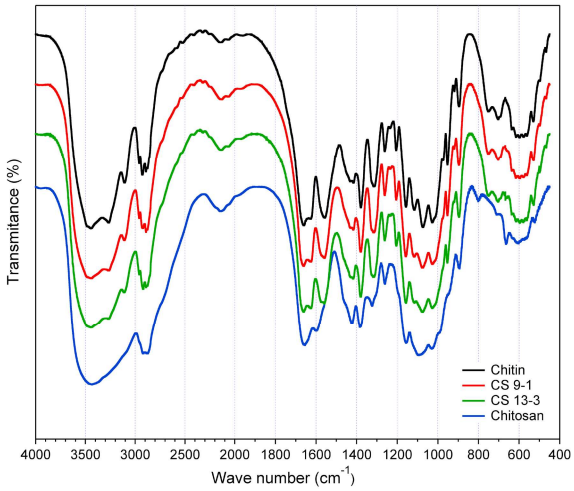

Figure 1: *FTIR spectra of chitin and its derivatives*

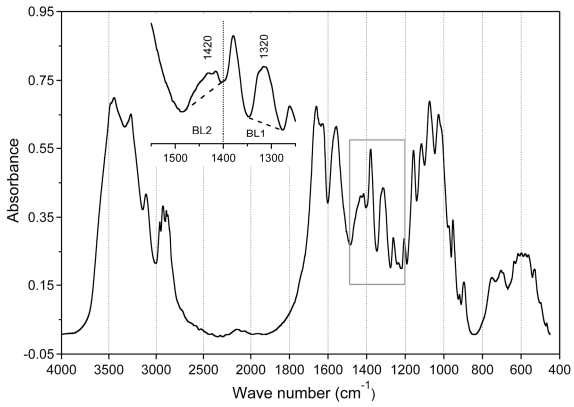

Figure 2: *FTIR spectra of chitin*

Table 4 records the mean values of DA of chitin as a function of process variables (Tab. 2). The error was calculated using Student's *t*-test at 95% of confidence ($t_{2;\,0.05}$ = 4.303) as indicated by Equation 2.1.

$$error = \frac{t_{\nu;\alpha/2} \times s}{\sqrt{n}} \qquad \text{Eq. 2.1}$$

were $t_{\nu,\alpha/2}$ is Student's *t* at ν freedom degree and α/2 significance level.

Table 4: *Degree of acetylation as a function of process variables using FTIR*

Sample	DA (%)	Error (%)
CS9-1	84.0	4.1
CS9-3	80.2	4.3
CS11-2	75.5	5.8
CS13-1	77.3	3.9
CS13-3	65.5	6.8

Factorial designed experiment can be appropriately analysed using the DEX interaction effect plot (Fig. 3). This plot showing mean values for the levels of each factor and that of interaction between them will indicate the significance on changing from one level to another as well as the interdependence of the factors. This plot shows that the most significant variable is the temperature followed by the time. The interaction between temperature and time was apparently not significant in the range studied. All factors indicate that higher chitin deacetylation, using 50% aqueous NaOH, can be obtained for temperatures higher than 130 °C and/or at reaction times higher than 3 h.

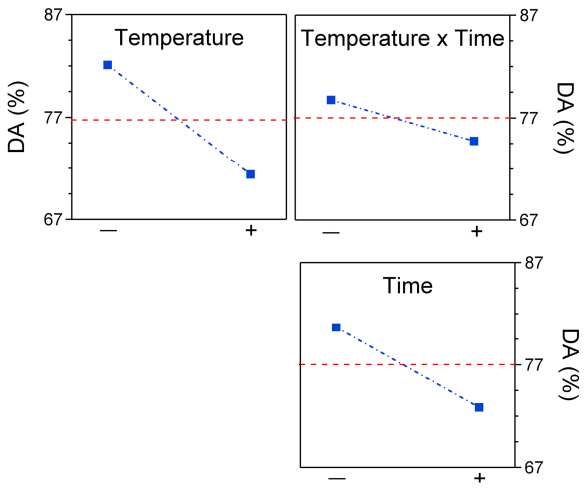

Figure 3: DEX interaction effect plot for DA values

The analysis of variance (ANOVA) is summarized in Table 5 including as source of variation the "pure quadratic" to check for pure quadratic curvature effect. This check was performed with the center points of the 2^2 factorial design. The cut-off value of *F*-test at 95 % of confidence with 1 and 10 freedom degrees ($F_{0.05;\ 1;10}$) is 4.96. The F_0 values for the main effects and interaction are higher than that of cut-off and it can be concluded that they are statistically significant. On the other hand, pure quadratic effect is not significant and a first order model can be used adequately to fit results. The ANOVA confirmed the observations of DEX plot including that there is some interdependence between temperature and time although small for the range of variables studied.

Table 5: *ANOVA for factorial model*

Source of Variation	Sum of Squares	Degrees of Freedom	Mean Square	F_0
A (Temperature)	343.68	1	343.68	79.74
B (Time)	184.55	1	184.55	42.82
AB	48.24	1	48.24	11.19
Pure quadratic	3.20	1	3.20	0.74
Error	43.12	10	4.31	
Total	622.79	14		
Model	576.47	3	192.16	44.58
R^2=0.926				

Considering the above remarks, the regression model for the chitin deacetylation process is

$$\hat{y} = 76.8 - 5.3x_1 - 3.9x_2 - 2x_1x_2 \qquad \text{Eq. 2.2}$$

The relationship between coded and natural variables is

$$x_1 = \frac{Temp - (Temp_{low} + Temp_{high})/2}{(Temp_{high} - Temp_{low})/2} \quad \text{Eq. 2.3}$$

$$x_2 = \frac{Tempo - (Tempo_{low} + Tempo_{high})/2}{(Tempo_{high} - Tempo_{low})/2} \quad \text{Eq. 2.4}$$

Consequently, the fitted model of Eq. 2.2 with the natural variables is

$$\hat{DA} = 118.64 - 0.22T - 6.34t - 0.02Tt \quad \text{Eq. 2.5}$$

where, *T* and *t* are Temperature and time variables.

The ANOVA for the model is included in Table 5. The cut-off value of $F_{0.05;\ 3;10}$ is 3.71 that is lower than that found for the model. This means that at least one coefficient of the model is different of zero. Beside, below the ANOVA of model, are reported a statistic to check adequacy of fit of the model. This statistic represents the fraction of the variation about the mean that is explained by the fitted model. So, R^2 value suggests that the model can be explain about 93% of DA variability.

Using the model represented by Eq. 2.5 it can be said that to obtain chitosan with 20% of DA using NaOH at 50% and a reaction temperature of 100°C it is needed about 9 hours.

2.4.2 TGA

The TGA method for chitin and chitosan derivates has been used principally on thermodegradation kinetic studies [29,30]. However, a simple way to determine chitin DA was proposed by Alonso *et al*. [31] They take the weight loss in air atmosphere that corresponded to the maximum of DTG peak of chitin and chitosan degradation traces and correlated with DA of chitin standards. They demonstrated that the empirical correlation obtained could be a fast way to control DA.

Figure 4 shows typical TG and DTG traces for chitin and its derivates in air atmosphere and TG data are reported in Table 6.

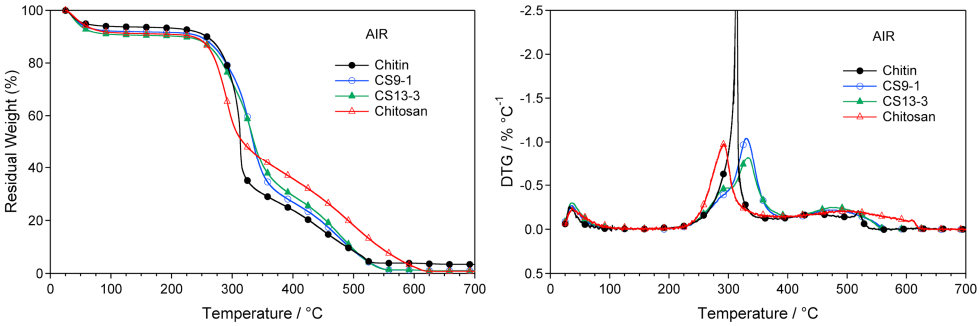

a) b)

Figure 4: *Typical (a) TG and (b) DTG traces of chitin and its derivatives in air atmosphere.*

As the time for a TG analysis is long, only the center point of the 2^2 factorial design was replicated to allow the evaluation of the error other than to check the presence of curvature in the fitting model.

The first step in the temperature range of 30-150 °C corresponds to the equilibrium moisture of samples with that of ambient, which appears in the Table 6 as volatile. The second thermo-oxidation step appeared as an overlapped peak only for the sample CS13-3 (DA = 65.5 from FTIR – see Tab. 4) with maximum at 296 °C and which is slightly higher than that measured for commercial chitosan (see insert inside Fig. 4 b). For other chitin derivates, this step appeared as a shoulder. So, the maximum rate peak of second step around 325 °C is associated to chitin, which is in accordance with literature [31]. The last step of thermo-oxidation in the range 350-600 °C seems to have some correlation with the capacity of the molecule to uptake moisture as indicated by the same tendency presented by the volatile value in Table .6. Peniche-Covas *et al*. observed that up to 430 °C both pyrolysis and thermo-oxidation TGA traces of chitosan overlap. They considered that up this temperature the decomposition is independent of atmosphere [29]. Consequently, as this step is related to oxidation reaction of the residue it can be supposed that depends on DA.

Commercial chitosan that has a DA around 80 % contain *ca.* 9 % of adsorbed moisture that is only *ca.* 2.5 % higher than that of chitin. However, the behaviour of chitin derivatives does not follow the DA values presented in the Table 4. The first approach to

explain this result can be related to the formation of some kind of intermolecular interaction that turn less accessible the hydrophilic groups for moisture adsorption. The thermo-oxidation temperature defined at 2 wt-% of weight loss after that of volatile (T_d) for chitin was 243 °C suggesting be 2 °C less stable than chitosan (DA=80%). However, considering the replication of the experiment with the center point sample (CS11-2) and using Student's *t*-test at 95% of confidence (Eq. 2.1), it can be said that the error of the experiment is around 3.8 °C. In conclusion, the difference observed on T_d value between chitin and chitosan is not significant. The same statement can be formulated for chitin derivates.

Table 6. *TGA data of chitin and its derivatives in air atmosphere* [a)]

Sample[b)]	Volatile (%)	T_d (°C)	ΔM_1 (%)	T_{p1} (°C)	ΔM_2 (%)	T_{p2} (°C)	R_{600} (%)
Chitin	6.3	243	61.8	313	28.0	519	3.9
CS9-1	8.1	248	63.6	330	27.0	479	1.3
CS13-1	6.7	244	61.4	324	29.7	475	2.2
CS9-3	7.1	244	65.7	324	25.5	479	1.7
CS13-3	3.4	245	64.7	329	29.5	481	2.4
CS11-2	3.9	240	65.0	324	29.8	477	1.3
CS11-2	3.9	243	64.0	325	30.6	485	1.5
CS11-2	3.3	241	64.2	325	30.0	487	2.5
Chitosan	8.8	245	54.0	292	34.2	493	3.0

[a)] Volatile means the weight loss up to 150 °C. T_d is the decomposition temperature defined at 2 wt-% of weight loss from 150 °C; T_p is the first derivative peak; and R_{600} is the residual weight at 600°C. [b)] See Table 2.2 for code definition.

The residue at 600 °C (R_{600}) was a white powder that characterize the inorganic molecules present in the crustaceous shell. Pristine chitin left *ca*. 4% and the commercial chitosan 3%. The R_{600} values of the chitin derivatives were lower than the two limits of kind of 2-deoxy-β-D-glucopyranose materials. This is one indication that the presence of inorganic impurities depends on the purification method used. Although the results suggest

that the time and temperature in NaOH concentrated solution could be factors on materials inorganic impurities, the error observed from CS11-2 of 1.6 % weaken this possibility.

Typical traces of TG and DTG of chitin and its derivates under nitrogen atmosphere are presented in Figure 5. DTG traces (Fig. 5 b) show clearly that pyrolysis occur in two steps in the range 200-600 °C. The first weight loss up to 150 °C takes place moisture volatilization as previously verified for samples decomposed in air atmosphere. Unlike the DTG profile in air atmosphere, the second step of chitin derivates in the range 200-330 °C overlap the third step assigned to chitin but it is possible to take both maximum peak temperatures (T_p). Table 7 reports pyrolysis data.

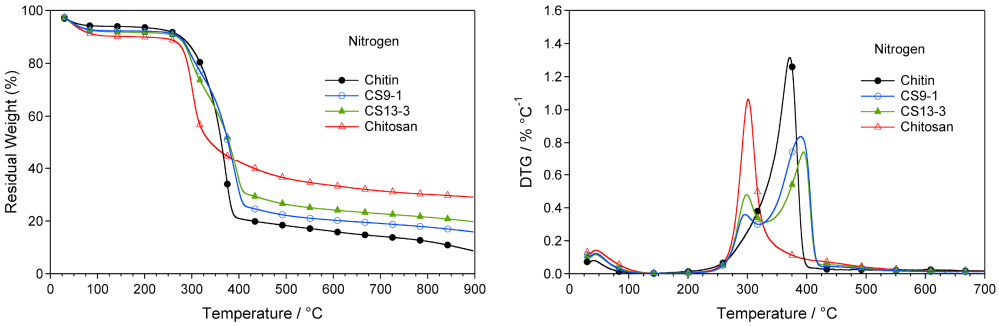

a) b)

Figure 5. Typical TG (a) and DTG (b) traces of chitin and its derivates in nitrogen atmosphere.

2.4.3 UV Spectrophotometry

The method of the first derivative UV spectrophotometry is one of the most used for determination of the DA [19, 20]. It is the simplest and the most convenient among all the presently available methods. Besides, provides accurate and precise results in a simple and fast way for highly deacetylated chitin. This method requires only very small amounts of sample and relies on simple reagents and instrumentation. In addition, the results obtained from method are reasonably independent of protein contamination. The main disadvantages of this method are the requirement of an accurate determination of the weight, particularly difficult for the highly hygroscopic chitosan samples.

Table 7. TGA data of chitin and its derivates in air atmosphere.[a)]

Sample[b)]	Volatile (%)	T_d (°C)	ΔM_1 (%)	T_{p1} (°C)	ΔM_2 (%)	T_{p2} (°C)	ΔM_3 (%)	R_{600} (%)
Chitin	6.0	257	—	—	73.0	371	4.8	16.2
CS9-1	7.7	271	15.7	296	50.7	389	5.5	20.4
CS13-1	5.8	268	19.1	297	49.5	391	5.4	20.2
CS9-3	6.4	270	16.5	297	53.6	390	4.4	19.1
CS13-3	5.1	270	18.5	298	42.7	395	6.4	24.3
CS11-2	5.5	275	17.9	299	50.9	393	5.4	20.3
Chitosan	10.3	270	57.7	302	—	—	—	32.0

[a)] Volatile means the weight loss up to 150 °C. T_d is the pyrolysis decomposition temperature defined at 2 wt-% of weight loss from 150 °C; T_p is the first derivative peak; ΔM is the range of weight loss and R_{600} is the residual weight at 600°C. [b)] See Table 2.2 for code definition.

The two models substances, GluNAc and GluN, are UV chromophoric groups, which contribute in a simple addictive way to the total absorbance of the material at a particular wavelength. Based on this evidence Liu *et al* derived a linear relationship between absorbance and the total molar concentration of the monomers permitting DA determination [32].

The high absorbance of the acetic acid at the working concentration disturbs the determination of both GluNAc and GluN residues when using the zero order UV spectra. The 1st derivative spectra of the AcOH solutions share a common point at around 202 nm for concentrations from 0.005 up to 0.03 M, designated as the zero crossing point by Muzzarelli and Rocchetti [19]. Consequently, the determination of the amine and N-acetyl containing concentration should be relatively insensitive to fluctuations in the acetic acid concentration. Individual calibration curves for both GluNAc and GluN were drawn through a linear regression between the concentration and the 1st derivative UV signal arising from each one (Fig. 6 and 7, respectively). This was deduced from the Beer's lamberts law for diluted

solutions, which correlates the concentration *(C)* with the absorbance *(A)*, for a given wavelength (λ) as shown in Equations 2.6-2.9. Each spectrum shown in Figures 6 a) and 7 a) represents the average of two independent data sets.

$$A(\lambda) = \varepsilon(\lambda) l_{uv} C \qquad \text{Eq. 2.6}$$

Where ε is the molar absorptivity and l_{UV} is the optical length that in the present work is 1 cm. Since both *l* and *C* are independent on the wavelength,

$$\frac{dA}{d\lambda} = \frac{d\varepsilon}{d\lambda} lC = \varepsilon'(\lambda) l_{uv} C \qquad \text{Eq. 2.7}$$

It should be noticed that the acetic acid (AcOH) gives also a signal at λ = 202 nm, thus Eq. 2.7 should be corrected as shown below,

$$A - A_{AcOH} = \varepsilon l_{UV} C \qquad \text{Eq. 2.8}$$

$$\frac{dA}{d\lambda} - \left(\frac{dA}{d\lambda}\right)_{AcOH} = \varepsilon' l_{UV} C \qquad \text{Eq.2.9}$$

Denoting the 1st derivative of the GluNAc and GluN molar absorptivities as ε_a and ε_g respectively, the linear regression of the experimental data gives,

$\varepsilon_a' l_{UV}$= -459.5 M^{-1} and $\varepsilon_g' l_{UV}$= -33.3 M^{-1}

The method for the determination of DA by means of 1st derivative UV is based on the assumption that the molar absorptivities of both GluN (ε_g) and GluNAc (ε_a) chromophoric groups does change when they are covalently bound through β-(1→4) glycosidic linkages. Consequently, the monosaccharides contribute in an addictive way to the total absorbance, which in the presence of acetic acid can be expressed as,

$$A = \varepsilon_a l_{UV} C_a + \varepsilon_g l_{UV} C_g + \varepsilon_{AcOH} l_{UV} C_{AcOH} \qquad \text{Eq. 2.10}$$

where the concentrations (C_i) are in mol/L.

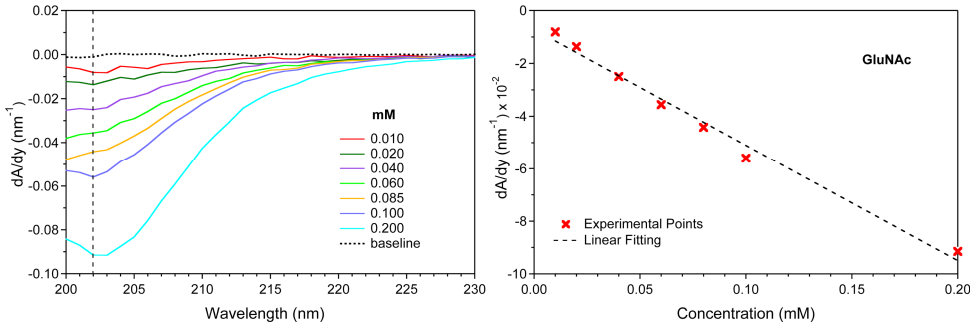

a) b)

Figure 6: *First Derivative UV spectra of GluNAc at 202 nm*

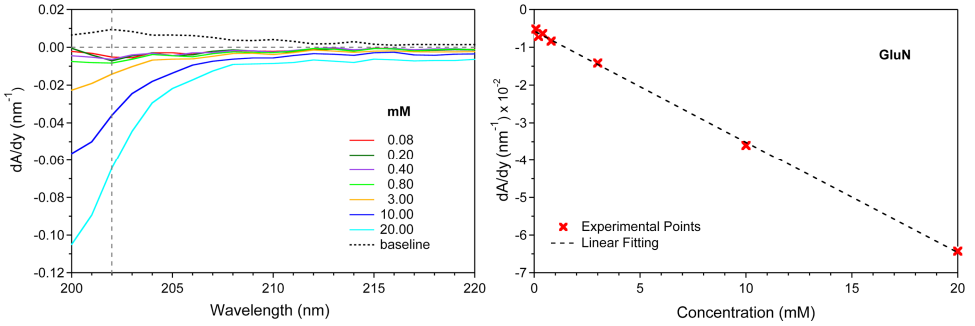

a) b)

Figure 7: *First derivative UV spectra of (a) GluN at λ=202 nm and (b) respective calibration curve*

Since the optical path length (l) and the concentration (C_i) are independent of the wavelength, differentiating Equation 2.10 gives,

$$\frac{dA}{d\lambda} - \left(\frac{dA}{d\lambda}\right)_{AcOH} = \varepsilon'_a l_{UV} C_a + \varepsilon'_g l_{UV} C_g \qquad \text{Eq. 2.11}$$

The degree of deacetylation (DD) is defined as the molar fraction of the GluN units and can be expressed as the ratio between the GluN and total monosaccharides concentrations (C_t),

$$DD = \frac{C_g}{C_a + C_g} = \frac{C_g}{C_t} \qquad \text{Eq. 2.12}$$

Combining Equations 2.11 and 2.12 and rearranging, it is obtained,

$$\frac{1}{C_t}\left[\frac{dA}{d\lambda} - \left(\frac{dA}{d\lambda}\right)_{AcOH}\right] = \varepsilon'_a\, l_{UV} - \left(\varepsilon'_a\, l_{UV} - \varepsilon'_g\, l_{UV}\right)DD \qquad \text{Eq. 2.13}$$

The Equation 2.13 is the basis of the method proposed herein. It is interesting to notice that the method developed by Muzzareli and Rocchetti is a particular case of the last equation [19]. In fact, since $\varepsilon_g >> \varepsilon_a$, Equation 2.13 can be simplified as follow,

$$\frac{1}{C_t}\left[\frac{dA}{d\lambda} - \left(\frac{dA}{d\lambda}\right)_{AcOH}\right] = \varepsilon'_a\, l_{UV} - \left(\varepsilon'_g\, l_{UV}\right)DD \qquad \text{Eq. 2.14}$$

C_t within a chitosan sample cannot be achieved without knowing the DD. Thus, it is more convenient to express the copolymer concentration in terms of solute mass ($\overline{C}_t$) in g/L, which is defined experimentally. These two concentration values are related by the next Equation,

$$\frac{\overline{C}_t}{C_t} = M_a - (M_a - M_g)DD \qquad \text{Eq. 2.15}$$

Where M_a and M_g are the molecular weights of the GluNAc and GluN units within the copolymer. Combining Equations 2.13 and 2.15, it is obtained,

$$\frac{1}{C_t}\left[\frac{dA}{d\lambda} - \left(\frac{dA}{d\lambda}\right)_{AcOH}\right] = \frac{\varepsilon'_a\, l_{UV} - \left(\varepsilon'_a\, l_{UV} - \varepsilon'_g\, l_{UV}\right)DD}{M_a - (M_a - M_g)DD} \qquad \text{Eq. 2.16}$$

Following rearranging, the following results,

$$DD = 1 - \left[\frac{\varepsilon'_g\, l_{UV} - \frac{M_g}{\overline{C}_t}\left(\frac{dA}{d\lambda} - \left(\frac{dA}{d\lambda}\right)_{AcOH}\right)}{\frac{M_a - M_g}{\overline{C}_t}\left(\frac{dA}{d\lambda} - \left(\frac{dA}{d\lambda}\right)_{AcOH}\right) - (\varepsilon'_a\, l_{UV} - \varepsilon'_g\, l_{UV})}\right] \qquad \text{Eq. 2.17}$$

The molecular weight of N-acetyl and amino glucopyranoses comonomers are M_a=203 g/mol and M_g=161 g/mol, respectively. Therefore, Equation 2.17 allows a straightforward determination of the DD. DD can also be expressed in terms of percentage. Consequently, the value of DA (%) can be obtained by the difference.

$$DA(\%)=100-DD(\%)$$

The results obtained for the different chitin derivate samples are reported in Table 8.

Table 8: *Degree of acetylation (DA%) as a function of process variables using UV*

Sample	DA (%)	Error (%)
Chitin	99.7	1.4
Chitosan	5.9	0.9
CS9-1	81.5	4.8
CS11-1	77.1	2.9
CS13-1	66.9	2.7

2.5. Conclusion

Using a statistical approach, temperature and time as process variables of the chitin deacetylation reaction were analysed. Taking on FTIR as one of the most traditional method to determine chitin deacetylation degree, it was verified that the higher level of both variable studied (130 °C-3h) resulted a chitin derivative with ca. 65% of DA. The ANOVA indicated that the most important variable is the temperature and that there is a slight interdependence between both variables in the range studied.

Thermo-oxidation data from TGA showed that the equilibrium moisture of the chitin derivates is equivalent to that of pristine chitin for samples that resulted a DA higher than 75% which value was around 7%.

The values of DA assessed from the 1st derivative UV is in accordance with that using FTIR.

2.6. References

[1] Kurita, K.; *Mar. Biotechnol.*; **2006,** 203.

[2] Sannan, T.; Kurita, K.; Iwakura, Y., *Makromolekulare Chemie-Macromolecular Chemistry and Physics* **1976,** 3589.

[3] Wei, W.; Bo, S. Q.; Li, S. Q.; Wen, Q.; *Int. J. Biol. Macromol.*, **1991,** 281.

[4] Errington, N.; Harding, S. E.; Varum, K. M.; Illum, L.; *Int. J. Biol. Macromol.*,**1993,** 113.

[5] Rinaudo, M.; Milas, M.; Ledung, P., *Int. J. Biol. Macromol.*,**1993,** 281.

[6] Varum, K. M.; Ottoy, M. H.; Smidsrod, O.; *Carbohydr Polym*.,**1994,** 65.

[7] Zydowicz, N.; Vachoud, L.; Domard, A. In *Influence of the acetylation degree of a chitin gel on its physical and chemical properties*, Proceedings of the 1st International Conference of the European Chitin Society, Lyon.. 1996; A. Domard, C. J., R. Muzzarelli, G. Roberts, Ed. Jacques Andre Publisher: Lyon.. 1996; pp 262-270.

[8] Shigemasa, Y.; Saito, K.; Sashiwa, H.; Saimoto, H.; *Int. J. Biol. Macromol.*,**1994,** 43.

[9] Hutadilok, N.; Mochimasu, T.; Hisamori, H.; Hayashi, K.; Tachibana, H.; Ishii, T.; Hirano, S.; *Carbohydr Polym*.,**1995,** 143.

[10] Nordtveit, R. J.; Varum, K. M.; Smidsrod, O.; *Carbohydr Polym.*, **1996,**163.

[11] Peluso, G.; Petillo, O.; Ranieri, M.; Santin, M.; Ambrosio, L.; Calabro, D.; Avallone, B.; Balsamo, G.; *Biomaterials*, **1994,** 1215.

[12] Curotto, E.; Aros, F.,; *Anal. Biochem.*,**1993,** 240.

[13] Ke, H.; Chen, Q.; *Huaxue Tongbao* **1990**, 44.

[14] Rathke, T. D.; Hudson, S. M., *J Polym Sci A Polym Chem*., **1993,** 749.

[15] Hirai, A.; Odani, H.; Nakajima, A.; *Polymer Bulletin* ,**1991,** 87.

[16] Baxter, A.; Dillon, M.; Taylor, K. D. A.; Roberts, G. A. F.; *Int. J. Biol. Macromol.* **1992,** 166.

[17] Domszy, J. G.; Roberts, G. A. F.; *Makromolekulare Chemie-Macromolecular Chemistry and Physics* ,**1985,** 1671.

[18] Sannan, T.; Kurita, K.; Ogura, K.; Iwakura, Y.; *Polymer* **1978,** 458.

[19] Muzzarelli, R. A. A.; Rocchetti, R., *Carbohydr Polym.*, **1985,** 461.

[20] Tan, S. C.; Khor, E.; Tan, T. K.; Wong, S. M., *Talanta.*,**1998,** 713.

[21] Roberts, G. A. F., Thirty years of progress in chitin and chitosan. *Progress in the Chemistry and Application of Chitin and its Derivatives* **2008,** XIII, 7-15.

[22] Bristow, J. Chitosan manufacturing process including demineralization, deproteination, and deacetylation of chitin. WO2009/117499, 20090318., 2009.

[23] Montgomery, D. C., *Design and Analysis of Experiments*. 3rd ed.; John Wiley & Sons: New York, 1991.

[24] Kasaai, M. R.; *J. Agric. Food Chem*., **2009,** 1667.

[25] Kasaai, M. R.; *Carbohydr Polym.*, **2008,** 497.

[26] Duarte, M. L.; Ferreira, M. C.; Marvao, M. R.; Rocha, J.; *Int. J. Biol. Macromol.*, **2002,** 1.

[27] Khan, T. A.; Peh, K. K.; Ch'ng, H. S.; *J Pharm Pharm Sci* **, 2002,** 205.

[28] Brugnerotto, J.; Lizardi, J.; Goycoolea, F. M.; Arguelles-Monal, W.; Desbrieres, J.; Rinaudo, M.;*Polymer*, **2001,** 3569.

[29] Peniche-Covas, C.; Arguellesmonal, W.; Sanroman, J.; *Polym. Degrad. Stab*., **1993**, 21.

[30] Zohuriaan, M. J.; Shokrolahi, F.; *Polymer Testing.*,**2004**, 575.

[31] Alonso, I. G.; Penichecovas, C.; Nieto, J. M.; *J Therm Anal Calorim.*, **1983,** 28, (1), 189-193.

[32] Liu, D. S.; Wei, Y. N.; Yao, P. J.; Jiang, L. B.; *Carbohydr Polym.*, **2006**, 782.

3. CHITOSAN BASED BEADS FOR CONTROLLED RELEASE OF PROTEINS

3.1. Abstract

Chitosan is biocompatible polymer of natural origin widely investigated for applications in drug delivery and regenerative medicine. In this chapter, Chitosan's capability of forming water gelling beads in the presence of non-toxic polyanion was exploited for the loading of two model proteins. Human Serum Albumin (HSA) and porcine trypsin were successfully loaded into chitosan-tripolyphosphate (TPP) beads. Both proteins were highly incorporated when the cross-linking process was allowed to occur for 24 h at room temperature (RT). The release profiles of the two proteins were compared and the faster diffusion of trypsin was associated to its smaller molecular weight. Moreover, in vitro degradation experiments, aimed to mimic physiological degradation pattern of the beads displayed a complete degradation of the material in almost 30 days. Certainly, the preliminary experimental data acquired in the present work represent a starting study for the promising application of chitosan-TPP beads for the controlled release of proteins of therapeutic interest.

3.2. Introduction

Chitosan is a cationic polysaccharide composed of β-1,4 linked 2-amino-2-deoxy-D-glucopyranose (D-glucosamine). In nature it is found in fungi, but it is conventionally produced by deproteinization, demineralization and deacetylation of chitinous material which is widely distributed in living organisms (arthropods, fungi, algae, mollusca, etc.) [1]. Chitosan is biocompatible, it does not cause allergic reactions and rejection. Moreover, chitosan has antacid and antiulcer characteristics, which prevents or weakens drug irritation in the stomach [2]. Under the action of ferments, i*n vivo* it degrades slowly to harmless products (amino sugars), which are completely absorbed by the human body. It is known to possess antimicrobial property and absorbs toxic metals such as mercury, cadmium, lead, etc. In addition, it has good adhesion properties [3], coagulation ability and immunostimulating activity [4].

Chitosan is a widely investigated biopolymer, thanks to its gelling capability and the possibility of applying this natural polymer in regenerative medicine and drug delivery.

In particular, chitosan vehicles appear promising for the administration of therapeutic peptides and proteins such as vaccines, cytokines, enzymes, hormones and growth factors, which are becoming a very important class of both therapeutics and agents for regenerative medicine. Despite the potential of many proteins and peptides, their application in medical treatments is hampered by difficulties in the *in-vivo* administration, related to their chemical and conformational instability, presence of denaturing agents, pH and changes in ionic strength.

Chitosan has been extensively studied as carriers for drugs [5, 6], protein carriers [7] and gels for the entrapment of cells or antigens [8] as a viable route of parenteral drug delivery. Through parenteral drug delivery, especially intravenous injection, one can gain easy access to the systemic circulation with rapid drug absorption and delivery to the site of drug action. Unfortunately, this rapid drug absorption is usually concomitant with a rapid decline in drug levels in the systemic circulation by the reticuloendothelial system. For effective treatment, it is often desirable to maintain systemic drug levels within a therapeutically effective concentration range for as long as treatment is needed [9]. Consequently, considerable effort has been invested in the development of parenteral controlled release formulations.

The depot form, as microspheres/ beads, was found to be the most favorable due to their facile fabrication, long acting controlled drug delivery to the systemic circulation and specific orientation of the drug carrier via active or passive targeting to the treatment site of the body. The carrier matrix should be biocompatible, biodegradable and easily shaped into microsphere/ beads forms, therefore, chitosan is a good matrix for this purpose.

Chitosan microspheres and beads have been prepared using several different methods. The most applied processing methods include internal or external iontropic gelation, which allows for the obtainment of a wide range of products, from micro beads to nanosized particles. Among these, the most popular one is the suspension-crosslinking technique. The following is a typical procedure; an aqueous acidic solution of chitosan is added in the form of small droplets via a syringe into a phase (water/mineral/ oil) as the suspension medium. To this suspension, a chemical/physical crosslinking agent, usually a bifunctional chemical reagent such as; glutaraldehyde, hexamethylene diisocyanate or ethylene glycol diglycidyl ether [8,10] is added. A schematic representation of the technique is given in *figure 1*. The chitosan microspheres obtained are washed with petroleum ether, sodium bisulfide and acetone, respectively, to remove excess crosslinking agent and oil [10,11]. Chitosan microspheres have been evaluated for delivery of different types of active agents such as drugs, proteins and antigens [12-21]. Entrapped drugs can be released via

diffusion from the microspheres; consequently, the swelling ratio significantly affects the release rate.

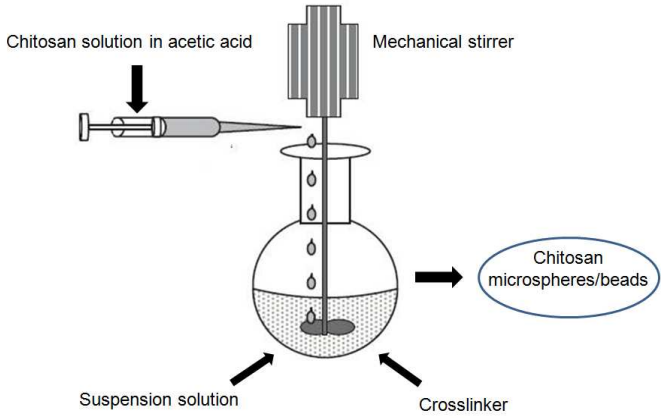

Figure 1. *Schematic representation of the suspension crosslinking technique.*

According to previous studies, drug release from chitosan microparticles could be controlled by crosslinking the matrix using chemical crosslinking agents such as glutaraldehyde [22, -25], NaOH [26-28] and ethylene glycol diglycidyl ether [8]. However, these chemical crosslinking agents have possibility of inducing undesirable effects and are toxic to living systems. Chemically synthesized glutaraldehyde can cause irritation to mucosal membranes due to its toxicity [27,6,29]. To overcome this disadvantage of chemical crosslinking agents, ionic crosslinking agents can be used such as tripolyphosphate (TPP), genipin and alginate [30-33]. For example, chitosan beads, micro or nanoparticles were produced by ionic crosslinking with tripolyphosphate (TPP) [34-36]. Shu and Zhu *et al.* reported the chitosan bead, which was prepared with TPP, increased the drug loading efficiency as well as prolonging the drug release period, and they also showed that citrate cross-linked chitosan film possessed pH sensitive swelling and drug controlled release properties[32,53]. Mi *et al.* reported that the chitosan microspheres prepared with genipin, a naturally occurring crosslinking reagent, affected the release behavior of the drugs in microspheres [6]. TPP is nontoxic and multivalent anions. It can form gel by ionic interaction between positively charged amino groups of chitosan and negatively charged counterion of TPP [29, 32, 37, 38]. This interaction could be controlled by the charge density of TPP and chitosan, which is dependent on the pH of solution. The chitosan matrix could be depended on molecular weight (MW) of chitosan. Puttipipatkhachorn *et al.* (2001) reported

that the higher the MW and degree of deacetylation of chitosan, the lower the release rate of chitosan film [39].

The advantage of iontropic gelation stands in the safeness for the operator, since it avoids the use of hazardous organic solvents and it is based on the cationic nature of chitosan, able to crosslink with multivalent anions such as sulfate, citrate, and tripolyphosphate [40,41]. Tripolyphosphate (TPP) is a non-toxic polyanion which easily interacts with chitosan and has previously been used for the preparation of chitosan beads, microspheres and nanoparticles [38].

In this chapter, two model proteins are applied for the preparation of protein loaded chitosan-TPP beads. HSA has been chosen as middle-size protein model and applied for preliminary evaluation on loading and release kinetics. Porcine trypsin has been applied as model of active agent, due to its enzymatic activity it is generally applied for the assessment of activity maintenance after loading into a polymeric system [42, 43].

3.3. Materials and Methods

3.3.1 Materials

Chitosan and sodium tripolyphosphate(TPP) were purchased from Sigma Aldrich. Molecular weight was in the range of 190,000 - 375,000 as indicated by the supplier, viscosity was about 200 cps . Degree of deacetylation (DD) was >85%. All other reagents and solvents were of reagent grade purity. Human Serum Albumin used as a model protein and lysozyme (hen egg-white) were purchased from Sigma-Aldrich.

3.3.2 Methods

3.3.2.1 Preparation of crosslinked Chitosan beads

Chitosan powder(0.6 g) was dispersed in 20 mL of water containing 1 (v/v)% acetic acid. The mixture was stirred and left overnight to prepare dissolved chitosan solution. The TPP powder was dissolved in distilled water to prepare 1%(w/v) TPP aqueous solutions. The chitosan solution was dropped through a syringe needle into gently agitated TPP solution and the gelled spheres formed instantaneously.

3.3.2.2 Preparation of protein loaded Chitosan beads

The chitosan and TPP solutions of the same concentrations as above were made. The model protein HSA was dissolved directly into the TPP solution. The concentration of the protein in TPP solution is 0.1%. The pH of the TPP solution was maintained at 7. The solution of TPP and albumin was stirred for 10 min to attain homogeneity. The chitosan solution was dropped through a syringe needle into gently agitated TPP solution and the gelled spheres formed instantaneously. The chitosan droplets were stood in the solution for 2 hrs and 24 hrs to cross-link the gel beads and examine the effect of time on crosslinking. To analyse the effect of temperature on cross linking and encapsulation of the protein the beads were allowed to crosslink at room temperature as well as at -4°C. After cross linking, the solidified gel beads were separated and the supernatant collected for further analysis.
Porcine trypsin was loaded under the same conditions of albumin loading, by allowing the crosslinking at room temperature for 24hrs.

3.3.2.3 Morphological characterization

The surface and cross-sectional morphologies of the dried beads were examined using scanning electron microscopy (SEM) and Field Emission Microscopy (FEM).

3.3.2.4 Swelling of Chitosan-TPP beads

The water sorption capacity of the beads was determined by swelling the beads in three media: distilled water, phosphate buffer saline solution (PBS) pH 7.4, cell DMEM growth media. A known weight (16 mg) of the chitosan beads was placed in different media. The wet weight of the swollen beads was determined by first blotting the beads with filter paper to remove the adsorbed water and then weighed immediately on an electronic balance. The percentage swelling of chitosan beads in the media were calculated by the formula:

$$BSR\% = [(W_e - W_o)/W_o]*100 \qquad (1)$$

Where BSR is the beads swelling ratio percent at equilibrium. We denote the weight of the beads at equilibrium swelling and W_o is the initial weight of the beads.

3.3.2.5 Degradation of Chitosan-TPP beads

The in vitro degradation of chitosan TPP beads was followed in 1ml PBS pH 7.4 at 37 °C containing 1.5 µg/ml lysozyme. The concentration of lysozyme was chosen to correspond to the concentration in human serum [44]. Briefly, beads of known dry weights were incubated in the lysozyme solution with gentle mechanical agitation for the period of study. The lysozyme solution was refreshed daily to ensure continuous enzyme activity [45]. After 7, 14, 21 and 28 days, samples were removed from the medium, rinsed with distilled water, dried under vacuum and weighed. The extent of in vitro degradation was expressed as percentage of weight loss of the beads after lysozyme treatment.

3.3.2.6 Evaluation of protein encapsulation efficiency

The supernatants of the drug loaded beads were analysed both by U.V spectrophotometric method for preliminary protein evaluation and by BCA micro assay kit. The BCA Micro Assay Kit was used as per the guidelines mentioned on the kit and the reading was taken at 540nm. All the samples are analysed in triplicate.

The Encapsulation Efficiency (EE%) was calculated from the following expression:

EE%= [Loaded Protein(mg) / Protein Formulation (mg)] *100 (2)

The experiment was performed in two sets: one for 2h cross linking and 24h cross linking and the other for temperature difference during cross linking process i.e. cross linked at room temperature and at -4°C.

The Loading(%) was also calculated by using the formula:

Loading (%)=[Loaded Protein(mg)/lyophilised beads (mg)]*100 (3)

3.3.2.7 Protein release studies

Either albumin or trypsin loaded beads were suspended into 50 mL PBS pH 7.4 and incubated on a shaking water-bath at 37°C. A total of 2 ml supernatant were withdrawn, at appropriate intervals and protein content was determined by BCA micro assay kit. An equal volume of the same dissolution medium was added immediately to maintain a constant volume.

The activity of the released trypsin was also evaluated by a colorimetric assay using N-α-benzoyl-DL-arginine-4-nitroanilide (BApNA) as synthetic substrate for the enzyme.

3.4. Results and Discussion

3.4.1 Preparation of Crosslinked Chitosan Beads

The chitosan gel beads were obtained by using ionotropic gelation method. This method employs the reinforcement of TPP as crosslinking agent. This results in the formation of insoluble chitosan beads, without involving addition of dialdehydes. The electrostatic interaction between TPP and chitosan has been reported and exploited in the pharmaceutical industry to prepare TPP cross linked beads for long time [46]. The TPP treatment of chitosan beads is expected to improve their stability and their applicability in controlled drug delivery [47].

The interaction of a strong polycation chitosan, with tripolyphosphate (TPP) results in a polycation-multivalent anion complex. The nature and extent of ionic reactions have been found to be sensitive to some variable such as the molecular weight, the unit molar ratio, and the charge density of both electrolytes [38]. Depending on these parameters, different types of the chitosan-TPP complexes have been prepared in the recent years [38]. According to the intrinsic pK (pK_0) of chitosan (6.3), chitosan dissolves in acid to present -NH^{3+} site. Tripolyphosphoric acid ($H_5P_3O_{10}$) is a weak polyprotic acid-like phosphoric acid. Due to this reason, sodium tripolyphosphate ($Na_5P_3O_{10}$) dissolves in water to dissociate both OH^- and tripolyphosphoric ions in the TPP solution. The dissociation constant is about $7.453* 10^{-4}$, this means that $P_3O_{10}^{5-}$, $HP_3O_{10}^{4-}$, and $H_2P_3O_{10}^{3-}$ could co-exist in the tripolyphosphate aq. solution in all pH ranges. In original TPP aq. solution (basic, pH not adjusted), the concentration of $P_3O_{10}^{5-}$ and $HP_3O_{10}^{4-}$ is high but the concentration of OH^- is also present. The OH^- or tripolyphosphoric ions ($P_3O_{10}^{5-}$ and $HP_3O_{10}^{4-}$) in this medium could competitively react ionically with the bind site -NH^{3+} in chitosan by deprotonation or ionic crosslinking, respectively (*figure. 2*) which is, what expected in our case as well. This result has also been reported by Mi *et al.*[38], who proposed that at the pH value of 9.7 of TPP , the TPP ions ($P_3O_{10}^{5-}$) competed with OH^- ions to bind with –NH^{3+} in chitosan, resulting in the decrease of binding sites for OH^- ions and increased pH. And hence, the precipitations of complexes in this state were formed both by deprotonation and ionic crosslinking. By adjusting the pH value of TPP solution from 9.7 (initial) to 4.0, only $P_3O_{10}^{5-}$ anions existed and that the precipitations of complexes were formed only by ionic crosslinking between -NH^{3+} and TPP ions.

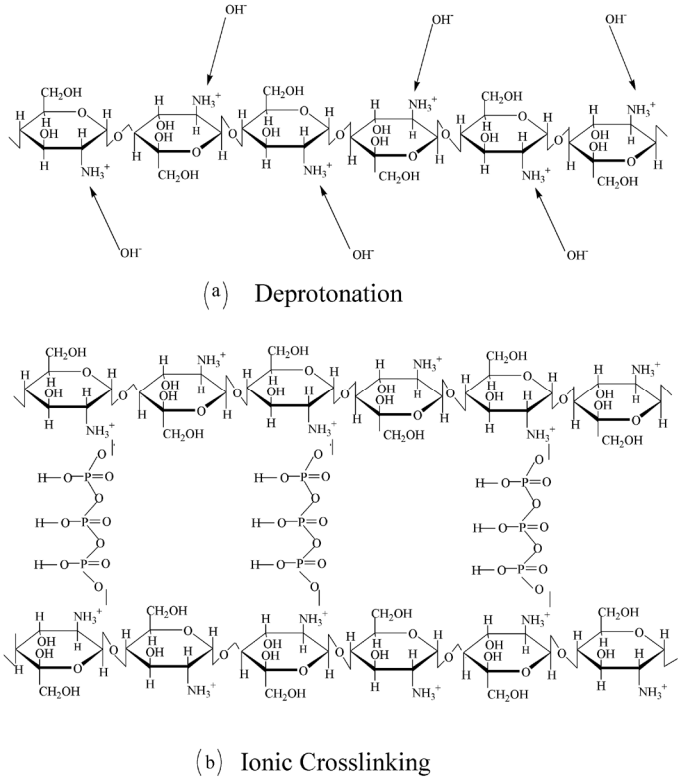

Figure 2. *Ionic reaction of chitosan in TPP aq. solution: (a) deprotonation; (b) ionic crosslinking.*

Mi *et al*. [38] also suggested that, a reversible chitosan-TPP structural change occurs by varying the pH value of curing agent, TPP, as shown in *figure 3*. In the higher pH region, chitosan may take a randomly coiled conformation because of the decrease of ionized amino group and of a weak charge repulsion. However, in the lower pH region, chitosan used possibly takes a more extended form both by hydration of the protonated amino group and by strong positive charge repulsion between NH_3^+ groups. Thus, in the higher pH range region, the chitosan-TPP complexes contain several times more chitosan repeating unit than tripolyphosphate expressed as mole ratio and may accept the looped shape ("loop" means, in this case, TPP combined with chitosan in a "slackened state").

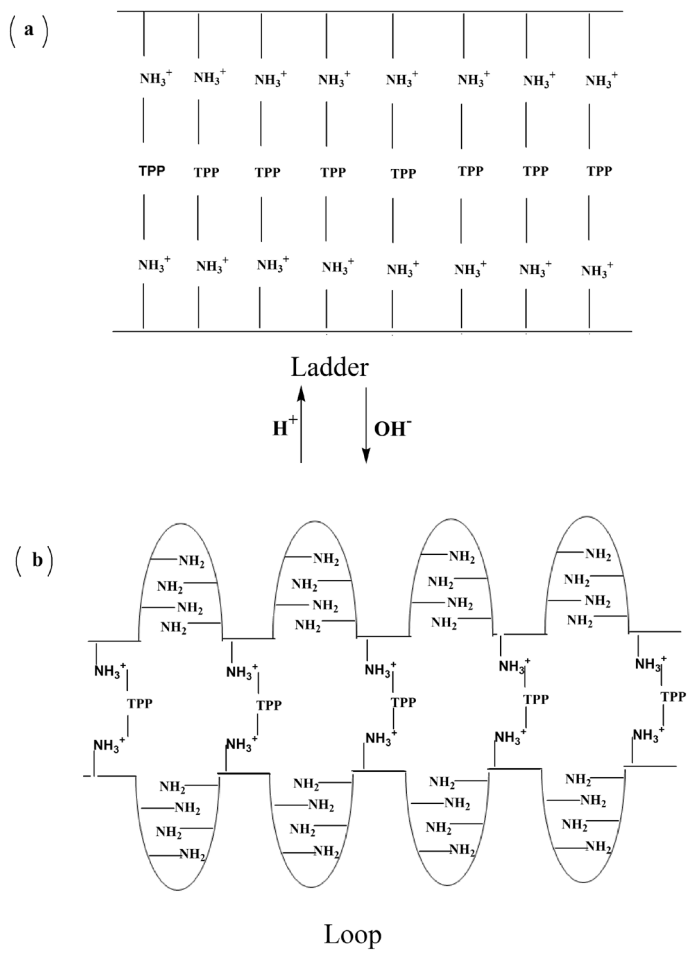

Figure 3. *Ladder-loop transition of chitosan-TPP complex structures: (a) ladder type (b) loop type.*

In this state, the ionic reaction of chitosan-TPP complex should be a pH-dependent coacervation accompanied with slightly ionic-crosslinking. Though according to the facilitation of ionizing chitosan in lower pH range region, the chains of chitosan accept a more extended conformation and they form a complex with TPP in a ladder shaped structure. In this state, chitosan forms complex with multivalent counterions, TPP, through the formation of intermolecular or intramolecular linkages by ionic interaction. Chitosan-TPP complexes were formed only by the ionic interaction between the positively charged amino group and negatively charged counterions, TPP ions. The gelation mechanism of chitosan–TPP complexes in this state should be fully ionic crosslinking controlled.

3.4.2 Morphological Observation

The prepared beads were mostly spherical in their hydrated state (*figure 4*). SEM micrographs of the dry chitosan-TPP beads (*figure 4(b)*) display the formation of beads with drop-like shape of about 800µm diameter for the spherical portion, and a wrinkled surface with little cracks (*figure 4(c)*). The loading of the two model proteins, HSA and trypsin, did not affect the iontropic gelation process. Similarly to plain chitosan-TPP beads, the prepared protein loaded beads were macroscopically spherical in the hydrated form. The SEM micrographs of the dry state display a preserved spherical shape, with about 1-1.5 mm diameter and a more irregular surface with higher rugosity. (*figure 5(a), 5(b)*).

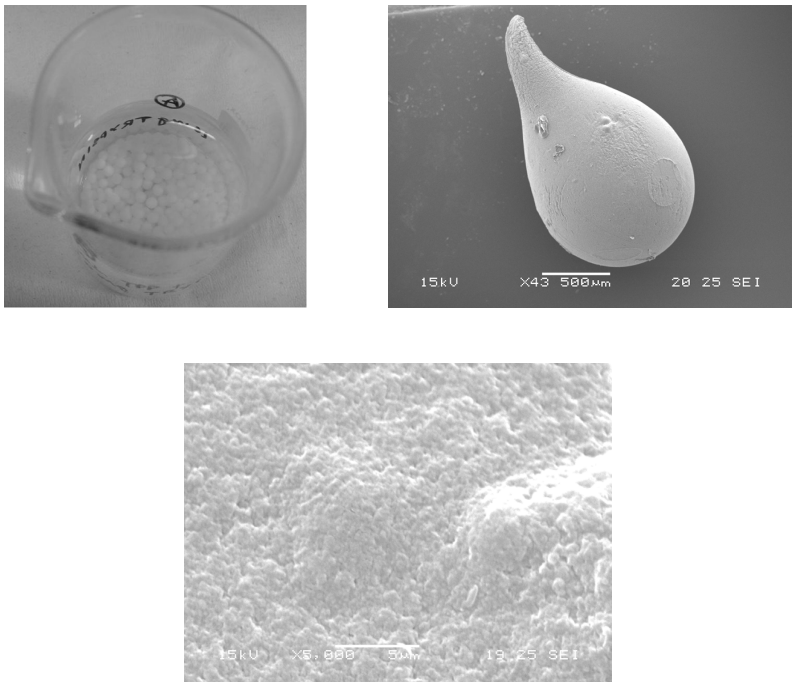

Figure 4: *(a)Macroscopic features of TPP crosslinked Chitosan beads(b) SEM micrographs of Chitosan beads shape (c) SEM of the beads surface*

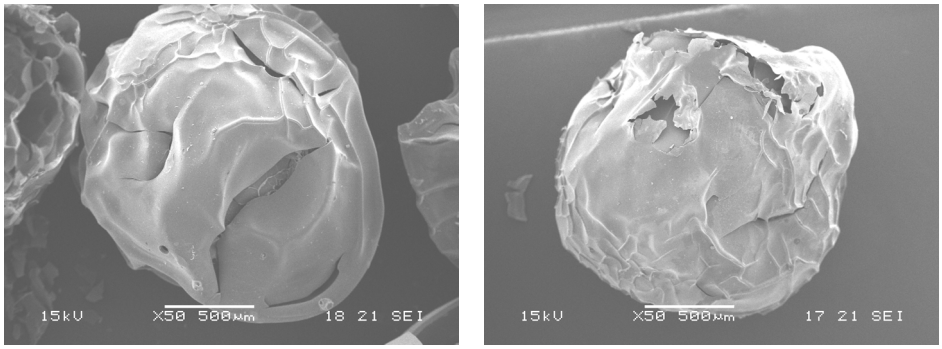

Figure 5: *SEM micrographs of(a) HSA, and (b) trypsin loaded TPP cross linked Chitosan beads.*

3.4.3 Swelling Ratio

The swelling behaviour of plain chitosan-TPP beads was investigated in deionised water, PBS at pH7.4 and DMEM cell culturing medium (Table 1). The swelling equilibrium is reached in about 20h in all the media, leading to swelling ratios values of 120-130%.

Table 1: *Swelling ratios of the TPP cross linked Chitosan beads in water, DMEM and PBS.*

Medium	Water	PBS	DMEM
Swelling%±SD	119.4±3.5	121.2±1.1	131.0±1.9

3.4.4 Degradation of Chitosan-TPP Beads

It is well known that, in human serum N-acetylated chitosan is mainly depolymerised enzymatically by lysozyme and not by any other enzymes or other depolymerisation mechanism [49]. The enzyme biodegrades the polysaccharide by hydrolysing the glycosidic bonds present in the macromolecular backbone. Lysozyme contains hexameric binding site [49] and hexasaccharide sequences, containing 3-4 or more acetylated units, contribute mainly to the initial degradation rate of N-acetylated chitosan [50]. The pattern of degradation of chitosan found in our studies can, in part, be explained by this mechanism of enzymatic degradation. As can be seen in *figure 6*, almost linear enzymatic degradation occurred within 15-17 days and complete degradation of the beads is expected in about 30 days.

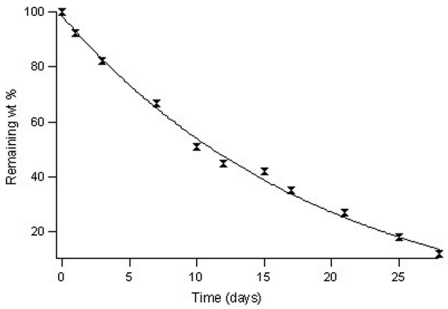

Figure 6: *Enzymatic degradation profile of TPP crosslinked Chitosan beads.*

3.4.5 Protein Encapsulation and Release Studies

The model protein HSA was successfully encapsulated into chitosan-TPP beads. The influence of the crosslinking time and temperature on encapsulation efficiency was evaluated. In particular as reported in Table 2, 2 h of crosslinking were not sufficient to achieve a high EE%, but 24 h were required. Moreover, when the process was performed at 4°C, a lower value of EE% was recorded, probably due to kinetic limitations of the specific low temperature.

When trypsin was applied for the loading, no significant variation of beads formation was observed macroscopically. The loading was performed in this case at room temperature for 24hrs and the EE% was 55%.

The applied formulation parameters involve quite a small amount of protein which is highly incorporated in the beads, EE% up to 64%, and correspond to about 4.1% of beads dry weight.

Table 2:.*Encapsulation Efficiency (EE%) and Loading % of Albumin into the TPP cross linked Chitosan beads, related to cross-linking temperature and duration.*

Run	Cross-Linking		EE %	Loading %
	Temp (°C)	Time (h)		
B-HSA1	RT	2	49	4.1
B-HSA2	RT	24	64	4.1
B-HSA2	4	2	27	3.6

In-vitro drug release was monitored for 5 h. Both proteins easily diffused out of the chitosan-TPP beads under physiological conditions. Results of drug release versus time for albumin and trypsin are shown in *figure 7(a),(b).* As expected, in case of albumin the release of the protein was slower than for trypsin reaching around 17% of cumulative release in 5 h whereas under the same release conditions trypsin was released up to a level of 50%. The difference in molecular weight of the two protein is reflected in their inherent volume and certainly into their diffusion constant.

Anyway, the measurements of the activity of the trypsin released from the beads (*figure 7(c*)) highlight a loss of 15-20% of activity after 30 minutes. Actually, the enzyme released from the beads is accumulated in the releasing medium because only a small amount of volume (2 ml on total 50 ml) are replaced when sampling. It known that trypsin is extremely sensitive to auto-digestion under physiological conditions [51]. The correct evaluation of the activity of the released trypsin would be better performed with the complete withdrawn of the medium at each time, or after addition of calcium ions to the solution, to limit protein autolysis [52].

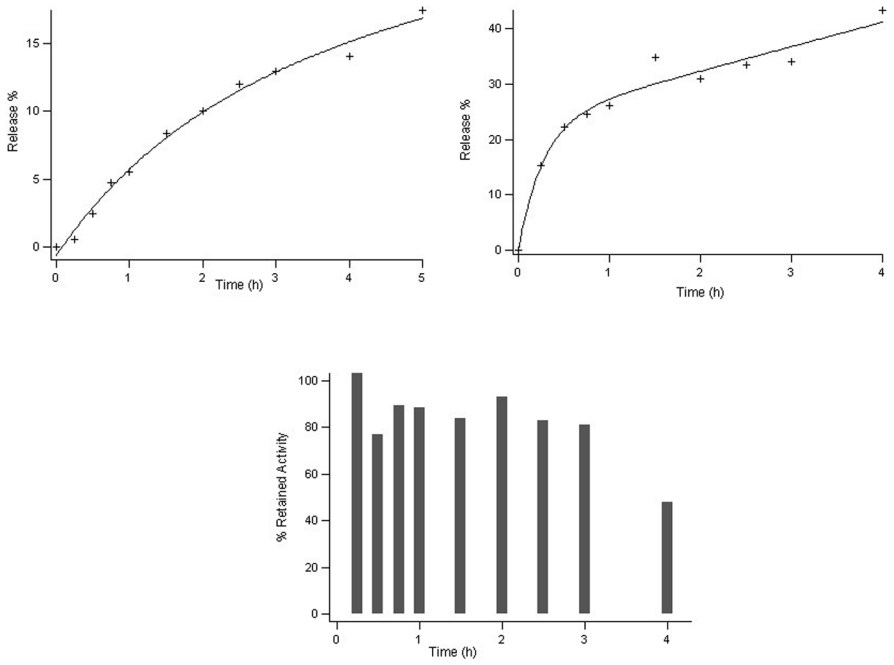

Figure 7: *Drug release profiles of (a) HSA loaded (b) trypsin loaded TPP crosslinked Chitosan beads and (c) Retained activity of trypsin loaded into TPP crosslinked Chitosan beads in the releasing medium.*

3.5. Conclusion

In this work, the conditions for the preparation of protein loaded TPP crosslinked chitosan beads were optimized for the achievement of high protein loading. The activity of the model enzyme was not significantly affected by the process and the observed reduction of activity of the released protein is mostly associated with trypsin autolysis. Under physiological conditions the release profiles of the loaded proteins seem related to their molecular weight and the complete degradation of the TPP crosslinked chitosan beads under lysozyme digestion occurs in 30 days. The present work represent a starting study for the promising application of chitosan-TPP beads for the controlled release of proteins of therauputic interest. Forthcoming studies will be focussed on the reduction of bead size to micro-nanostructures with the same properties of the prepared beads, but with the ability to reach all body areas after conventional administration.

3.6. References

[1].Steinbüchel, A (Ed.) *Biopolymers*, Volume 5-6. *Polysaccharides* I and II Vandamme EJ, De Baets S and Steinbüchel A. WILEY-VCH Verlag GmbH, Weinheim, Germany (2002).

[2]. Gupta, K.C., Ravi Kumar, M.N.V.; *Polym. Int.*, **2000**, 141.

[3]. Bravo-Osuna, I., Vauthier, C., Farabollini, A., Palmieri, G.F., Ponchel, G.; *Biomaterials*, **2007**, 2233.

[4]. Muzzarelli, R.A.A., Muzzarelli, C.; *Adv Polymer Sci*, **2005** ,151.

[5]. Bayomi, M.A., Al-Suwayeh, S.A., El-Helw, A.M., Mesnad, A.F.; *Pharmaceutica Acta Helvetiae*, **1998**, 187.

[6]. Mi, F.L., Sung, H.W., Shyu, S.S.; *J. Appl. Polym. Sci.* **2001**, 1700.

[7]. Calvo, P., Remun˜a´n-Lo´pez, C., Vila-jato, J.L., Alonso, M.J.; *J. Appl. Polym. Sci*. **1997**, 125.

[8]. Mi, F.L., Shyu, S.S., Chen, C.T., Schoung, J.Y.; *Biomaterials*, **1999**, 1603

[9]. 38. Chein, Y.W. (1992). Novel Drug Delivery Systems, 2nd edn, revised and expanded, p. 381, Marcel Dekker Inc., New York.

[10]. Denkbas, E.B., Odabasc, M.; *J. Appl. Poly. Sci.*, **2000,** 1637.

[11]. Denkbas, E.B., Odabasc, M., Kılıçay, E. , Özdemir, N.; *J. Appl. Poly. Sci.*, **2002,**3035.

[12]. Denkbas, E.B., Seyyal, M., Pisckin, E.; *J. Microencapsulation*, **1999,** 741.

[13]. Gupta, K.C. , Ravi Kumar, M.N.V.; *Biomaterials*, **2000,** 1115.

[14]. Hata, H., Onishi, H. and Machida, Y. *Biomaterials*, **2000,** 1779.

[15]. Mi, F.L., Lin, Y.M., Wu, Y.B., Shyu, S.S. , Tsai, Y.H. *Biomaterials*, **2002,** 3257.

[16]. Shi, X.Y., Tan, T.W.; *Biomaterials*, **2002,** 4469 .

[17]. Mi, F.L., Tan, Y.C., Liang, H.F., Sung, H.W.; *Biomaterials*, **2002,**181.

[18]. Takechi, M., Miyamoto, Y., Momota, Y., Yuasa, T., Tatehara, S., Nagayama, M., Ishikawa, K. , Suzuki, K. ; *J. Mater. Sci. Mater. Med.*, **2002,** 973.

[19].Vandenberg, G.W., Drolet, C., Scott, S.L. , Noue, J.D.; *J. Control. Release*, **2001,** 297.

[20].Vila, A., Sanchez, A., Toblo, M., Calvo, P. , Alonso, M.J.; *J. Control. Release*, **2002,**15.

[21]. Zhou, S.B., Deng, X.M., Li, X.H.; *J. Control. Release*, **2001,** 27.

[22]. Jameela, S.R., Jayakrishnan, A.; *Biomaterials*, **1995**,769.

[23]. Genta, I., Perugini, P., Conti, B., Pabanetto, F.; *Int. J. Pharm*. **1997**, 237.

[24].Genta, I., Costatini, M., Asti, A., Conti, B., Montanari, L.; *Carbohyd. Polym*. **1998**, 81.

[25]. Blanco, M.D., Go´mez, C., Olmo, R., Mun˜ iz, E., Teijio´n, J.M.; *Int. J. Pharm.* **2000,** 29.

[26]. Chandy, T., Sharma, C.P.; *Biomaterials*, **1996**, 61.

[27]. Lim, L.Y., Wan, L.S.C., Thai, P.Y.; *Drug Dev. Ind. Pharm*. **1997**, 981.

[28]. Vasudev, S.C., Chandy, T., Sharma, C.P.; *Biomaterials*, **1997**, 375.

[29].Shu, X.Z., Zhu, K.J.; *J. Microencapsulation*, **2001**, 237.

[30]. Ko, J.A., Park, H.J., Hwang, S.J., Park, J.B. , Lee, J.S.; *Int. J. of Pharm.*, **2002,** 165.

[31]. Tan, T., Hu, B., Jin, X. and Zhang, M.; *J. Bioact. Comp. Pol.*, **2003,** 207.

[32]. Shu, X.Z., Zhu, K.J.; *Int. J. Pharm.*, **2000,** 51.

[33]. Mi, F.L., Sung, H.W., Shyu, S.S.; *J. Appl. Polym. Sci.*, **2001,** 1700.

[34]. Bodmeier, R., Oh, K.H., Pramar, Y.; *Drug Dev. Ind. Pharm.* **1989**, 1475.

[35]. Shiraishi, S., Imai, T., Otagiri, M.; *J. Control. Release*. **1993**, 217.

[36].Calvo, P., Remun˜a´n-Lo´pez, C., Vila-jato, J.L., Alonso, M.J.;. *J. Appl. Polym. Sci.*, **1997**, 125.

[37].Aral, C., Akbug˘a, J.; *Int. J. Pharm*. **1998**, 9.

[38]. Mi, F.L., Shyu, S.S., Lee, S.T., Wong, T.B.; *J. Polym. Sci: Polym. Phys.* **1999b**, 1551.

[39]. Puttipipatkhachorn, S., Nunthanid, J., Yamamoto, K., Peck, G.E.; *J. Control. Release*. **2001**, 143.

[40]. Agnihotri, S.A., Mallikarjuna, N.N., Aminabhavi, T.M.; *J. Control Release*, **2004**, 5 .

[41]. Denkbas, E.B., Ottenbrite, R.M; *J Bioact Compat Polym* ,**2006**, 351.

[42]. Chiellini, F., Bartoli, C., Dinucci, D., Piras, A.M., Anderson, R., Croucher, T.; *Int J Pharm*, **2007**, *90*.

[43]. Piras, A.M., Chiellini, F., Fiumi, C., Bartoli, C., Chiellini, E., Fiorentino, B., Farina, C.; *Int J Pharm*, **2008**, 260.

[44]. Porstmann, B. Jung, K., Schmechta, H., Evers, U., Pergande, M., Porstmann, T., Kramm, H.J., Krause, H.; *Clin Biochem*, **1989**, 349.

[45]. Masuda, T., Ueno, Y., Kitabatake, N.; *J Agric Food Chem* **, 2001**, 4937.

[46]. Shu, X.Z., Zhu, K.J.; *Int J* Pharm, **2002**, 217.

[47]. Anal, A.K., Stevens, W.F., Remunan-Lopez, C.; *Int J Pharm*,**2006**,166.

[48]. Varum, K.M., Myhr, M.M., Hjerde, R.J.N.O.; *Carbohydr Res*, **1997**, 99.

[49]. Pangburn SH, Trescony PV, Heller J, Biomaterials, 1982, 105.

[50]. Nordtveit, R.J., Varum, K.M., Smidsrod, O.; *Carbohydr Polym*, **1994**, 253.

[51]. Li, X. F., Nie, X., Tang, J.G.; *Biochem. Biophys. Res. Commun*., **1998**, 235

[52]. Vajda, T., Garai A.; *J Inorg Biochem* **, 1981**, 307.

[53]. Shu, X.Z., Zhu, K.J., Song, W.; *Int. J. Pharm*. **2001,** 19.

4. HYBRID NANOPARTICLES BASED ON CHITOSAN AND POLY(METHACRYLOYLGLYCYLGLYCINE)

4.1. Abstract

A novel polyelectrolyte complex nanoparticles were prepared based on chitosan and poly(methacryloylglycylglycine) [poly(MAGlyGly)]. The physical-chemical properties of the complexes were investigated by means of dynamic light scattering, scanning electron microscopy, zeta potential and X-ray photo electron spectroscopy (XPS). The results indicated that the addition of chitosan into MAGlyGly in DMSO and polymerized subsequently resulted in the formation of nanoparticles in the size range of 100-120 nm with proper chitosan and MAGlyGly weight ratios. Variation of the ratio of the different components revealed that the formation of the nanoparticles depended strongly on the ratio of chitosan and MAGlyGly. The particles also showed difference in size and morphology before and after polymerization. Zeta potential studies highlighted a positive surface charge and the results were well supported by XPS analysis.

4.2. Introduction

Nanotechnology is of great interest in most fields, since it allows manipulating matter at the nanoscale level [1,2] and tailoring final product properties. Among the various tools used in nanotechnology, nanoparticles represent a widely studied area. Nanoparticle synthesis is currently intensely researched due to its wide variety of potential applications, including food processing [3,4] and biomedical [5], optical [6], and electronic devices [7]. The use of natural polysaccharides in the preparation of nanoparticles has attracted attention [8-11] due to their biocompatibility, biodegradability, and hydrophilicity, which are favorable characteristics in various applications. Chitosan nanoparticles [12,13] stand out due to their unique properties. Chitosan is a polysaccharide derived from chitin, which may be obtained from crustaceans, insects, fungi, etc. [14]. Several appealing properties have been reported, such as film-forming ability, gelatinous characteristics, bioadhesion, and skin penetration-enhancing effects, which may be explained by the opening of tight epithelial cell junctions. Due to its polymeric cationic characteristics, Chitosan may interact with negatively charged molecules and polymers [15]. In detail, chitosan is a weak base with a pKa value of the D-glucosamine residue of about 6.2-7 and therefore is insoluble at neutral

and alkaline pH values. Chitosan is readily soluble in dilute acidic solutions below pH 6.0. The presence of the amino groups indicates that pH substantially alters the charged state and properties of chitosan [16]. At low pH, these amines get protonated and become positively charged, making chitosan a water-soluble cationic polyelectrolyte. It is this cationic property that makes it easy for processing into various formulations.

In the specific field of biomedicine, natural and synthetic polymers that are biocompatible, biodegradable, capable of binding with proteins, genes, nucleic acids, acidic lipids as well as having the ability of absorption enhancing and mucosal adhesion without toxicity are required [17]. Chitosan, as a polymer best suits for the above said applications. On the basis of these considerations, many types of nanosized polymeric carriers were developed, including polymeric micelles [18], polymer modified liposome [19], and some other colloidal systems [20]. Among them, biocompatible polymeric nanoparticles have been extensively investigated for both therapeutic (e.g., drug delivery) and diagnostic (e.g., imaging) purposes [21-24]. As a successful drug delivery vehicle, polymeric nanoparticles should have the ability to deliver drug to desirable sites and to escape from the biological particulate filter known as the reticuloendothelial system (RES), resulting in long circulating in vivo [25]. To use them for the incorporation of bioactive macromolecules and vaccines such as monoclonal bodies, plasmids, antigens, oligonucleotides, enzymes, recombinant proteins, and peptides for therapeutic applications, the design/preparation of these systems must be monitored in terms of particle shape and morphology, size distribution, surface chemistry, and polymer nature [26]. Among the methods of development of polymer dispersions for biomedicine, the employment of polyelectrolyte complexes represents a very attractive approach, mainly due to the simplicity involved in the preparation [27].

Nanoparticles made of polyelectrolytes complexation (PEC) have shown potential for use as drug delivery systems [28,29]. Polyelectrolyte complexes are formed by interactions between macromolecules that carry oppositely charged ionisable groups [30]. During the last years PECs on the base of natural and synthetic polymers evoked a particular interest. Chitosan, whose structure is shown in *figure 1*, is a well-known natural cationic polyelectrolyte that processes primary amine groups ($–NH_2$) and as mentioned earlier also, can be protonated in acidic environments to become $–NH_3^+$. Recently the use of complexation of oppositely charged macromolecules to prepare chitosan complexes and nanoparticulate structures as controlled drug release formulations has attracted much attention [31-35], because this process is simple, feasible, and can usually be performed under mild conditions. Moreover, it has attracted interest as a biocompatible, stimulus–responsive, mucoadhesive material for use in biomedical applications [36-38].

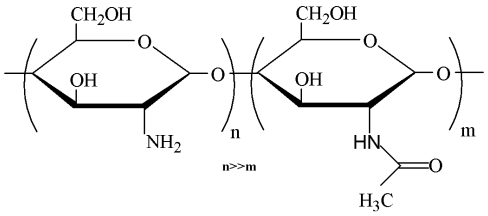

Figure1: *Chitosan*

These complexes made up of polymeric systems can be used to physically trap an antitumor agent and release it in a sustained form directly at the tumor site [39,40]. They also allow for controlling the release pattern of drug and sustaining drug levels for a long time by appropriately selecting the polymeric carrier [41].

Water-soluble polymers such as *N*-(2-hydroxypropyl)-methacrylamide (HPMA) co-polymers are a class of synthetic polymers that are frequently employed as drug carriers because of their ability to improve the solubility of hydrophobic compounds, reduce non-specific toxicity, and increase the therapeutic index of low molecular weight anticancer drugs [42]. Anticancer drugs chemically bound to water-soluble polymeric carriers such as HPMA co-polymers (polymeric prodrugs) have exhibited decreased systemic toxicity, as a result of the altered biodistribution of polymer-bound drugs as compared to free drugs [43]. Several drug-polymer conjugates based on HPMA co-polymers have been studied clinically. A doxorubicin-(HPMA co-polymer) conjugate, known as PK1, was the first drug-polymer conjugate to enter clinical trials [44]. Targeted HPMA co-polymer-bound doxorubicin conjugates have previously been shown to have a significant anti-tumor effect *in vitro* and *in vivo* [45,46] and have shown greater potency than free doxorubicin in the treatment of ovarian cancer *in vivo* and *in vitro* [47]. Recently authors have reported the first endocrine-chemotherapy combination in the form of the model compound HPMA co-polymer-aminoglutethimide doxorubicin [48]. In our laboratory, nanoparticles based on bioeliminable co-polymers poly(methacryloylglycylglycine-OH_x-*co*-hydroxypropylmethacrylamide$_y$) were prepared and loaded with HSA as model drug [49].

Based on this approach methacryloylglycylglycine (MAGlyGly) was prepared and used for preparing nanoparticles employing compelexation with chitosan. MAGlyGly is a biocompatible synthetic polyelectrolyte with polyanionic character, its wide applicability as a co-monomer in the field of drug delivery is impressive. It has carboxylic groups which ionize to become COO- groups that can effectively react with the NH_3^+ groups of chitosan to form a polyelectrolyte complex. Various reaction parameters have been optimized to form

nanoparticles with this PEC's. When ionized, both polyelectrolytes have intrinsic biological properties. In parallel, the production of nanoparticles through in situ polymerization appears to be an interesting route as well. In the present work, the possibility to prepare chitosan based nanoparticles by the polymerization of the anionic monomer MAGlyGly was investigated and the effect of subsequent polymerization observed. Hence, the objective of the present study was to optimise the preparative conditions of chitosan$_x$-poly**(**MAGlyGly)$_y$ nanoparticles and to establish the interaction between the two using various techniques.

4.3. Materials and Methods

4.3.1 Materials

Glycyl-glycine (GlyGly), methacryloyl chloride, ammonium persulphate [$(NH_4)_2S_2O_8$], sodium metabisulfite ($Na_2S_2O_5$) and Chitosan (Mw = 71.3 kDa, degree of deacetylation 93%) were purchased from Sigma-Aldrich and used as received.

4.3.2 Methods

4.3.2.1 Synthesis of MAGlyGly

GlyGly (one equivalent) was added to a solution of sodium hydroxide (one equivalent) in water (19,8 w/v). Methacryloyl chloride was cooled to 0°C (one equivalent) and to it a solution of sodium hydroxide (one equivalent) in water (19,8 w/v) was added dropwise and simultaneously. The reaction mixture was stirred at room temperature for two hours than acidified with concentrated hydrochloric acid to pH 2. The crystal that precipitated from solution was isolated by recrystallization from 1:1 water/ethanol solution. The crystalline white monomer was dried in vacuum. The obtained yield was 50%.

FT–IR (KBr): $\overline{\nu}$ = 3380-3100 (ν OH, NH), 1740 (ν C=O carboxylic), 1647.4 (ν C=O amide I band), 1605.9 (ν C=C), 1540.4 (δ N-H and ν C-N amide II band), 1431 (ν C-O and O-H carboxylic) and 1337.9 cm^{-1} (δ CH_3).

^{1}H NMR (200 MHz, DMSO-d_6): δ (ppm) 1,8(s, 3H), 3,8(m, 4H,), 5,3 (s, 1H,), 5,7 (s, 1H,) and 8,2 ppm (m, 2H).

4.3.2.2 Preparation of Chitosan-MAGlyGly nanoparticles [CS_x-$(MAGlyGly)_y$]

Nanoparticles were prepared for 50:50 (w/w) and 25:75 (w/w) ratio of chitosan and MAGlyGly respectively. Data relevant to individual experiments are summarized in Table 1, whereas a typical experiment is described as follows.

10 mg of chitosan was dissolved in a solution of 25,5 mg of MAGlyGly in 5 mL of 1:9 dimethyl sulphoxide/water mixture for two hours under magnetic stirring. With the slow dissolution of chitosan in the solution mixture, opalescence was observed. After two hours under magnetic stirring the suspension was stored at 4°C and submitted to further investigations.

After the dissolution of chitosan in the MAGlyGly solution, the suspension was stored at 4°C.

4.3.2.3 Preparation of Chitosan-polymerized(MAGlyGly) nanoparticles [CS_x-poly$(MAGlyGly)_y$]

CS_x-poly$(MAGlyGly)_y$ nanoparticles were obtained by polymerizing MAGlyGly in DMSO solution containing chitosan as described below. Nanoparticles were prepared for both the ratios of 50:50 (w/w) and 25:75 (w/w) of chitosan and MAGlyGly respectively also in this case. Data relevant to individual experiments are summarized in table 1, whereas a typical experiment is described as follows.

10 mg of chitosan was dissolved in a solution of 25,5 mg of MAGlyGly in 5 mL of 1:9 dimethyl sulphoxide/water mixture for two hours under magnetic stirring. After the dissolution, 10 µL each of 1% w/v $[(NH_4)_2S_2O_8]$ and 1% w/v $(Na_2S_2O_5)$ solutions were added to the chitosan-MAGlyGly formulation and the mixture was maintained under stirring at 70°C for an additional hour then cooled in an ice bath for 20 minutes. The nanoparticle suspension was stored at 4°C.

For purification, the nanoparticle suspension was placed in a polypropylene conical tube and centrifuged at 8000 *g* for 45 min at 25 °C by using an ALC PK121 R refrigerated centrifuge. The resulting pellet was suspended in distilled water.

Table 1 *Formulations of CS_x-$(MAGlyGly)_y$ nanoparticles.*

Sample	MAGlyGly (mg)	Chitosan (mg)	$(NH_4)_2S_2O_8$[a] (µL)	$Na_2S_2O_5$[a] (µL)
CS_{50}-poly$(MAGlyGly)_{50}$ (50/50 w/w)	177,5	177,5	71	71
CS_{50}-$(MAGlyGly)_{50}$ (50/50 w/w)	177,5	177,5	-	-
CS_{25}-poly$(MAGlyGly)_{75}$ (25/75 w/w)	255	100	100	100
CS_{25}-$(MAGlyGly)_{75}$ (25/75 w/w)	255	100	-	-

[a] 1% aqueous solution

4.3.2.4 Granulometry in suspension

Dimensional analyses were carried out using a Coulter LS230 Laser Diffraction Particle Size Analyzer, equipped with *small volume module plus*. Nanoparticle suspension were added into the cell unit until a 30-50% obscuration of polarization intensity differential scattering (PIDS) detector was reached. Deionised water was used as background and diameter distribution was processed using the Fraunhofer optical model. Three runs were performed on each sample.

4.3.2.5 Morphological analysis

Nanoparticle morphology was investigated by means of scanning electron microscopy (SEM), using a JEOL LSM5600LV scanning electron microscope. The nanoparticle samples were purified by centrifugation and the resulting pellets were resuspended in deionised water and lyophilised. Gold sputtering was performed before SEM analysis.

4.3.2.6 Spectroscopic analysis

Infrared (FT-IR) spectra were recorded on liquid films and KBr pellets by using a Jasco FT–IR 410 spectrophotometer.

Nuclear Magnetic Resonance (NMR) spectra were recorded on 5–10% (w/v) solutions, in deuterated solvents, at 25 °C by using a Varian Gemini 200 spectrometer and tetramethylsilane (TMS) as internal standard. ^{1}H–NMR spectra were recorded at 200 MHz, using the following spectral conditions: 3 KHz spectral width, 30 ° impulse, 2s acquisition time, 1–16 transients. Chemical shifts (δ) are reported in ppm and referred to tetramethylsilane as standard. Peak multiplicity is denoted by the following: s = singlet, d = doublet, dd = double doublet, t = triplet, m = multiplet.

CS_x-poly(MAGlyGly)$_y$ and CS_x-(MAGlyGly)$_y$ nanoparticles were pressed into KBr pellets (1:100 copolymer/KBr ratio) and the FT-IR spectra were recorded by using the same, Jasco FT-IR 410 spectrophotometer

4.3.2.7 Surface chemical characterization

X-ray Photoelectron Spectroscopy (XPS) was used to assess the surface chemical composition of CS_x-(MAGlyGly)$_y$ and of CS_x-poly(MAGlyGly)$_y$ nanoparticles. Surface chemical characterization of the nanomaterials was performed using a Thermo VG Theta probe spectrometer equipped with a microspot monochromatized Al Kα source and a flood gun combined with an argon gun for compensation of electrostatic charging of samples.

The Al Kα line (1486.6 eV) was used throughout the work and the base pressure of the instrument was 10^{-9} mbar. Survey and high-resolution spectra were acquired in fixed analyzer transmission mode with pass energies of 150 and 50 eV, respectively. Data analysis was performed using the *Avantage* software package, which consists of a non-linear least-squares fitting program. The surface composition was determined by using the manufacturer's sensitivity factors.

The fractional concentration of a particular element X (% X) was computed using the following equation:

$$\% X = [(I_x/f_x)/ \Sigma(I_i/f_i)] \cdot 100$$

where I_i and f_i are the integrated peak areas of each of the n detected elements and their sensitivity factors, respectively. The values of binding energies (BE–eV) were taken relatively to the binding energy of C1s-electrons of hydrocarbon contaminants on the sample

surface (from an adventitious carbon), which is accepted to be equal to 285.0 eV. The curve fitting process was done by imposing the same peak full width at half maximum (FWHM) to the all N1s peaks.

4.3.2.8 Zeta potential analysis

Zeta potential analyses were performed on CS_x-$(MAGlyGly)_y$ and CS_x-poly$(MAGlyGly)_y$ samples purified by centrifugation and resuspended in saline (NaCl 0.9%) so that the final concentration of nanoparticles was about 0.1 mg / ml and the pH around 3.5-4. The tests were performed using Beckman Coulter DELSA 440SX at 25 ° C with a maximum deviation of 0.4 °C between the ends of the cell and setting constant values of current. Statistically significant results were obtained from the average of 3 replicates for each matrix used.

4.3.2.9 Thermal analysis

Thermal Gravimetric Analysis (TGA) measurements of were carried out on 5-10 mg nanoparticles samples in the 30–900°C temperature range in a nitrogen atmosphere at 10 °C/min heated with a Thermogravimetric Analyzer TGA Q500.

4.4. Results And Discussion

4.4.1 Preparation & Characterization of MAGlyGly

A similar amidation reaction between methacryloyl chloride and glycylglycine, conducted in a basic aqueous media with NaOH, led to the formation of the monomer, methacryloylglycylglycine-OH (MAGlyGly). The system was obtained pure after recrystallization from methanol with yield of 50% *(Scheme 1).*

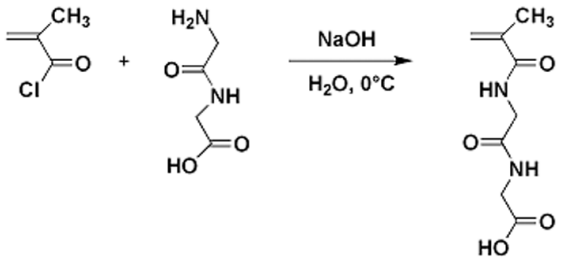

Scheme 1: *Synthesis of MAGlyGly.*

The formation of the product was confirmed by spectroscopic characterizations *(figure 2).*

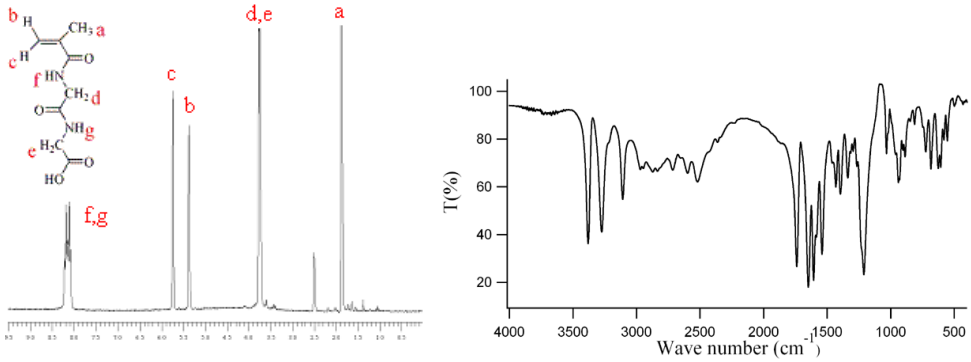

Figure 2 *Spectroscopic characterization of MAGlyGly: (a) ^{1}H- NMR spectrum, (b) FT-IR spectrum.*

4.4.2 Synthesis & Characterization of [CS_x-(MAGlyGly)$_y$] and [CS_x-poly(MAGlyGly)$_y$] nanoparticles

In this study, a novel nanoparticle system composed of chitosan and poly(MAGlyGly) was prepared with a simple and mild method under magnetic stirring. Briefly, chitosan was added to a solution of MAGlyGly in DMSO under stirring for two hours. This technique is promising because the nanoparticles can be prepared under mild conditions without using harmful solvents. It is well known that organic solvents may cause denaturation of peptide or protein drugs that are unstable and sensitive to their environments [50]. The prepared nanoparticles are intended to be used for drug delivery applications and hence such mild conditions are congenial. In our case, when chitosan is added to MAGlyGly solution, it goes into a polyelectrolyte form, which establishes electrostatic interactions with MAGlyGly and leads to the formation of CS_x-$MAGlyGly_y$ nanoparticles. This phenomenon is observed immediately by the appearance of opalescence. It is important to point out that

opalescence has been used as an indication of nanoparticle formation in several other systems, whereas precipitation indicates the production of an unstable suspension due to a much larger particle size and/or the formation of agglomerates or unstable surface property balance [51]. This leaded us to investigate the particles at this stage of preparation. It was observed that the formed particles appeared in small clusters *(figure 3)*. It is also significant to note here that the formation of chitosan nanoparticle is strongly correlated to the presence of MAGlyGly. In fact, experiments carried out in the same conditions but without MAGlyGly showed no nanoparticles formation.

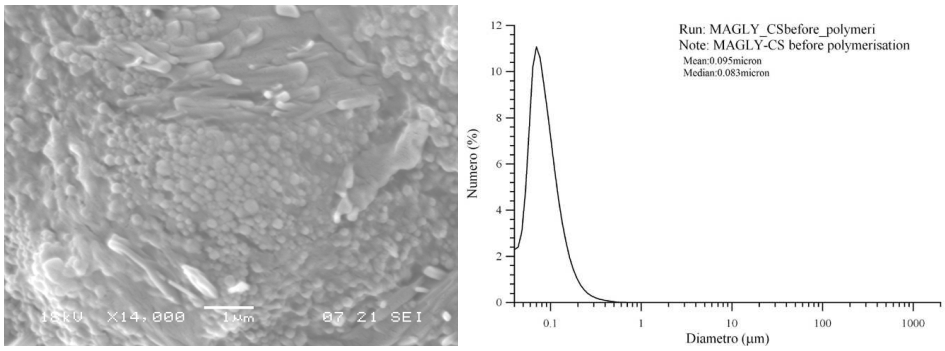

Figure 3 *(a) SEM microphotographs of CS_{25}-$(MAGlyGly)_{75}$ nanoparticles; (b) Diameter distribution of CS_{25}-$(MAGlyGly)_{75}$ nanoparticles.*

In particular, the fact that we are more interested in is in the formation of a polyelectrolyte complex, and by definition, a polyelectrolyte complex is formed by the reaction of two oppositely charged polymers. The electrostatic interaction between the positive charge of —NH_3^+ group and the negative charge of carboxyl group is one of the most important factors. Even though this interaction was sufficient to lead to the formation of nanoparticles, it would be favourable to have MAGlyGly polymerized also for a toxicity point of view. Hence, in our experiments we polymerized MAGlyGly using [$(NH_4)_2S_2O_8$] and $Na_2S_2O_5$ as radical initiators. When chitosan is dropped into this solution, inter- and intra- molecular electrostatic attractions occur between the anionic carboxyl group of poly(MAGlyGly) and the cationic amino groups of chitosan. A schematic representation of the complex is shown in *scheme 2.* The formation and properties of the polymer complex depends on the charge ratio of the anionic-to-cationic species [52]. This type of interaction is also in agreement with similar systems using acrylic acid reported in the literature [53,54]. Three type of ratios in terms of weight namely, 50:50, 25:75 and 60:40 of chitosan and MAGlyGly respectively were used to see if the change in composition had some effect in the

formation of the nanoparticles. Nanoparticle formation was observed only in case of 50:50 and 25:75 of chitosan and MAGlyGly respectively, whereas the 60:40 ratio resulted in precipitation of chitosan in MAGlyGly solution.

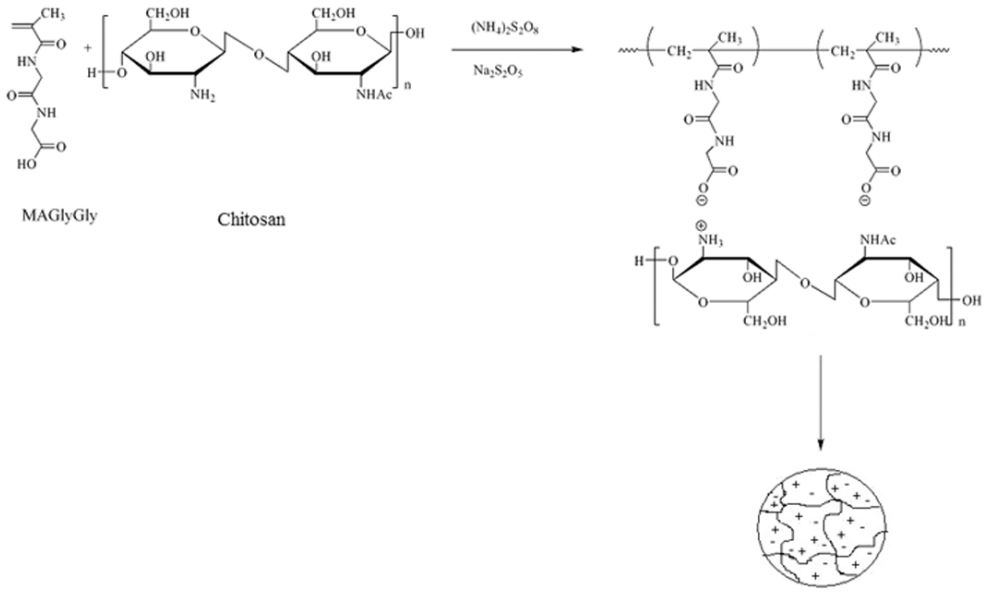

Scheme 2 *A schematic representation of the proposed structure of the nanoparticles* CS_x-poly(MAGlyGly)$_y$ *obtained.*

4.4.3 SEM Analysis

SEM analysis showed a homogeneous morphology with a uniform particle size distribution and a good spherical shape. Nanoparticles size resulted in the range of 120-140 nm.

Nanoparticles were formed for CS_{50}-poly(MAGlyGly)$_{50}$ and CS_{25}-poly(MAGlyGly)$_{75}$ and no difference in morphology and size of nanoparticles was observed *(figure 4(a),(b))*. However, a significant difference was observed when the nanoparticles were prepared after polymerization. Subsequent in situ polymerization of MAGlyGly in the presence of chitosan led to a considerable increase in the number of nanoparticles and to an increase in their size as confirmed by SEM and granulometry in suspension analysis *(figure 3, 4).*

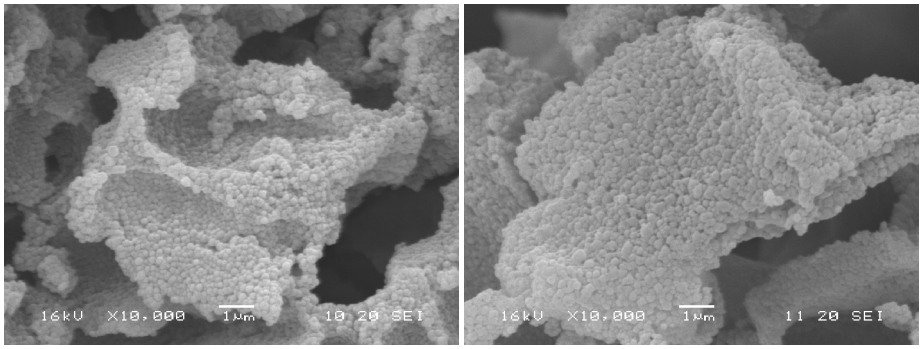

(a) (b)

Figure 4: *SEM microphotographs of (a) CS_{25}-poly(MAGlyGly)$_{75}$ nanoparticles; (b) CS_{50}-poly(MAGlyGly)$_{50}$ nanoparticles.*

4.4.4 FT-IR Analysis

The interaction of chitosan, MAGlyGly was investigated using FT-IR spectroscopy. The spectrum of chitosan (*figure 5(a))* presents characteristics peaks at 3435 cm^{-1} assigned to stretching vibration of NH_2 and OH groups and at 1651.7 cm^{-1} due to C=O of amide I. The MAGlyGly spectrum, also *(figure 5(b))* shows peculiar peaks at 1740cm^{-1} due to C=O stretching, at 1540cm^{-1} related to N-H bending vibration of amide II, at 1647 cm^{-1} due to the stretching of amide I and at 1432 cm^{-1}assigned to the OH of carboxylic group.

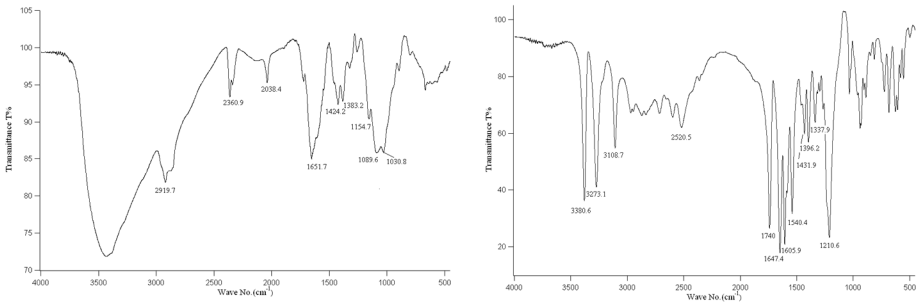

Figure 5: *Representative FT-IR transmittance spectra of (a) Chitosan (b) MAGlyGly*

On comparing the spectra of MAGlyGly, chitosan and CS_x-poly(MAGlyGly)$_y$ nanoparticles, it was observed the absence of the band at 1740 cm^{-1} and the presence of two new bands at 1642 and 1393.8 cm^{-1} due to C=O asymmetric and symmetric stretching respectively of COO^- and of a band at 1539.4 cm^{-1} related to symmetrical stretching of NH_3^+ group *(figure 6).* The appearance of these new bands indicates the occurring of ionic

interaction between poly(MAGlyGly) and chitosan associated with the formation of nanoparticles *(figure 6).* This observation was valid for both CS_{50}-poly(MAGlyGly)$_{50}$ and CS_{25}-poly(MAGlyGly)$_{75}$

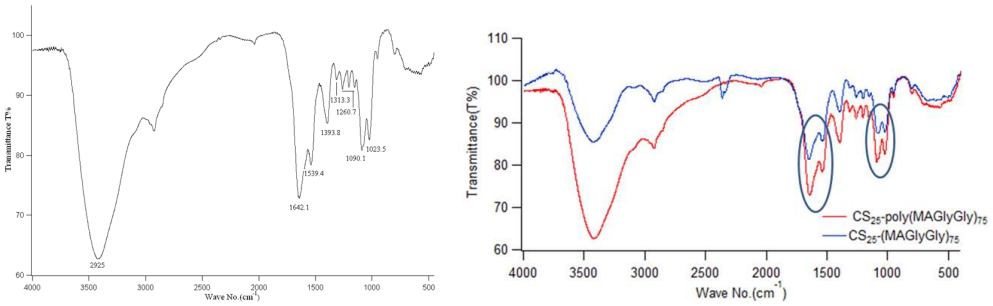

Figure 6 *Representative FT-IR transmittance spectra of (a) CS_{25}-poly(MAGlyGly)$_{75}$ nanoparticles.(b)comparison of CS_{25}-(MAGlyGly)$_{75}$ and CS_{25}-poly(MAGlyGly)$_{75}$ nanoparticles.*

As can be seen in *figure 6(b),7(b),* no significant difference between the spectrum of the polymerized and unpolymerised system of CS_x-(MAGlyGly)$_y$ nanoparticles were observed.

Another important observation that was made on comparing the spectra's was that the spectra of CS_{25}-poly(MAGlyGly)$_{75}$ showed a strong similarity with the spectrum of MAGlyGly in the region between 1260 and 1394 cm^{-1}, while the spectra of nanoparticles of CS_{50}-poly(MAGlyGly)$_{50}$ had less resemblance with the spectrum of MAGlyGly, confirming the presence of a lower percentage of MAGlyGly in their composition.

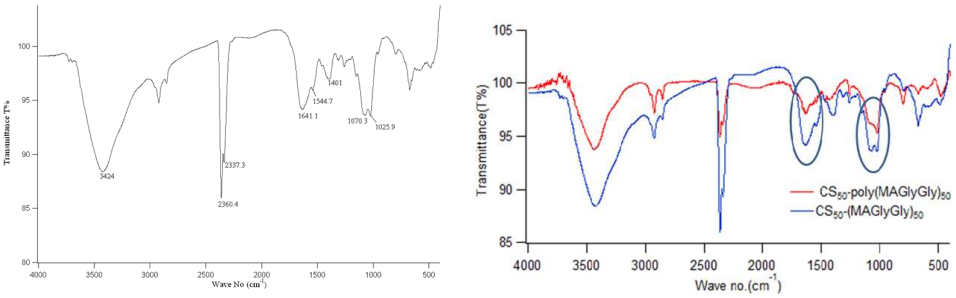

Figure 7 *Representative FT-IR transmittance spectra of (a) CS_{50}-poly(MAGlyGly)$_{50}$ (b) comparison of CS_{50}- (MAGlyGly)$_{50}$ and CS_{50}-poly(MAGlyGly)$_{50}$*

4.4.5 X-Ray Photoelectron spectroscopy

Additional information about the composition and structure of CS_x-$(MAGlyGly)_y$ and CS_x-poly$(MAGlyGly)_y$ nanoparticles in upper layers have been obtained by recording and examining XPS spectra. In order to discriminate the different chitosan and MAGlyGly contributions in the hybrid nanoparticles, pure materials have been also analyzed.

The following CS_x-$(MAGlyGly)_y$ formulations have been analyzed:

1) CS_{50}-$(MAGlyGly)_{50,}$ CS_{50}-poly$(MAGlyGly)_{50}$
2) CS_{25}-$(MAGlyGly)_{75,}$ CS_{25}-poly$(MAGlyGly)_{75}$

The most abundant elements detected on the surface of the nanomaterial are carbon, oxygen and nitrogen, while sulphur, silicon and chlorine are detected at lower concentrations. In particular, in *figure 8* , the survey spectra of chitosan, MAGlyGly, CS_x-$(MAGlyGly)_y$ and CS_x-p$(MAGlyGly)_y$ samples are reported. Atomic percentages of the relevant detected elements are reported in Table 2.

By these data an evaluation of the O1s/N1s corrected areas ratio was performed, giving the following results: 4/1 and 2.3/1 in chitosan and MAGlyGly, respectively (both as the expected stoichiometric value), 3/1 and 3.2/1 in CS_{50}-$(MAGlyGly)_{50}$ and CS_{50}-poly$(MAGlyGly)_{50}$, respectively and 3.4/1 and 3.3/1 in CS_{25}-$(MAGlyGly)_{75}$ and CS_{25}-poly$(MAGlyGly)_{75}$, respectively. These quantitative informations resulted in general agreement with the stoichiometry of the chemicals employed for the nanoparticles synthesis.

Table 2: *Atomic percentages relevant to Chitosan, MAGlyGly, CS_{50}-$(MAGlyGly)_{50,}$ CS_{50}-poly$(MAGlyGly)_{50,}$ CS_{25}-$(MAGlyGly)_{75}$ and CS_{25}-poly$(MAGlyGly)_{75}$ samples*

Element	**Atomic percentage %**					
	CS	***MAGlyGly***	***CS_{50}-$(MAGlyGly)_{50}$***	***CS_{50}-poly$(MAGlyGly)_{50}$***	***CS_{25}-$(MAGlyGly)_{75}$***	***CS_{25}-poly$(MAGlyGly)_{75}$***
C1s	63	59	62	61	62	65
O1s	29	23	25	24	24	26
N1s	7	10	8	8	7	8
Cl2p	-	1	0.4	-	-	-
Si2p	1	7	5	6	8	5
S2p	-	-	0.4	0.6	-	-

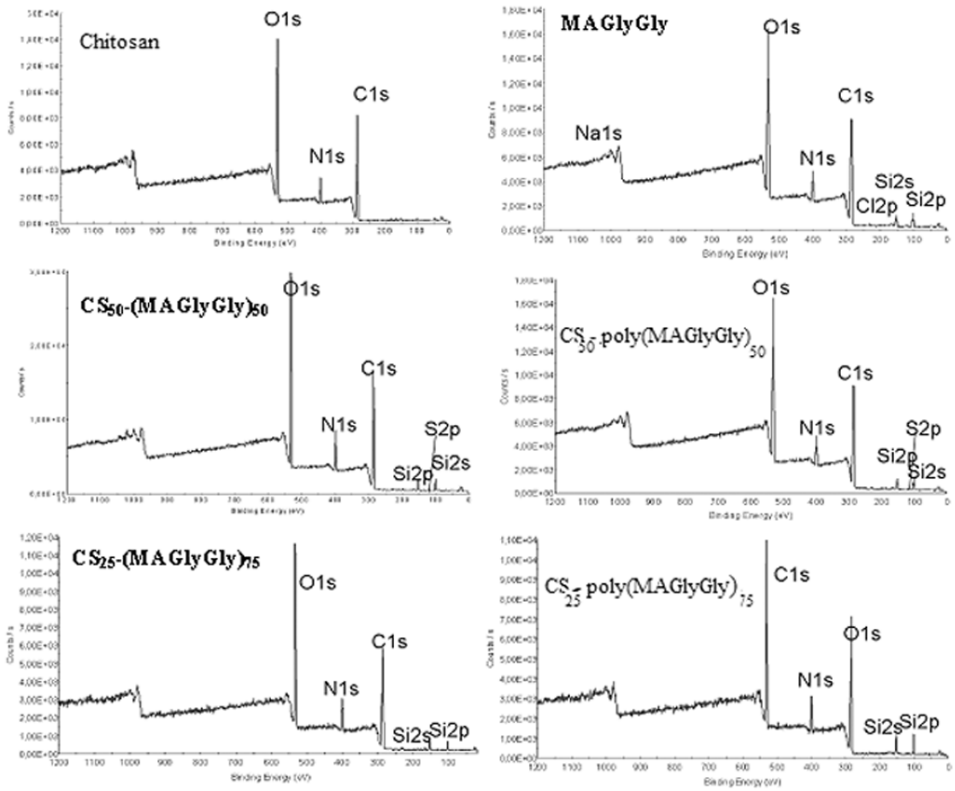

Figure 8 *Survey spectra relevant to Chitosan, MAGlyGly, CS_{50}-$(MAGlyGly)_{50}$, CS_{50} poly$(MAGlyGly)_{50}$, CS_{25}-$(MAGlyGly)_{75}$ and CS_{25}-poly$(MAGlyGly)_{75}$ samples*

Contamination of polymer surfaces by adsorbed monolayers of hydrocarbons is common in XPS unless preparation of the samples for measurement is done in clean chambers [55]. Thus, examination of the C1s region spectra for chitosan derivatives supports the encapsulation of MAGlyGly moieties, but unfortunately quantitative evaluation could result very inexact.

In this respect, this information could be extracted by curve-fitting of N1s signals *(figure 9-12)*. Results of the XPS characterization of the individual nitrogen-containing groups of all the analyzed samples are reported in the Table 3 for comparison.

As far as chitosan N1s signal is concerned *(figure 9 b)*, two different types of N-containing species, e.g. N in amine ($–NH_2$) falling at 399.1 eV and amide form (–NHC(=O)-), at 400.6 eV, can be estimated from the ratio of the corrected peak areas. Indeed, N 1s core-level spectra of chitosan suitably predicted the degree of deacetylation of chitosan, the component of amide species being about 20% of the total N1s intensity. No appreciable presence of ammonium groups (at BE > 401 eV) attributable to $-NH_3^+$ was detected on our pure chitosan specimen.

Table 3 *Peak position and relative abundance of the N1s peak components relevant to Chitosan, MAGlyGly, CS_{50}-$(MAGlyGly)_{50}$, CS_{50}-poly$(MAGlyGly)_{50}$, CS_{25}-$(MAGlyGly)_{75}$ and CS_{25}-poly$(MAGlyGly)_{75}$ nanoparticles.*

Peak B.E (eV)	***Attribution***	***Atomic Percentage(%)***						
		Chitosan	***CS at pH 4.2***	***MAGlyGly***	***CS_{50}-$(MAGlyGly)_{50}$***	***CS_{50}-poly$(MAGlyGly)_{50}$***	***CS_{25}-$(MAGlyGly)_{75}$***	***CS_{25}-poly$(MAGlyGly)_{75}$***
399.1	-C-NH2	78.6	69.3	-	75.3	55.6	74.2	62.3
400.6	-C(=O)-NH	21.4	24.0	92.2	19.6	15.0	20.4	26.7
>402.0	$-NH_3^+$	-	6.6	7.8	5.1	29.4	5.3	11.0

Since in the formulation of composite nanoparticles, the pH of the solution was 4.2, XPS analysis of a sample of chitosan at this pH was also performed *(figure 9 a).* As expected, at pH 4.2 a peak at BE > 401 eV appeared, representing the 6.6 % of the total N1s signal.

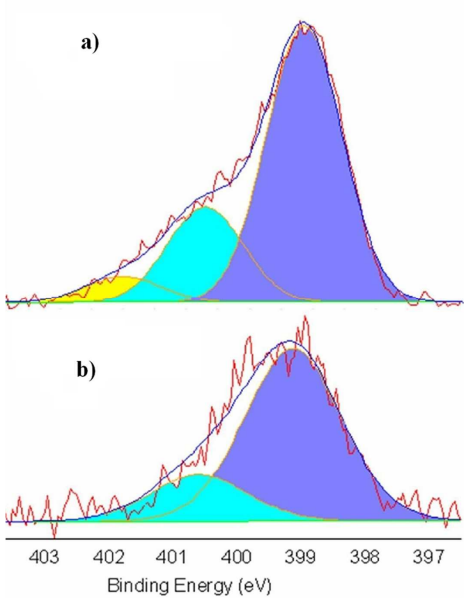

Figure 9 *N1s spectra curve fitting of (a) Chitosan at pH 4.2 and (b)Chitosan.*

In the case of MAGlyGly monomer N1s spectrum, a high contribution of amide form, the only one expected by its stoichiometric formula, is present. However, an appreciable presence of quaternary ammonium groups (401–402 eV) was detected.

Chatterjee A. *et al* reported a systematic XPS study of glycine, glycyl-glycine, diglycyl-glycine, and polyglycine [56]. In the case of glycilglycine (GlyGly), the precursor of MAGlyGly monomer synthesised in this work, they observed two N1*s* features at 400.7 and 402.2 eV, which they attributed, respectively, to the amide group and the protonated amino $–NH_3^+$ group of the zwitterion $-NH_3^+CH_2CONHCH_2COO^-$.

In this study, a low but appreciable presence of a peak at higher binding energies could be ascribed to a low amount of unreacted MAGlyGly in the investigated specimen. This was also confirmed by presence of Cl2p signal with a corrected area comparable to the $–NH_3^+$ group peak area *(figure 10).*

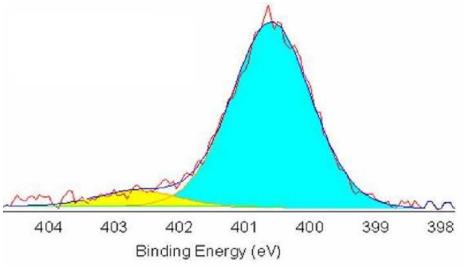

Figure 10 *N1s spectra curve fitting of MAGlyGly.*

As far as CS_x-$(MAGlyGly)_y$ nanoparticles are concerned, nanoparticles obtained by mixing chitosan with unpolymerized MAGlyGly and by mixing chitosan with polymerized MAGlyGly were investigated, in order to test if any difference between these two typologies of samples could be revealed in terms of surface distributions of elements and functional groups. In *figure 11* the curve-fitting of N1s relevant to CS_{50}-$(MAGlyGly)_{50}$ and CS_{25}-$(MAGlyGly)_{75}$ is shown.

The overall shape of the CS_x–$(MAGlyGly)_y$ nanoparticles N1s spectrum resulted almost similar to that of pure chitosan at pH 4.2 (*figure 9a*), thus qualitatively indicating that the unpolymerized nanoparticles surface composition is mainly dominated by the contribution of the chitosan dispersing matrix, while the surface availability of MAGlyGly monomers as well as their interactions with chitosan seem to be very low. This observation is valid for both the formulations, irrespectively to the ratio used.

In the case of CS_x-poly$(MAGlyGly)_y$, N1s spectra relevant to CS_{50}-poly$(MAGlyGly)_{50}$ and CS_{25}-poly$(MAGlyGly)_{75}$, reported in *figure 12*, resulted different.

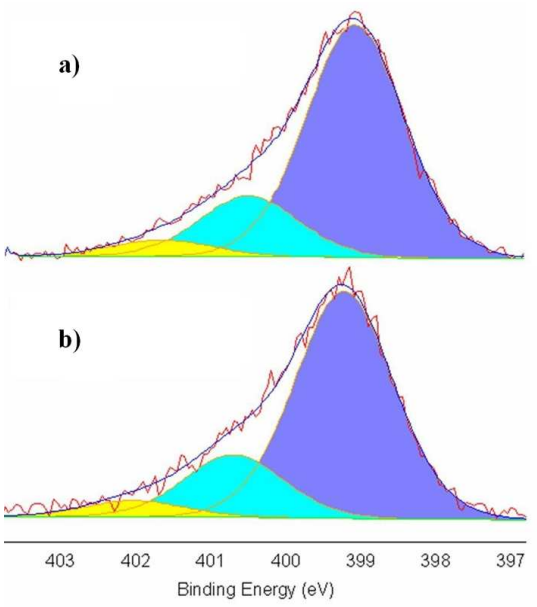

Figure 11 *N1s spectra curve fitting of (a) CS_{50}-$(MAGlyGly)_{50}$ (b) CS_{25}-$(MAGlyGly)_{75}$.*

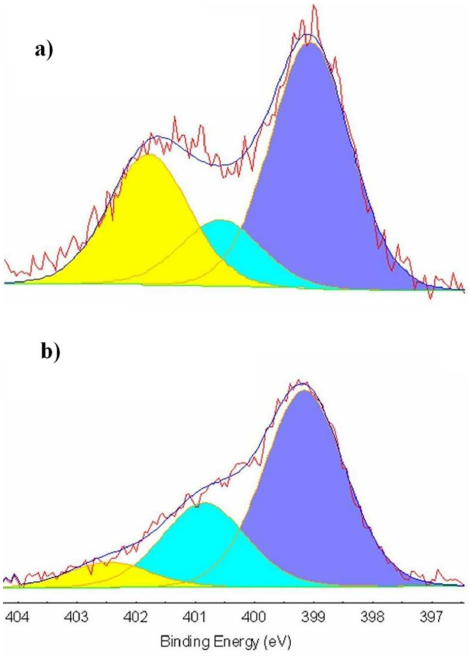

Figure 12 *N1s spectra curve fitting(a) CS_{50}-poly$(MAGlyGly)_{50}$ (b)CS_{25}-poly$(MAGlyGly)_{75}$.*

In the case of CS_{50}-poly$(MAGlyGly)_{50}$, N1s spectrum contains a very high amount of the ammonium groups signal *(figure 12a).* These ammonium groups could be ascribed to

interaction of chitosan with carboxylated MAGlyGly moieties present in the polymer, as represented in *Scheme 2*.

It is noteworthy that, calculating ($–NH_3^+$ peak area) / (-C(=O)-NH peak area), this value resulted equal to 0.09 for MAGlyGly, 0.26 for CS_{50}-$(MAGlyGly)_{50}$ and raised to 1.96 for CS_{50}-$poly(MAGlyGly)_{50}$. The results clearly show that a significant ionization of amine groups of chitosan occurred, probably as a result of interaction of poly(MAGlyGly) present on the surface of the nanosized materials.

In the case of CS_{25}-$poly(MAGlyGly)_{75}$, a slightly higher ammonium groups signal than in unpolymerized ones was also observed *(figure 12(b))*.

Calculating ($–NH_3^+$ peak area) / (-C(=O)-NH peak area), this value resulted equal to 0.26 for CS_{25}-$(MAGlyGly)_{75}$ and raised to 0.41 for CS_{25}-$poly(MAGlyGly)_{75}$. This can be attributed to the lower presence of chitosan, and consequently amine groups available to ionization, in the CS_{25}-$poly(MAGlyGly)_{75}$ sample than in the CS_{50}-$poly(MAGlyGly)_{50}$.

However, for both the samples, the evidence of a difference between unpolymerized *(figure 11)* and polymerized nanoparticles *(figure 12)* resulted quite evident.

4.4.6 Zeta-potential Studies

The zeta-potential analysis indicated that the surface of the nanoparticles carried a positive charge. It is well assessed that there is a dependence of the zeta potential with the pH of the solution, hence the variations of zeta-potential measurements with pH results in changes of nanoparticles surface charge density [57]. For our experiments, the pH at which the zeta-potential measurements were performed were 3.46 and 3.95 for preparation with and without polymerization respectively. The difference in pH of the two types of preparations were not significantly different. The positively charged nanoparticles surface indicated by the positive zeta-potential could be attributed to the cationic characteristic of chitosan at this pH [58]. The CS_{25}-$MAGlyGly_{75}$ and CS_{25}-$poly(MAGlyGly)_{75}$ nanoparticles did not show appreciable difference in the zeta potential values. The values were very close to each other, being 35.3 and 33.5 respectively (Table 3). However, when the concentration of chitosan in the formulation was changed, a difference in the zeta-potential values was observed. As can be seen from the table x, the zeta-potential value changes from 35.3 to 50.2 with the increase in the concentration of chitosan in the formulation. As the chitosan concentration increases, there is an excess of $–NH_3^+$ groups relative to COO^- groups from MAGlyGly, therefore resulting in an increased zeta-potential values.

Table 3: *Zeta-potential values of the different nanoparticle formulations.*

Sample	ζ Values
CS_{25} -$MAGlyGly_{75}$	33.5
CS_{25} –poly($MAGlyGly_{75}$)	35.3
CS_{50} –$MAGlyGly_{50}$	48.6
CS_{50} –poly($MAGlyGly_{50}$)	50.2

4.4.7 Thermal Analysis

TGA analyses were carried out in order to evaluate the thermal stability of the nanoparticles, in the perspective of their *in vivo* application. The TGA thermograms of raw Chitosan, CS_x-$(MAGlyGly)_y$ and CS_x-poly$(MAGlyGly)_y$ nanoparticles are shown in *figure13.*

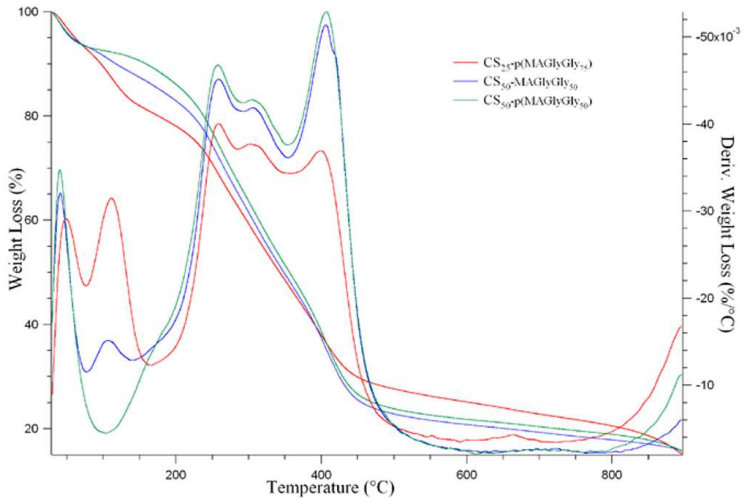

Figure 13 *Traces of the integral and the first derivative of weight loss (% ΔW) of CS_{50}-$(MAGlyGly)_{50,}$ CS_{50}-poly$(MAGlyGly)_{50,}$ and CS_{25}-poly$(MAGlyGly)_{75}$ samples*

The nanoparticles had three stages of degradation pattern in the range of 200°C to 400°C. These results indicate that CS_x-poly$(MAGlyGly)_y$ and CS_x-$(MAGlyGly)_y$ nanopartices are thermally stable up to 150°C. Hence, it is clear that nanoparticles stability shall not be affected under the physiological conditions.

4.5. Conclusion

Chitosan and MAGlyGly were used to prepare nanoparticles with 120-140 nm diameter. The interaction between the NH_3^+ groups from chitosan and COO^- groups arising from MAGlyGly formed the basis of the formation of the CS_x-$MAGlyGly_y$ particles. The nanoparticles were polymerized to form CS_x-$poly(MAGlyGly)_y$ and the effect of polymerization on the formed particles was also studied. Various techniques like FTIR, XPS were used to confirm the interaction between the two. The ratio of the polymer/monomer was varied and two kind of ratios namely 50:50 and 25:75 of chitosan, MAGlyGly respectively were prepared. With the FTIR studies it was successfully confirmed that the formed nanoparticles exhibited characteristic bands with some bands arising from the native materials used. This was observed for both with both the ratios of CS_x-$MAGlyGly_y$ nanoparticles. Similarly, XPS analysis also confirmed the presence of the two constituents on the surface of the formed nanoparticles with their amounts varying according to the ratio used. The surface of the nanoparticles exhibited a positive charge due to the chitosan at the formulation pH of 4.2. The results obtained showed that the polymerization of MAGlyGly in the presence of chitosan appears to be a very promising approach in the preparation of nanoparticles for applications in drug delivery.

4.6. Reference

[1] Lemarchand, C., Gref, R., Couvreur, P.; *Eur. J. Pharm. Biopharm.*, **2004**, 327.

[2] Xia, X., Hu, Z., Marquez, M.; *J. Control. Release*, **2005**, 21.

[3] Jiang, J.Z., Cai, C.; *J. Colloid Interface Sci.*, **2006**, 938.

[4] Pal, A., Esumi, K., Pal, T.; *J. Colloid Interface Sci.*, **2005**, 396.

[5] Montet, X., Funovics, M., Montet-Abou, K., Weissleder, R., Josephson, L.; *J. Med. Chem.*, **2006**, 6087.

[6] Endo, T., Yamamura, S., Nagatani, N., Morita, Y., Takamura,Y., Tamiya, E.; *Sci. Technol. Adv. Mater.* **2005**, 491.

[7] Koliopoulou, S., Dimitrakis, P., Goustouridis, D., Normand, P. Pearson, C. Petty, M.C., Radamson, H., Tsoukalas, D.; *Microelectron. Eng.*, **2006,** 1563.

[8] Huang, H., Yuan, Q., Yang, X.; *J. Colloid Interface Sci.*, **2005**, 26.

[9] Sarmento, B., Ribeiro, A., Veiga, F., Ferreira, D., *Colloids Surf. B*, **2006**, 193.

[10] Bertholon, I., Hommel, H., Labarre, D., Vauthier, C., *Langmuir* , **2006**, 5485.

[11] Vanthienen, T.G., Ralmdonck, K., Demeester, J., DeSmedt, S.C.; *Langmuir*, **2007**,9794.

[12] Douglas, K.L., Piccirillo, C.A., Tabrizian, M.; *J. Control. Release*, **2006**, 354.

[13] Bodnar, M. J., Hartmann, F., Borbely, J.; *Biomacromolecules*, **2005**, 2521.

[14] Boonsongrit, Y., Mitrevej, A., Mueller, B.W.; *Eur. J. Pharm. Biopharm*., **2006**, 267.

[15] Wang, L., Wang, A.; *J. Hazard. Mater.*, **2007**, 979.

[16] Yi, H., Wu, L.Q., Bentley, W.E., Ghodssi, R., Rubloff, G.W., Culver, J.N.; *Biomacromolecules*, **2005**, 2881.

[17]van der Lubben, I. M., Verhoef, J. C., Borchard, G., Junginger, H. E.; *Adv. Drug Delivery Rev*,. **2001**, 139.

[18] Hu, Y., Zhang, L. Y., Cao, Y., Jiang, X. Q.; *Biomacromolecules*, **2004**, 1756.

[19] Nobs, L., Buchegger, F., Gurny, R.; *J. Pharm. Sci.*, **2004**, 1980.

[20] Barratt, G.; *Cell. Mol. Life Sci.* **2003**, 21.

[21] Gref, R., Minamitake, Y., Peracchia, M. T., Trebetskoy, V. S., Torchilin, V. P., Langer, R.; *Science* **1994**, 1600.

[22] Yasugi, K., Nagasaki, Y., Kato, M., Kataoka, K.; *J. Control. Release* **, 1999**, 89.

[23] Hu, Y., Jiang, X., Ding, Y., Zhang, L., Yang, C. Z., Zhang, J., Chen, J.; Yang, Y. *Biomaterials* **2003**, *24*, 2395-2404.

[24] Kwon, G. S., Okano, T.; *Adv. Drug Delivery Rev.*, **1996**, 107.

[25] Moghimi, S. M., Hunter, A. C., Murray, J. C.; *Pharmacol. Rev.*, **2001**, 283.

[26] Hans, M. L., Lowman, A. M.; *Curr. Opin. Solid State Mater. Sci.*, **2002**, 319.

[27] Dumitriu, S., Chornet, E.; *Adv. Drug Delivery Rev.*, **1998**, 223.

[28] Lochmanna, D. Jaukb, E., Zimmer, A.; *Eur. J. Pharm. Biopharm*., 2004, 237.

[29] Cheng, W.P., Gray, A.I., Tetley, L., Hang, T.L.B., Schatzlein, A.G., Uchegbu, I.F.; *Biomacromolecules*, 2006, 1509.

[30] Peniche-Covas, C., Argu¨elles-Monal, W.; *Polym. Int.*, 1995, 45.

[31] Schtz, C., Lucas, J.M., Viton, C., Domard, A. Pichot, C., Delair,T.; *Langmuir*, **2004**, 7766.

[32] Schatz, C., Domard, A., Viton, C., . Pichot, C., Delair, T.; *Biomacromolecules*, **2004**,1882.

[33] Mao, H.Q., Roy, K., Troung-Le, W.L., Janes, K.A., Lin, K.Y., Wang, Y., August, J.I., Leong, K.W.; *J. Control. Release*, **2001**,399.

[34] Zheng,Y.L., Wu, Y., Yang, W.L., Wang, C.C., Fu, S.K., Shen, X.Z.; *J. Pharm. Sci.*, **2006**,179.

[35] Boonsongrit, Y., Mitrevej, A. Mueller, B.W.; *Eur. J. Pharm. Biopharm.*, **2006**,267.

[36] Liao, I.C., Wan, A.C.A., Yim, E.K.F., Leong,K.W.; J. *Control. Release*, **2005**, 347.

[37] Jameela, S.R., Jayakrishnan, A.; *Biomaterials*, **1995**, 769.

[38] Maestrelli, F., Garcia-Fuentes, M., Mura, P., Alonso, M. J.; *Eur. J. Pharm. Biopharm.*, **2006**, 79.

[39] Simeonova, M., Velichkova, R., Ivanova, G., Enchev, V., Abrahams, I.; *Int. J. Pharm.*, **2003**, 133.

[40] Elvire Fournier, E., Passirani, C., Colin, N., Breton, P., Sagodira, S., Benoit, J.P.; *Eur.J. Pharm. Biopharm.*, *2004*, 189.

[41] Vasir, J.K., Labhasetwar, V.; *Technol. Cancer Res. Treat.*, **2005**, 363.

[42] Kopecek, J., Kopeckova', P., Minko, T., Lu, Z.-R.; *Eur. J. Pharm. Biopharm.*,**2000**, 61.

[43] Nori, A., Jensen, K.D., Tijerina, M., Kopeckova, P., Kopecek, J.; *Bioconjug. Chem.*,**2003**, 44.

[44] Vasey, P.A., Kaye, S.B., Morrison, R., Twelves, C., Wilson, P., Duncan, R., Thomson, A.H., Murray, L.S., Hilditch, T.E., Murray, T., Burtles, S., Fraier, D., Frigerio, E., Cassidy, J.; *Clin. Cancer Res.*,**1999**, 83.

[45] Jelinkova, M., Strohalm, D., Plocova, V., Subr, V., Stastny, M., Ulbrich, K., Rihova, B.; *J. Control. Release*, **1998,** 253.

[46] Ulbrich, K., Strohalm 1, Subr, V., Plocova, D., Duncan, R., Rihova, B.; *Macromol. Symp.*, **1996,** 177.

[47] Malugin, A., Kopeckova, P., Kopecek, J.; *Mol. Pharm.*, **2006**, 351.

[48] Duncan, R., Vicent, M.J., Greco, F., Nicholson, R.I.; *Endocr. Relat. Cancer*, **2005**, 89.

[49] Chiellini, F., Bartoli, C., Dinuccio D., Piras, A. M., Anderson, R., Croucher, T.; *Int. J. Pharm.*, **2007**, 90.

[50] Kajihara, M., Sugie, T., Hojo, T., Maeda, H., Sano, A., Fujioka, K., Sugawara, S., Urabe, Y.; *J. Control. Release*, **2001**, 279.

[51] Hu, Y., Ding,Y., Ding, D. Sun, M. Zhang, L., Jiang, X., Yang, C.; *Biomacromolecules*, 2007, 1069.

[52] Baier, J., Koetz, J., Kosmella, S., Tiersch, B., Rehage, H. J.; *Phys. Chem. B* , **2007**, 8612.

[53] Wang, H., Li, W., Lu, Y., Wang, Z.; *J. Appl. Polym. Sci.*, **1997**, 1445.

[54] De Vasconcelos, C.L., Bezerril, P.M., Dos Santos, D.E.S., Dantas, T.N.C., Pereira, M.R., Fonseca, J.L.C.; *Biomacromolecules*, **2006,** 1245.

[55] Winkelmann, M., Gold, J., Hauert, R., Kasemo, C., Spencer, N.D., Brunette, D.M., Textor, M.; *Biomaterials***, 2003,** 1133.

[56] Chatterjee, A., Zhao, L., Zhang, L., Pradhan, D., Zhou, X., Leung, K.T.; *J. Chem. Phys.*, **2008**, 105.

[57] Moura, M.R., Aouada, F.A., Mattoso, L.H.C.; *J. Colloid Interface Sci*., **2008**, 477.

[58] Gan, Q., Wang, T.; *Colloids Surf. B*, **2007**, 24.

5. SYNTHESIS AND CHARACTERIZATION OF SEMI-INTERPENETRATING POLYMER NETWORK HYDROGEL BASED ON CHITOSAN AND POLY(METHACRYLOYLGLYCYLGLYCINE)

5.1. Abstract

The objective of the present work was to develop a strategy for the synthesis of semi-interpenetrating(semi-IPN) hydrogels using chitosan and poly(methacrylamides) under physiological conditions. Free radical polymerization of methacryloylglycylglycine was performed by using ethylene glycol dimethacrylate as the crosslinker and sodium metabisulphite and ammonium persulfate as the radical initiators. Chitosan and poly(methacryloylglycyl glycine) hydrogels were prepared with different composition of copolymers and amount of crosslinker . The hydrogels were evaluated for swelling studies under physiological conditions. Scanning electron microscopy led to understand the morphology of the semi-IPN's. Fourier transformation infrared spectroscopy was employed to gain insight into the structure of the prepared semi-IPN hydrogels. Thermal studies were carried out to investigate and confirm the presence of the comonomers involved. The type of water was assessed by differential scanning calorimetric studies. Degradation behavior of the hydrogels was also studied.

5.2. Introduction

Hydrogels are crosslinked macromolecular networks swollen in water or biological fluids. The term hydrogel is composed of ''hydro'' (¼water) and ''gel,'' and it refers to aqueous (water-containing) gels, or to be more precise, to polymer networks that are insoluble in water, where they swell to an equilibrium volume but retaining their shapes [1]. The hydrophilicity of the network is due to the presence of chemical residues such as hydroxylic (–OH), carboxylic (–COOH), amidic (–CONH–), primary amidic ($–CONH_2$), sulfonic ($–SO_3H$), and others that can be found within the polymer backbone or as lateral chains. Nevertheless, it is also possible to produce hydrogels containing a significant portion of hydrophobic polymers, by blending or co-polymerizing hydrophilic and hydrophobic polymers, or by producing interpenetrating or semi-interpenetrating polymer networks [2] (respectively, IPN and semi-IPN) of hydrophobic and hydrophilic polymers [3]. The

insolubility of the gel in water is due to the presence of a three-dimensional network, where an equilibrium between dispersing (acting on hydrated chains) and cohesive (preventing further penetration of water) forces exist [4-6]. These cohesive forces are generated by covalent bonds between the chains of the polymer network (permanent or chemical hydrogel) or by cooperative and associative forces such as:

(1) hydrophobic associations/Van der Waals forces [6-10]

(2) micellar packing [11-13]

(3) hydrogen bonding [14-17]

(4) ionic bonding [18-20]

(5) crystallizing segments [21] or

(6) combinations of the above (reversible or physical hydrogel).

As mentioned earlier, these structures expand when are placed in contact with water. However, these materials can be also designed to swell or shrink when they are exposed to particular signals such as temperature, pH, ionic strength, electrical field, particular aqueous solution composition, and light, as it was on command [22,23].

Hydrogels can be formed either by crosslinking, by formation of interpenetrating networks (IPNs), or by crystallization that induces crystallite formation and drastic reinforcement of their structure [24,25]. IPNs are an important class of hydrogel materials, defined as two independent crosslinked synthetic and/or natural polymer components contained in a network form. A semi-IPN is an IPN where one of the components is a crosslinked polymer while the other component is a non-crosslinked polymer (*scheme 1*). Polymer complexes are formed by the association of two or more complementary polymers, and may arise from electrostatic forces, hydrophobic interactions, hydrogen bonding, Van der waals forces or combinations of these interactions. The formation of complexes may strongly affect some properties such as the mechanical properties, permeability, and electrical conductivity etc. of the polymeric systems. Particularly, polyelectrolyte complexes are formed by the reaction of a polyelectrolyte with an oppositely charged polyelectrolyte in an aqueous solution. Thus, electrostatic polyelectrolyte complexes exhibit unique physical and chemical properties with reasonable biocompatibility, hence special attention has been focused on their application in ecology, biotechnology, and medicine [26–28].

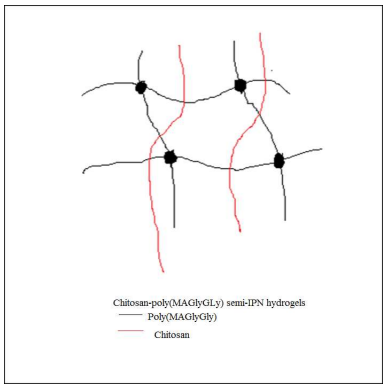

Scheme 1: *Schematic representation of semi-IPN of Chitosan -poly(MAGlyGly).*

Chitosan is a (1,4)-linked 2-amono-2-deoxy-b- D-glucan and can be presented by *N*-deacetylation of chitin. Chitosan, as a cationic polyelectrolyte, is able to form polyelectrolyte complexes by reaction with various natural and synthetic anionic polyelectrolytes. The electrostatic attraction between the cationic amino groups of chitosan and the anionic groups of the other polyelectrolyte is the main interaction leading to the formation of the polyelectrolyte complex. It is stronger than most secondary binding interactions [29]. These complexes are generally water insoluble and form hydrogels. Formation of chitosan hydrogels by polyelectrolyte complexation is an interesting alternative to covalently crosslinked hydrogels. The polyelectrolyte complex undergoes slow erosion, which gives a more biodegradable material than covalently crosslinked hydrogels [30,31]. Polyelectrolyte complexes of chitosan with other polysaccharides, DNA, proteins and different synthetic anionic polyelectrolytes have been extensively investigated in literature due to their wide variety of applications in medicine, pharmacy (especially as drug delivery systems), technology and other fields [32,33].

In the present work, polymerized MAGlyGly[(poly(MAGlyGly)] has been used as a polyanionic polymer for complexation with chitosan. Poly(MAGlyGly) has anionically charged groups that forms polymer complexes with chitosan. The preparation of the investigated network was performed by free radical polymerization of MAGlyGly in the presence chitosan acid solution by using ethylene glycol dimethacrylate (EGDMA) as crosslinking agent and the couple sodium metabisulfite ($Na_2S_2O_5$) and ammonium persulfate [$(NH_4)_2S_2O_8$] as radical initiator. The synthetic scheme is presented in *figure 1*.

The fundamental investigation of the prepared hydrogel involved the Fourier Transformation Infrared spectroscopy (FTIR) for the structure of the prepared hydrogel and

at the same time to confirm the presence of both chitosan and poly(MAGlyGly). Physical and chemical properties of hydrogels depend on their molecular and supramolecular structure, water content and the type of water. The nature of water in ionic hydrogel membranes is important in understanding their dynamic and equilibrium swelling behavior as well as in analyzing solute transport and other diffusive properties of such systems. For these reasons, the swelling behavior along with the thermal characterizations and state of water investigation of the hydrogels were performed. Degradability, another important feature in materials for Regenerative Medicine applications, was performed in the presence of lysozyme under physiological conditions.

5.3. Materials and Methods

5.3.1 Materials

Chitosan (Mw = 71.3 KDa, degree of deacetylation 93%), ammonium persulfate [$(NH_4)_2S_2O_8$], sodium metabisulfite ($Na_2S_2O_5$) and ethylene glycol dimethacrylate(EGDMA) were purchased from Sigma-Aldrich and they were used without any preliminary purification. Lysozyme (hen egg-white) was also purchased from Sigma-Aldrich. All other chemicals were extra pure reagent grade and were used as received.

5.3.2 Methods

5.3.2.1 Preparation of the monomer

Methacryloylglycylglycine (MAGlyGly) was synthesized according to a described procedure in chapter 4 (§ 4.3.2.1).

5.3.2.2 Silanization of glass

2 mm thick square plates (4x4 cm) were exposed to trimethylclorosilane vapours for 24 hours at room temperature, then rinsed with distilled water and dried.

5.3.2.3 Synthesis of semi-IPN's

Various compositions in terms of weight % of Chitosan/methacryloylglycylglycine based semi-IPN's were prepared. Details of the various runs are reported in table 1. Chitosan dissolved in 2M acetic acid solution was well mixed with MAGlyGly solution in DMSO (Acetic acid solution/DMSO = 9/1) to form a homogeneous solution. Then, different wt % of EGDMA (refer to table 1) as crosslinker and subsequent amount of initiators were added to the mixture. After few pumping/degassing cycles, the mixture was injected with a syringe between two silanized glasses separated by a 1 mm thick silicon spacer. Clamps were applied onto the glasses in order to ensure a perfect sealing, and the mixture was cured at 40°C for 4 hours. After 4 hrs, the hydrogels were washed with deionized water to remove any unreacted monomers and polymers that were not incorporated into the network. Then, the washed hydrogels were neutralized with phosphate buffer saline (PBS) solution. The neutralised hydrogels were again washed carefully with distilled water to remove salts followed by freeze drying.

Table 1. *Composition and designation of semi-IPN of Chitosan-poly(MAGlyGly).*

Run	**Ratio Chitosan/MAGlyGly** ***(in wt%)***	**Amount of crosslinker** ***(in wt% to MAGlyGly)***	**Hydrogel formation**
1	20/80	8	+
2	20/80	4	+
3	20/80	2	+
4	50/50	8	-
5	80/20	8	-

+ indicates hydrogel formation
- indicates no hydrogel was formed

5.3.2.4 Determination of swelling degree

To measure the equilibrium water content, pre-weighed dry samples were immersed in distilled water and 0.01 M pH 7.2 phosphate buffer saline at 37°C until the equilibrium was reached. After, excessive surface water was removed with filter paper, the weight of swollen samples was measured at various time intervals. The procedure was repeated until there was no further weight increase. The swelling ratio (SR%) was determined according to the following equation:

$$SR\% = [(W_s - W_d)/W_s] * 100$$

where W_S and W_d represent the weight of swollen and dry samples, respectively.

5.3.2.5 Morphological Analysis

The morphology of the prepared hydrogels were investigated by scanning electron microscopy (SEM), using a JEOL LSM5600LV scanning electron microscope. Lyophilized hydrogels were used and gold sputtering was done before SEM analysis.

5.3.2.6 Fourier transform infrared (FTIR) spectroscopy measurements

FTIR spectra of chitosan, chitosan-poly(MAGlyGly) hydrogels, poly(MAGlyGly) in KBr disc form were recorded on Jasco FT–IR 410 spectrophotometer from 400 to 4000 cm^{-1} with a resolution 4 cm^{-1} and 32 scans.

5.3.2.7 Differential scanning calorimetry (DSC) measurements

A Mettler DSC-822 (Mettler Toledo, Milan, Italy) differential scanning calorimeter equipped with a liquid nitrogen cooling accessory was used. DSC was used to analyse the type of water in the semi-IPN hydrogels. Samples (about 4 mg) were weighed in an aluminum pan designed for volatile samples and sealed. The samples were cooled to -70°C at 10°C/min and then heated to 50°C/ at a heating rate of 10°C/min under 80mL/min of nitrogen flow.

5.3.2.8 Thermogravimetric (TGA) studies

Thermogravimetric analyses were carried out by using Thermogravimetric Analyzer TGA Q500 (TA Instruments-Waters Division, Milan, Italy). All measurements were performed with approximately an equal amount (20mg) of samples in aluminum pans. The experiments were performed from 30°C to 900°C at a scanning rate of 10°C/min under a 60ml/min nitrogen flow.

5.3.2.9 In-vitro degradation

The in vitro hydrogels degradation tests were carried out in 4 ml phosphate-buffered solution (PBS, pH 7.4) at 37 °C containing 1.5 mg/ml lysozyme. The concentration of lysozyme was chosen to correspond to the concentration in human serum [34,35]. Briefly, hydrogels of known weight were incubated in the lysozyme solution for the period of study. The lysozyme solution was refreshed daily to ensure continuous enzyme activity [36]. After 7, 14, 21 and 28 days samples were removed from the medium, rinsed with distilled water carefully, dried under vacuum and weighed. The extent of in vitro degradation was expressed as percentage of weight loss of the dried films (n = 3 samples of each week) after lysozyme treatment. To separate between enzymatic degradation and dissolution, control samples were stored for 28 days under the same conditions as described above, but without the addition of lysozyme.

5.4. Results and Discussion

5.4.1 Preparation of Chitosan-poly(MAGlyGly) semi-IPN's

Figure 1 represents the scheme of the synthesis of IPN composed of chitosan and poly(MAGlyGly). The preparation of the investigated network was performed by free radical polymerization of MAGlyGly in the presence chitosan acid solution by using ethylene glycol dimethacrylate as the crosslinking agent and the couple sodium metabisulfite and ammonium persulfate as the radical initiator. Briefly, chitosan in acetic acid solution was mixed well in MAGlyGly solution to form a homogeneous solution. Then the crosslinker EGDMA and the couple initiators were added to this solution and after a few pumping /degassing cycles, the resulting mixture were injected between two silanized glasses where it was polymerized at 40°C for 4 hours *(figure 2 a)*. By this technique, homogeneous films with constant thickness and shape similar to that of the mould *(figure 2 b)* were obtained**.** The silanization of the glasses were done in order to facilitate the hydrogel removal at the end of the polymerization. The glass surface was silanized by exposure to trimethylchlorosilane vapours for 24 hours at room temperature and rinsed afterwards with distilled water.

Silanization is a gas-solid reaction that modifies the wettability and adhesion features of glass by transforming the hydrophilic silica surface in hydrophobic trimethoxysiloxane groups.

It is expected that amino groups of linear chitosan chain form polyelectrolyte complex with carboxylic acid groups of the poly(MAGlyGly) network and this interaction leads to the formation of the semi-IPN's. As shown in table 1, the concentration of chitosan/MAGlyGly and EGDMA are the two parameters that were varied to evaluate how the different composition affects the mechanical, chemical-physical and biological properties of the materials.

Hydrogels were not formed when the concentration of chitosan was increased more than 20 wt% irrespective of the concentration of the crosslinker EGDMA. In order to form a polyelectrolyte complex, both polymers have to be ionized and bear opposite charges. During complexation, polyelectrolytes can either coacervate, or form a more or less compact hydrogel. However, if ionic interactions are too strong, precipitation can occur, which is quite common [37] and hinders the formation of hydrogels. With the increase in concentration of chitosan, the complexion is enhanced and does not allow for the formation of the hydrogels. Whereas in case of the variation of EGDMA concentration, hydrogels were formed in all the three concentrations reported and they showed different properties.

All the described hydrogels were subjected to purification. Infact materials that are intended to be used for biomedical applications must be free from all components that may be harmful for the body. The compounds that could be possibly present in the synthesized hydrogels include initiator and their decomposition products, unreacted monomers, oligomers and impurities coming form the reagents.

Therefore, at the end of the polymerization, hydrogels were rinsed under running water for at least 24 hours. The prepared hydrogels were thereafter washed with PBS until the pH was neutral.

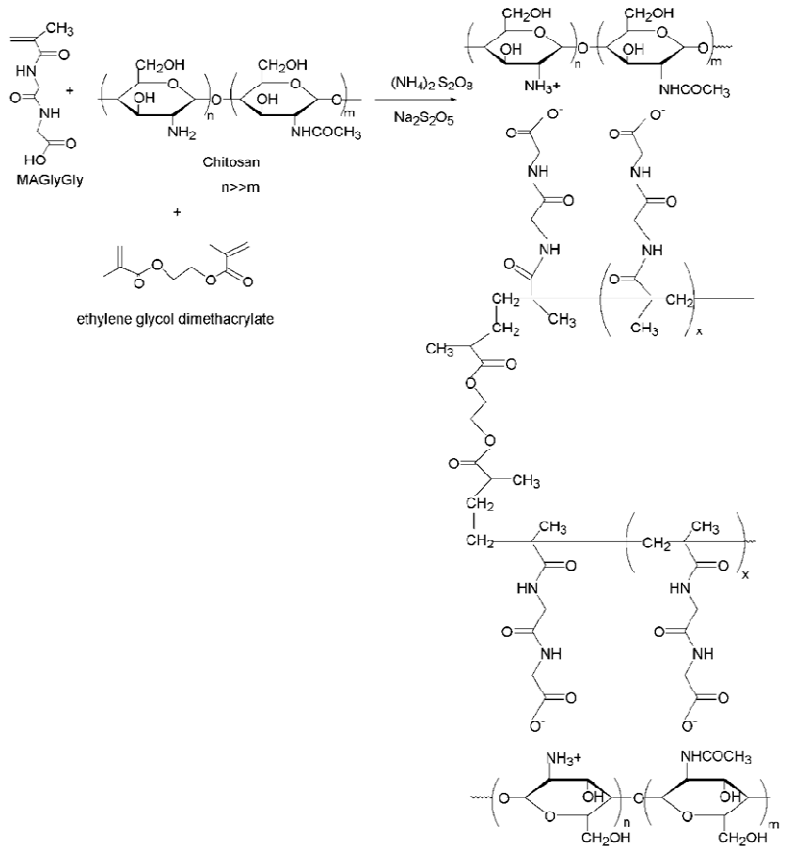

Figure 1: *Mechanism of synthesis of semi-IPN of Chitosan -poly(MAGlyGly.*

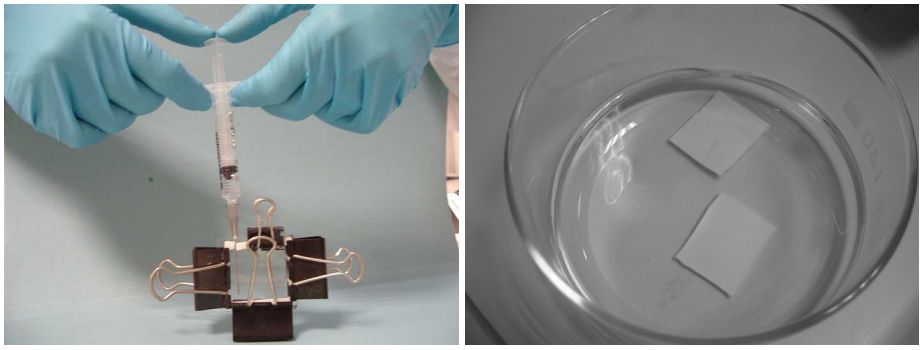

(a) (b)

Figure 2: (a) *Preparation of semi-IPN of Chitosan -poly(MAGlyGly);*(b) *Semi-Interpenetrating network of-Chitosan poly(MAGlyGly).*

5.4.2 Degree of Swelling and Swelling Kinetics of Semi-IPN Hydrogel in Different Solvents

In a crosslinked hydrogel, the solvent does not dissolve it but instead swells it. Thus, the total volume increases to that of the network and the solvent.

In a polymer that has been cross-linked into a network, the chains are in an entangled and relaxed conformation between two network junctions. However, when the solvent enters inside the polymer, the solvent molecules move the network junctions away from each other (as the polymer swells in the solvent). As the network junctions move away, the chains attached to these junctions experience a stress that is counteracted by the tendency of the polymer chain to return back to the relaxed state. At some stage, an equilibrium is reached wherein the polymer refuses to accept anymore of the solvent. Clearly, this equilibrium depends on how long the chains between network junctions are and the degree to which the polymer chains "like" (energetically) to have solvent molecules around them. Swelling property of hydrogels determines some important properties such as diffusion and transport of oxygen, essential nutrients and metabolic waste through the hydrogel network hence water absorption represents one of the main parameters that characterize hydrogels [4].

Swelling kinetics demonstrated a very high swelling ratio of semi-IPN sample in both water and PBS and as it can be observed from the figure below both kinetics showed a similar trend with equilibrium being achieved within 20 minutes. It was observed that the swelling in case of water was higher than in PBS in all the three concentrations of crosslinker as depicted in *figure 3*. The swelling studies also indicated that with the increase in crosslinker concentration, the swelling ratios decreased. Swelling of the network is mainly governed by the intermolecular crosslinks [38]. The hydrogels with lower amount of crosslinker exhibited much faster swelling kinetics. The observed difference in swelling with the crosslinker amount could be attributed to the fact that with higher amount of cross-linker, the hydrogel material becomes denser, reinforcing the hydrogel and leading to a more physical restriction. So, water molecules could not easily diffuse into hydrogel network causing a lower swelling kinetics.

The water contents of the hydrogels were lower in PBS than in distilled water (*figure 3*). The effect of the media on the swelling behaviour could be attributed to the shielding of COO^- repulsion. There occurs some kind of interactions between COO– groups in MAGlyGly and the ions present in the PBS. As discussed previously by the literature, in the presence of PBS, the hydrophilic –COO– groups hinder the dehydration of the polymer

chains, expanding the collapsed structure [39]. In PBS, the presence of ions produce an ionic shielding of the –COO– groups, this ionic shielding disrupts the swelling content of the hydrogels in PBS in comparison to distilled water.

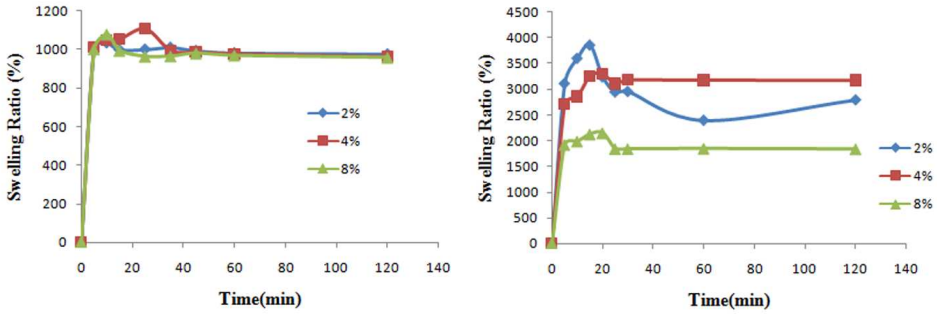

Figure 3: *Swelling studies of Chitosan-poly(MAGlyGly) hydrogels in (a) PBS (b) water*

5.4.3 Morphological Analysis

The morphological characteristics of the chitosan-poly(MAGlyGly) hydrogels after exposure to washings with water and PBS and subsequent freeze drying have been examined by SEM. The microstructure of a scaffold has a prominent influence on cell proliferation, function, and migration, all of which are key issues in tissue engineering. Microstructures of the networks surface investigated by scanning electron microscopy are presented in *figure 4*. It could be seen that the semi-IPN hydrogels displayed interconnected porous surface. The porosity increased with the increase in the crosslinker concentration from 2 % to 8 %.

5.4.4 FT-IR Analysis

Fourier transform infrared (FT-IR) spectroscopy was used to confirm the structure of chitosan -poly(MAGlyGly) semi-IPN hydrogels. *Figure 5* shows FT-IR spectra of chitosan, semi-IPN of chitosan -poly(MAGlyGly) and the MAGlyGly network.

On analyzing the spectrum of chitosan, a characteristic broad band at 3431 cm^{-1} is observed due to the overlapping of the stretching vibrations of hydroxyl O-H and amine N-H_2 groups. C-O stretching vibrations of chitosan appear at around 1030 cm^{-1} . The characteristic bands of amide I, amide II and amide III appear at around 1651, 1606 and 1383 cm^{-1}respectively. Peaks observed at 2875 and 2919 cm^{-1} are typical of C-H stretching

vibrations. The peaks around 894 and 1155 cm^{-1} correspond to saccharide structure. The observed peak at 1424 cm^{-1} is assigned to CH_3 symmetrical deformation mode [40].

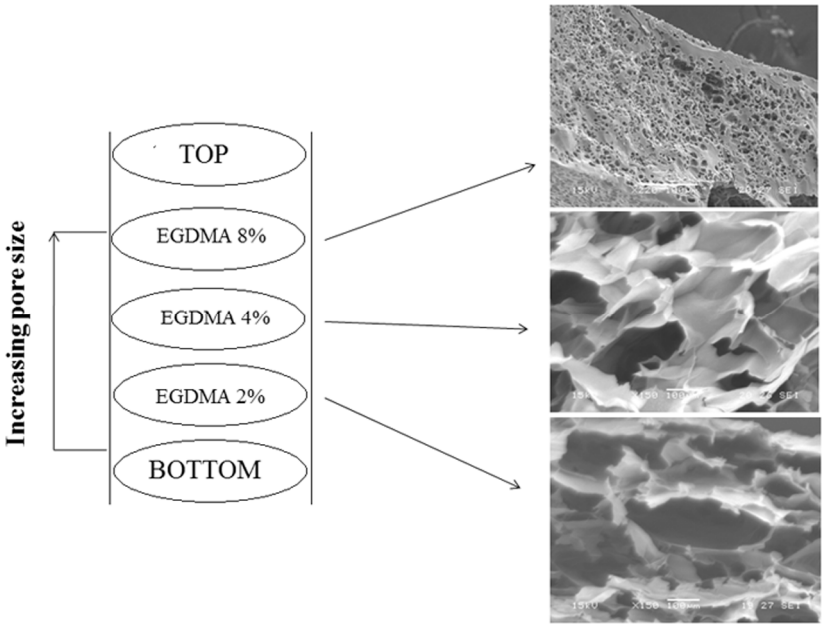

Figure 4: *SEM micrographs of Chitosan-poly(MAGlyGly) hydrogels with(a) 8% EGDMA(b)4% EGDMA (c)2% EGDMA*

On observing the MAGlyGly hydrogel spectrum, carbonyl stretching vibration (amide I) at 1672 cm^{-1} and 1540 cm^{-1}due to the N-H bending vibration (amide II) can be confirmed.

In the chitosan-poly(MAGlyGly) hydrogel , the overlapping of the stretching vibrations of hydroxyl O-H and amine N-H_2 groups appeared at 3432 cm^{-1} is observed which is similar to chitosan spectrum. Another similarity to chitosan could be seen in the presence of the peaks at 2960 and 2919 cm^{-1} which are typical of C-H stretching vibrations. Moreover it can be observed peaks at 1656.6 and 1387cm^{-1} that can be assigned to COO^{-1} stretching. Hence, it could be concluded that in the semi-IPN-Chitosan/(MAGlyGly), all the bands of both chitosan and MAGlyGly hydrogel are observed.

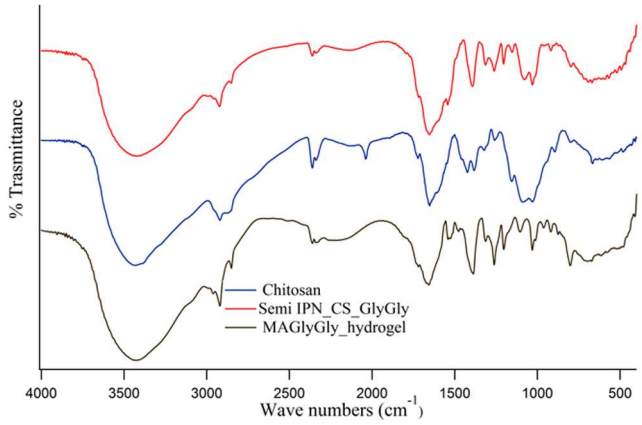

Figure 5: *FT-IR spectra of Chitosan, semi-IPN of Chitosan-poly(MAGlyGly) and MAGlyGly network.*

5.4.5 Thermogravimetric (TGA) studies

The thermal properties of the systems were investigated using thermogravimetric analysis. The thermogravimetric curves of chitosan, MAGlyGly raw materials and the hydrogel is shown in *figure 6*. Thermogravimetric analysis curve of chitosan shows a single stage degradation. The 7.1% weight loss at around 150°C is due to loss of absorbed water. The second stage starts at 240 °C and reaches a maximum at 380 °C with a weight loss of 56.66%. The residue was calculated to be 29.11% at 900°C. This result is similar to the ones of Nieto *et al* [41] and Neto *et al*. [42] The second stage corresponds to the decomposition (thermal and oxidative) of chitosan, vaporization and elimination of volatile products. According to the literature [41], pyrolysis of polysaccharides starts by a random split of the glycosidic bonds, followed by a further decomposition forming acetic and butyric acids and a series of lower fatty acids, where C2, C3 and C6 predominate.

The poly(MAGlyGly) hydrogel showed multiple stages of degradation. It could be observed four main steps. The first step of degradation appeared at 309.6°C with a weight loss of 10.4%, the second step is at 381.7°C with a 40.4% weight loss. The third step is observed at 770°C with 31.75% and the fourth step occurs at 809°C with 4.4% weight loss. The residue at 900°C was about 8%.

The TGA revealed that the hydrogel has three stages of degradation similar to poly(MAGlyGly). Being the onset temperature of chitosan and MAGlyGly close to each other, it was difficult to observe two different peaks of degradation for chitosan and

MAGlyGly, but the appearance of the peak was distinguishable, and it was possible to observe that the degradation curve of semi-IPN network contains both the peaks of degradation of chitosan and of MAGlyGly hydrogel as is highlighted in *figure 6*. In case of the hydrogel, the peak of degradation appeared to be broad and the onset of degradation started at a temperature closer to chitosan indicating clearly that both chitosan and MAGlyGly were present in the hydrogel matrix. On comparing the profiles of hydrogels with the three different EGDMA concentrations *(figure 7),* we observe that there is not much difference between the three types of hydrogels but in all cases it could be concluded that both chitosan and MAGlyGly are present in the hydrogel matrix.

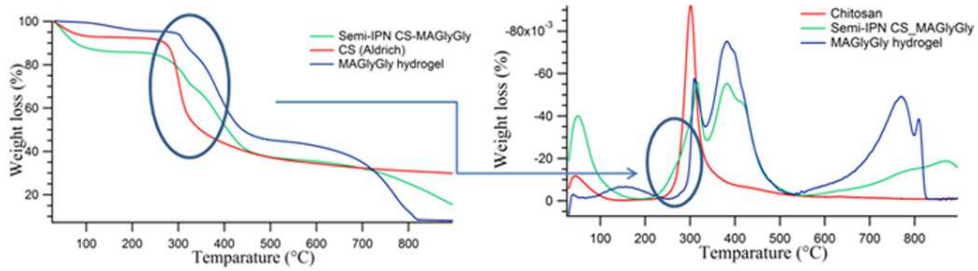

Figure 6: *Traces of the integral and the first derivative of weight loss (% ΔW) of Chitosan, MAGlyGly hydrogel and semi-IPN network of Chitosan -poly(MAGlyGly).*

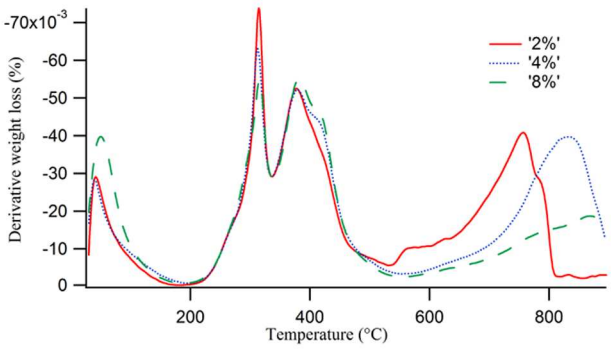

Figure 7: *Traces of the first derivative of weight loss (% ΔW) of semi-IPN of Chitosan-poly(MAGlyGly) with 8%, 4% and 2% of EGDMA.*

5.4.6 Differential Scanning Calorimetric (DSC) studies

In the literature on hydrogels, it is well established that water exists in polymer networks in three different physical states: free water, intermediate water and bound water.

Biomedical or pharmaceutical activity depends significantly on how the water molecules associate with the polymer. There is a variety of techniques for the study of water binding in polymers. Differential scanning calorimetry (DSC) is in many ways the most convenient and informative method [43]. Much research on the water-swollen polymers by means of DSC, Nuclear Magnetic Resonance (NMR) spectrometry, FTIR spectroscopy and other techniques has demonstrated that the state of water in polymer/water systems is different from that of bulk water [44-47]. Three energetically distinct states of water have been identified in water-swollen systems. The experimentally determined separate states of water within the polymer can be defined as follows [48-49] and depicted in *figure 8*:

(i) ***Free water***, which undergoes similar thermal transitions to that of bulk water, it has the same characteristics of pure water and does not interact with polymer chain.

(ii) ***Interfacial water*** or freezable bound water, which undergoes a thermal phase transition at a temperature shifted with respect to that of bulk water and

(iii) ***Bound water*** or non-freezable water, which is the tightly bound to the polymer and does not exhibit a first order transition over the range of temperatures normally associated with bulk water.

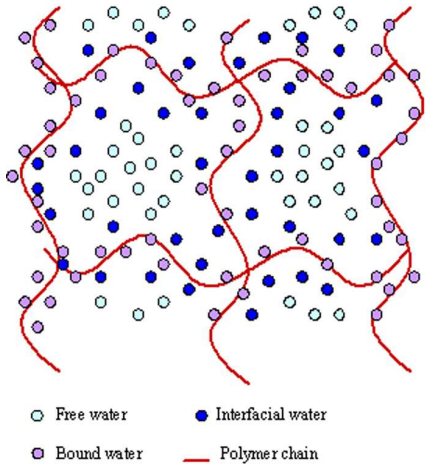

Figure 8: *Types of water present in hydrogel networks.*

Even for our studies DSC analysis was employed to assess the type of water present in the prepared semi-IPN's. This type of investigation of water structure in hydrogels is based on the hypothesis that on cooling *free* water freezes at the same temperature as pure water, whereas *bound* water does not freeze even at very low temperature, due to its strong

interaction with the polymer matrix [4]. According to this hypothesis the endotherm measured when warming the frozen gel represents the melting of *free* water and that value will yield the amount of free water in the hydrogel being tested.

The heat of crystallization of the freezing water (intermediate and free water) was determined from the area under the exothermic curve and was calibrated using pure distilled water as a standard (*figure 9*). In particular the amount of freezing water (W_f) was determined by comparing the ΔH of the crystallization peak of the hydrated sample with that of the pure water:

$$W_f = \frac{Q_w}{\Delta H°_w}$$

where Q_w is the crystallization enthalpy measured in Joule (J) and $\Delta H°_w$ is the solid-liquid transition enthalpy of hydration water in the hydrogel. By assuming that the crystallization enthalpy of hydration water is the same in pure water and in the hydrogel, the experimentally measured value of $\Delta H°_w$ turned out to be 495.31 $J \cdot g^{-1}$.

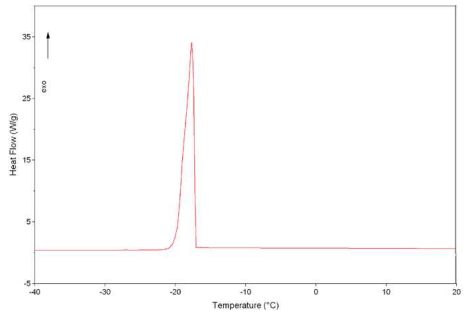

Figure 9 *DSC trace of pure water.*

The content of not-freezing water (W_{nf}) in the hydrogel was then evaluated as the total hydration water (W_t) minus the amount of freezing water (W_f):

$$W_{nf} = W_t - W_f$$

From the DSC analysis of the semi-IPN hydrogels, it was observed that most part of water is present as freezing water (*figure 10).* This result could be interpreted by considering the fact that with the formation of the polyelectrolyte complex between chitosan and poly(MAGlyGly) there are fewer hydrophilic groups available. When the amount of crosslinker is reduced to 4% and 2% , the amount of bound water in the system increases *(figure 10).* This could be explained on the basis that with lesser crosslinker amount, the pore

size is larger and hence more amount of water is able to enter the matrix and have some kind of interaction with the polymeric chains.

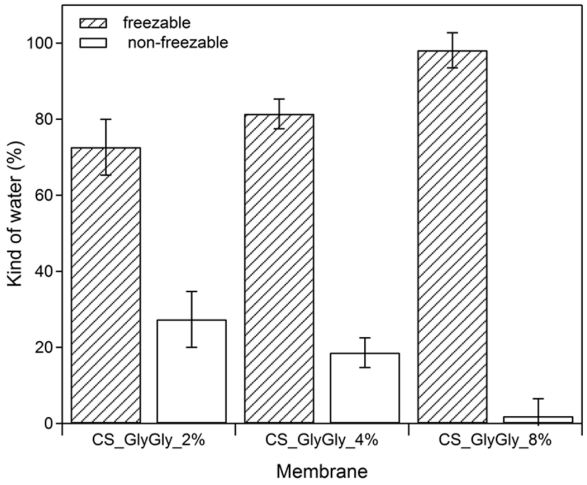

Figure 10: *Type of water in Chitosan-MAGlyGly semi-IPN hydrogels with (a) 2%(b)4%(c)8% EGDMA concentration*

5.4.7 In-vitro degradation studies

The degradation of chitosan based materials have already been tested in a number of *in vitro* studies [50-59]. Most of the studies were performed using physiological pH and enzyme concentrations as described herein. It is well known that, in human serum, N-acetylated chitosan is mainly depolymerized enzymatically by lysozyme, and not by other enzymes or other depolymerization mechanisms [51]. The enzyme biodegrades the polysaccharide by hydrolyzing the glycosidic bonds present in the chemical structure. Lysozyme contains a hexameric binding site [53], and hexasaccharide sequences containing three or more acetylated units contribute mainly to the initial degradation rate of N-acetylated chitosan [57].

To distinguish between enzymatic degradation and simple dissolution, we compared the mass loss after 28 days of samples that had been stored in PBS with lysozyme to those that had been stored in PBS without lysozyme. The semi-IPN network showed a progressive increase in mass loss over time (*figure 11(a)).* It was noticed that there was a 60%, 68% and 76% of degradation of chitosan-poly(MAGlyGly) IPN-network with 8%, 4% and 2% of EGDMA respectively in 28 days. The degradation values of the semi-IPN's were

significantly higher than the controls used which indicated enzymatic degradation of the semi-IPN's. However a minimum of loss in weight is detected also in the control samples. The increase in the degradation rate with the decrease in crosslinker amount was hard to interpret. With the decrease in crosslinker the pore size as well as the swelling increased, this caused more dissolution of the samples and their removal during subsequent refreshments. A comparison of the degradation values of the three kind of the semi-IPN hydrogels with their respective controls are shown in *figure 11(b).*

For MAGlyGly hydrogels, a clear distinction between degradation and dissolution could not be made under the adopted investigation conditions since the MAGlyGly hydrogels had a highly porous strucuture where dissolution could not be controlled.

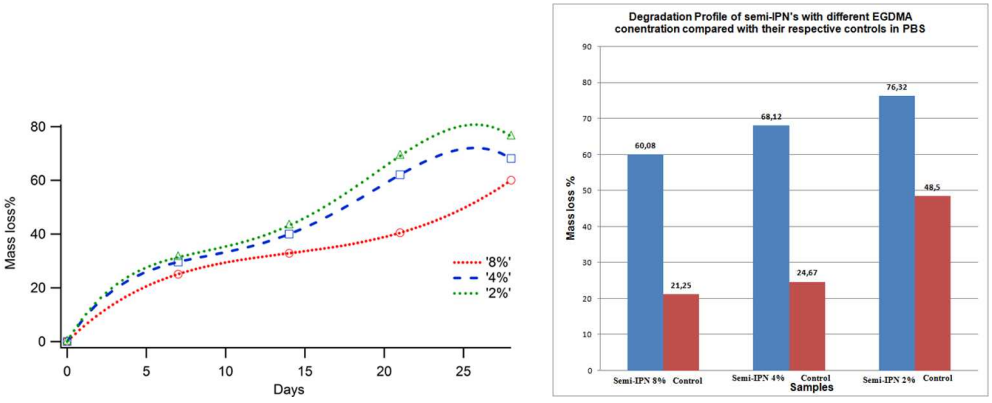

a) b)

Figure 11: (a)*Progressive mass loss of semi-IPN Chitosan- poly(MAGlyGly) after storage in PBS at 37°C with 1.5 µg/mL of lysozyme.* ***(b)*** *Comparison of the mass loss % of semi-IPN of Chitosan-poly(MAGlyGly) in lysozyme and their respective controls in PBS.*

5.5. Conclusion

The semi-IPN of chitosan-poly(MAGlyGly) were prepared. To gain insights on the influence of factors that could affect the formation of the hydrogels, the ratio of the concentration of the polymer/monomer were varied. The influence of the crosslinker on the type and properties of the hydrogels were also studied. Some important features of the hydrogels in terms of various applications like swelling, type of water etc. were studied in detail. It was observed that properties like swelling, morphology and type of water were inversely related to the amount of crosslinker. With the decrease in the amount of crosslinker, the semi-IPN's had a larger pore size. The semi-IPN's showed an increase in

swelling ratio and the percentage of bound water increased with the decrease in crosslinker amount. Physico-chemical characterizations like FT-IR and TGA led us to confirm the presence of both the constituents in the matrix of the hydrogel. Lysozyme degraded the hydrogel matrix to a maximum of 76% for the hydrogel with 2% EGDMA concentration. However, even if some dissolution was observed along with degradation under physiological conditions still the difference between the two was noticeable. The prepared semi-IPN constructs appear to be a promising material for regenerative medicine applications.

5.6. References

[1] Chen, J., Jo, S., Park, K.; Degradable hydrogels. In: Domb AJ, Kost J, Wiseman DM, editors. Handbook of biodegradable polymers. Amsterdam: Overseas Publishers Association, **1997** , 203

[2] Odian, G., Principles of polymerisation. New York: John Wiley and Sons, Inc.; **1991** , 149

[3] Ku° dela, V.,. Hydrogels. In: Kroschwitz JI, editor. Polymers: Biomaterials and medical applications. New York: John Wiley and Sons, Inc;**1989** , 228

[4] Hoffman, A.S.; *Adv Drug Deliv Rev*, **2002** ,3

[5] Peppas, N.A., Bures, P., Leobandung, W., Ichikawa, H. ; *Eur J Pharm Biopharm* , **2000**,27.

[6] Guenet, J.M.; Thermoreversible gelation of polymers and biopolymers. London: Academic Press, **1992**

[7] Cho, J., Heuzey, M.C., Begin, A., Carreau, P.J.; *Biomacromolecules*, **2005** ,3267.

[8] Rajagopal, K., Ozbas, B., Pochan, D.J., Schneider, J.P.; *Eur Biophys J* , **2006**,162.

[9] Kohler, K., Forster, G., Hauser, A., Dobner, B., Heiser, U.F., Ziethe, F., Richter, W., Steiniger ,F., Drechsler, M., Stettin ,H., Blume, A.;*J Am Chem Soc* , **2004**,16804.

[10] Nowak, A.P., Breedveld, V., Pakstis, L., Ozbas, B., Pine DJ, Pochan,D. ,Deming, T.J.;*Nature* **2002**, 388

[11] Determan, M.D., Guo, L., Thiyagarajan ,P., Mallapragada, S.K.;*Langmuir*, **2006**,1469.

[12] Grant, C.D., DeRitter ,M.R., Steege, K.E., Fadeeva, T.A., Castner, E.W. Jr.,. *Langmuir* , **2005**,1745.

[13] Wright, E.R., Conticello, V.P., Apkarian ,R.P., *Microsc Microanal*, **2003** ,17123.

[14] Kimura, M., Fukumoto, K., Watanabe, J., Ishihara, K., *J Biomater Sci Polym Ed* **2004**,631.

[15] Juszczak, L.J.,*J Biol Chem* , 2004,7395.

[16] Percec, V., Bera, T.K., Bufera, R.J., *Biomacromolecules*, 2002,272

[17] Kiyonaka, S., Shinkai, S., Hamachi, I.,*Chemistry* , 2003,976.

[18] Van Tomme, S.R., Van Steenbergen, M.J., De Smedt, S.C., Van Nostrum, C.F., Hennink, W.E., *Biomaterials*, **2005** ,2129

[19] Uludag, H., De Vos, P., Tresco, P.A., *Adv Drug Deliv Rev*, **2000** ,29.

[20] Baruch, L., Machluf, M., *Biopolymers*, **2006**,570.

[21] Stenekes, R.J., Talsma, H., Hennink, W.E.; *Biomaterials*, **2001,** 1891.

[22] Jeong, B., Kim, S.W., Bae, Y.H., *Adv Drug Deliv Rev*, **2002**,37.

[23] Qiu, Y., Park, K., *Adv Drug Deliv Rev* **,2001**,321.

[24] Aharoni, S. M.; *Plenum Press: New York*, **1992**.

[25] Klempner, O., Utracki, L. A. Sperling, L. H.; *Adv Chem Ser* ,**1991**, 239.

[26] Michaels, A. S. ;*Ind Eng Chem*, **1965**, , 32.

[27] Blumstein, A., Kakivaya, S. R., Salamone, J. C.; *J Polym Sci*, **1974**, 651.

[28] Scranton, A. B., Klier, J., Aronson, C. L.; ACS Symposium Series, **1992**, 171.

[29] Lee, J.W., Kim, S.Y., Kim, S.S., Lee, Y.M. , Lee, K.H., Kim, S.J.; *J. Appl. Polym. Sci.* **1999**,113.

[30] Torre, P.M., Enobakhare, Y., Torrado, G. , Torrado, S.; Biomaterials, **2003**, 1499.

[31] Noble, L., Gray, A.I., Sadiq, L. ,Uchegbu, I.F.; *Int, J. Pharm.*,**1999**, 173.

[32] Berger, J., Reist, M., Mayer, J. M., Felt, O., Gurny, R.*; Eur J Pharm Biopharm*, **2004**, 35.

[33] Berger, J., Reist, M., Mayer, J. M., Felt, O., Peppas, N. A., , Gurny, R.; *Eur J Pharm Biopharm*, 2004, 19.

[34] Brouwer, J., Van Leeuwen-Herberts, T., Otting-van de Ruit, M.; *Clin Chim Acta* ,**1984**, 21.

[35] Porstmann, B., Jung, K., Schmechta, H., Evers, U., Pergande, M., Porstmann, T., Kramm, H.J., Krause, H.; *Clin Biochem* ,**1989**,349.

[36] Masuda, T., Ueno, Y., Kitabatake, N.; *J Agric Food Chem* ,**2001**,4937.

[37] Yao, K.D., Tu, H., Cheng, F., Zhang, J.W., Liu, J., *Angew Makromol*. Chem. 1997, 63.

[38] Reddy, T. T., Lavenant, L., Lefebvre, J., Renard ,D.; *Biomacromolecules* ,**2006**, *323*

[39] Yue-qin, Yu., Yang, X., Hansheng, Ning., Shu-sheng, Z.; Colloid Polym Sci ,**2008**,1165.

[40] Al-Kahtani, A.A., Sherigara, B.S.; *J. Mater. Sci.: Matr. Med.*, **2009**, 1437.

[41] Nieto, J. M., Peniche-Covas, C., Padron, G.;*Thermochimica Acta*, **1991**, 63.

[42] Neto, C.G.T., Giacomettib, J.A., Jobb, A.E., Ferreirab, F.C., Fonsecaa, J.L.C., Pereiraa, M.R.; *Carbohydrate Polymers*, **2005,** 97

[43] Corkhill, P. H., Jolly, A. M., Ng, Ch. O., Tighe, B. J.; *Polymer*, **1987**, 1758.

[44] Hatakeyama, H., Hatakeyama, T.; *Thermochimica Acta*, **1998**, 3.

[45] McBrierty, V. J., Martin, S. J., Karasz, F. E.; *J Mol Liq*, **1999**,179.

[46] Ping, Z. H., Nguyen, Q. T., Chen, S. M., Zhou, J. Q., Ding, Y. D.; *Polymer*, **2001**,8461.

[47] Tamai, Y., Tanaka, H., Nakanishi, Y.; *Macromolecules*, **1996**,6750.

[48]Higuchi, A., Komiyama, J., Iijima, T.; *Polymer Bulletin*, **1984**, 203.

[49] Hodge, R. M., Edward, G. H., Simon, G. P.; *Polymer*, **1996**, 1371.

[50] Tomihata ,K., Ikada, Y.; *Biomaterials* **1997**,567.

[51] Varum, K.M., Myhr, M.M., Hjerde, R.J.N., Smidsrod, O.; *Carbohydr Res*, **1997**,99.

[52] Lee ,K.Y., Ha, W.S., Park, W.H.; *Biomaterials*, **1995**,1211–6.

[53] Pangburn, S.H., Trescony, P.V., Heller, J. ; *Biomaterials*, **1982**,105.

[54] Hirano, S., Tsuchida, H., Nagao, N.; *Biomaterials*, **1989**,574.

[55] Sashiwa, H., Saimoto, H., Shigemasa, Y.; *Int J Biol Macromol* ,**1990**,295.

[56] Aiba, S.; *Int J Biol Macromol*, **1992**,225–8.

[57] Shigemasa, Y., Saito, K., Sashiwa, H., Saimoto, H.; *Int J Biol Macromol* ,**1994**,43.

[58] Nordtveit, R.J., Varum, K.M., Smidsrod, O.; *Carbohydr Polym* ,**1994**,253.

[59] Nordtveit, R.J., Varum, K.M., Smidsrod, O.; *Carbohydr Polym*, **1996**,163.

OVERALL CONCLUSIVE REMARKS AND FUTURE PERSPECTIVES

Materials for Tissue Engineering (TE) have significantly progressed over the years, from being initially viewed as biologically inert structural supports to platforms capable of providing signals to cells and tissues to orchestrating tissue regeneration. Current trends suggest that biomaterial development will continue to create more life-like multi-functional materials that are able to simultaneously provide complex biological signals (chemical, structural and mechanical), replace mechanical function and respond to environmental stimuli. A continuing challenge for this approach will be to find ways of exploiting these sophisticated tools without unduly complicating large-scale production for clinical research. We have summarized a wide range of materials that are frequently used to date, or will potentially be useful in TE in the future. Concluding remarks on individual section of the thesis have been listed below.

(1) Chitosan- A Versatile Material for Regenerative Medicine Applications

A review on the current status of chitosan usage in Regenerative Medicine applications has been done. Chitosan appears to be one of the most promising biomaterials in TE because it offers a distinct set of advantageous physico-chemical and biological properties such as non-allergenicity, biocompatibility, biodegradability and cationic surface charges in acidic medium allowing for applications in a variety of conventional and pharmaceutical areas. In this review, various techniques used for preparing chitosan micro/ nanoparticles and hydrogels have been listed.

An updated study of the various applications of chitosan in TE, Drug Delivery, Gene Therapy and the most emerging Boimaging areas has been done. In conclusion, the survey demonstrated that chitosan as a biopolymer holding valuable and immense promise.

(2) Statistical Approach of Chitin Deacetylation

Chitosan was prepared from chitin by a heterogeneous deacetylation process using alkaline medium. Two reaction parameters, namely reaction time and temperature were varied in order to prepare various chitosan grades characterized by different acetylation degrees (DA). Based on this data, a statistical model was developed that can be used to define reaction conditions to obtain a specific value of DA.

(3) Chitosan-Based Beads for Controlled Release of Proteins

Extensive research is being carried out to exploit chitosan as a drug carrier to attain the desirable drug release profiles. The preparation of microspheres or beads are based on a therapy that offer numerous advantages over the conventional dosage forms. These include improved efficacy, reduced toxicity and improved patient compliance. Our approach was similar, in preparing beads of chitosan and loaded with proteins (HSA and PT). Chitosan beads of 700-800 µm were obtained with a satisfactory degree of encapsulation of the two types of proteins Encapsulation efficiency was dependent on the time and temperature to which the beads were allowed to crosslink. It was observed that when beads were allowed to remain in the crosslinking medium for 24 hrs at room temperature, there was recorded maximum encapsulation of about 64% . The release of the two proteins depended on the molecular weight of the respective proteins with trypsin being released faster than HSA. The degradation profile of the beads has been presented in a medium containing lysozyme. Although a lot of work is still included in our future perspective, we were able to optimise the basic conditions of preparation of the beads, encapsulation and release of the proteins.

(4) Hybrid Nanoparticles Based on Chitosan and Poly(Methacryloylglycylglycine)

In this chapter, our approach was focused on the preparation and characterization of nanoparticles based on chitosan. The nanoparticulate systems have great potentials, being able to convert poorly soluble, poorly absorbed and labile bioactive agents into promising deliverable drugs. The core of this system can enclose a variety of drugs, enzymes, genes and is characterized by a long circulation time due to the hydrophilic shell which prevents recognition by the Reticular-Endothelial System (RES). In our work, we tried to achieve the above said properties by combining the benefits of chitosan with that of an anionic poly(acrylamide) of carboxyl end capped of the glycine dimer,[poly(MAGlyGly)]. In this regard, we synthesized the monomer MAGlyGly and with their respective group interactions formed nanoparticles by using chitosan and poly(MAGlyGly) polymerized in-situ. Using various ratios of chitosan and MAGlyGly, nanoparticles of 100-120 nm were successfully prepared with good morphology and shape. Their interaction was established using FT-IR and XPS wherein the presence of all constituents in the nanoparticle matrix was confirmed. Our next step is to load drugs for a sustained release from the prepared nanoparticles.

(5) Synthesis and Characterization of Semi Interpenetrating Polymer Network Hydrogel Composed of Chitosan and Poly(methacryloylglycyl glycine)

Hydrogels have become increasingly studied as matrices for tissue engineering. These devices are usually passive exchange systems, but more recently experimental systems may contain entrapped or encapsulated cells from other human or animal sources. We synthesized hydrogels based on the concept of semi-IPN's wherein the monomers and/or polymers plus crosslinkers are mixed, followed by simultaneous polymerizations via non-interfering reactions. EGDMA was used as a crosslinker with $Na_2S_2O_5$ and $(NH_4)_2S_2O_8$ as the free radical initiator. Our prepared chitosan/poly(MAGlyGly) semi-IPN showed promising properties. The amount of the co-polymers and the crosslinking agent were varied to obtain semi-IPN's and observe their various properties. Evaluation of the preparation conditions were stressed on, it was found that above 20 %wt of chitosan semi-IPN's were not formed irrespective of the amount of crosslinker used. It was also observed that there was dependence of certain properties like swelling, morphology and type of water with the amount of crosslinker. The prepared semi-IPN's showed a very high swelling percentage in both PBS and water with most of the water present as free water. The interconnected porous hydrogels proved to be thermally stable under physiological conditions. Degradation of the prepared semi-IPN's were studied in the presence of lysozyme under physiological conditions. The biological investigations of the semi-IPN's will constitute the objective of further investigations.

The scientific and technology development are a never ended journey. Each closed research project opens a new range of questions and technological capabilities that can be explained and exploited in multiple directions. The worked developed in the scope of this thesis is not an exception. Herein, we intended to highlight some points that might be interesting and fruitful to exploit in forthcoming investigations.

ACKNOWLEDGEMENT

As I write the last part of my thesis, I have so many good memories to reminisce. This may not be the best occasion to disclose my feelings but this thesis being a very important accomplishment in my life, I would like to take this opportunity to thank so many around me, whom otherwise would be difficult to let them know how special they are for me.

To begin with, my family, who are far from me only in terms of distance, they dwell within me!. The three of them, *Mummy, Babu & Moon chua* have been an enormous source of strength invariably. They have always realised my dreams through their own eyes, standing strong as a pillar at times of need. It is, indeed, hard to put down on paper, what they mean to me.....

I would always remain obliged to Prof. Emo Chiellini for providing me this life time opportunity to do a Ph.D under his supervision. I learnt so much in his lab and had a great ambience to understand science along with having a possibility to feel another culture. Prof. Chiellini's level of energy is incredible as well as contagious!. I saw a supervisor who begins working before his students and finishes after them. Indeed, a very respectable and admirable personality!. A special word of thanks to my tutor Dr.Federica Chiellini, all through these years she was a constant support with ever encouraging words and has made substantial contribution in shaping the thesis. Besides, her role as tutor, I always felt a special relation with her. With a great smile that she has, she was always prompt in extending all kinds of help that she could. Whenever in need, I felt compassion and warmth in her approaches. Thank you! for everything, including "castagnaccio" from little *Eugenia*. Back in India, I would like to acknowledge, Prof. Banamali Pradhan, who has always persuaded me to achieve the highest standards in research and academics.

Beth - a fantastic teacher, she shaped and gave a attitude to my scientific thinking. Time spent with her are really brain stimulating. Thank you, Beth for being kind enough to spend those long hours, also during weekends, talking on diverse things from research to culture and for making an impressive contribution to this thesis. Here in Pisa, I spent a budding phase of my life both personally as well as professionally. I made friends that I am

proud of and will cherish their friendship all my life. My days in BIOLAB usually begun with a warm welcome by Dr. Ferri, I will really miss his gestures that made me feel at home. Anna, don't know what to tell about her, a person with so much positivity for life. Optimism and cheerfulness are synonymous to her and now these have been well inherited by our little *Letizia*. At times of stress, I always found her beside, alleviating me Thanks! Anna, for your guidance and affection. Marcella- I will do an injustice if I call her just a friend. She was a sister that this place gifted me. I have spent some really good time with her in the labs of BIOLAB, that served as spots to exchange almost each and every bits and pieces of our daily lives. Thank you for all your love and also for giving me a chance to see *Agnese*. It is also inevitable to acknowledge a good friend Stefania for professional assistance in doing the XPS analysis as well as for being kind enough to give me a lift back from BIOLAB, occasionally.

BIOLAB, was a place with fun and liveliness, a place that gave me a bag full of good friends. Veska, Cristina, Matteo, Andrea, Alberto- a great company to be with while working in labs, a wonderful musician- I wish him good luck to fulfil his dream of becoming a very famous musician someday, Cesare- I will miss cleaning the kitchen with him and also the BMP experiments, Silvia, even if she was far, I always knew I had a well-wisher, Dario, Nicola, Dino, Marco, Carlos, Muhammad, Shiva, Sudhakar, Ariana & all the new faces of this year.

A deep sense of acknowledgement also goes to both the Maria's and Michela. The help extended by Maria 1(as we address her to distinguish) is unforgettable for me. As a young girl with high aims, I admired so much her encouraging mails. I will forever remain grateful for all her assistance. The long hours of standing in Questura with Maria 2 is still so fresh in my memory. I cannot express how sorry I am, for bothering her and how thankful I am, for all those cooperation that I have received. Michela, with her courteous behaviour was ever ready to lend an ear to our problems.

To end, my stay in Pisa is indebted to my best friend, Shelly . To put it very candidly, I cannot thank Shelly in words for the contribution that she has made in my life during these years. I wish the best in life for her in all her endeavours.

Professional assistance provided by Mr.Peiro Narducci in performing the SEM is also duely acknowledged. The present thesis was performed within the framework of “NOE-Expertissues” CT-2004-500328 and PRIN-2006.

APPENDIX

PUBLICATIONS & LIST OF CONTRIBUTIONS IN CONFERENCES AND WORKSHOPS

Conferences:

M.Dash, M.Ferri, S.Cometa and F.Chiellini: Evaluation of hybrid nanoparticles of chitosan/methacryloylglycyl glycine for biomedical applications, 2nd International Congress on Biohydrogels, 10-15th November, Viareggio (Italy), 2009– oral presentation.

M.Dash, M.Ferri, S.Cometa and F. Chiellini: Preparation and characterization of chitosan/methacryloylglycyl glycine based nanoparticles for biomedical applications, VII CONVEGNO NAZIONALE INSTM SULLA SCIENZA E TECNOLOGIA DEI MATERIALI TIRRENIA(PI) 9-12 GUIGNO 2009-poster presentation

M.Dash, M.Ferri, F.Chiellini ; Biocompatible polymeric materials for regenerative medicine applications; 2° Forum Nazionale Giovani Ricercatori su Materiali Polimerici e Biomateriali, Genova (Italy), 4-5th July, 2008– poster presentation.

M.Dash, F.Chiellini, A.M. Piras and E. Chiellini: Micro and Nano Biomaterials for regenerative medicine. International Congress on Biohydrogels, 14–17th November, Viareggio (Italy), 2007– oral presentation.

M.Dash, F. Chiellini, E. Chiellini,; Bioactive polymeric material for regenerative medicine applications; 14th CIRMIB Biomaterials School on Nanomedicine: Imaging, Drug Release, Regenerative Medicine, 9–13th July, Ischia (Italy), 2007– oral presentation.

Book Chapter:

A.M.Piras, C.Errico, **M.Dash**, M.Ferri, E.Chiellini, F.Chiellini. Polymeric Nanoparticles for Targeted Release of Conventional and Macromolecular Drugs(preparation and characterization aspects). In Remaesh S. Chaughule and Raju V. Ramanujan (Ed)

NANOPARTICLES: From Synthesis to Application. American Scientific Publishers,25650 Lewis Way, Stevenson Ranch, California 91381-1439, USA.(2009). *In press*

M.Dash, A.M.Piras, F.Chiellini, "Chitosan based beads for controlled release of proteins" in Biohydrogels, Rolando Barbucci (Ed.), Springer-Verlag, Milan – Italy (2009), pp 111 –120.